CENTER FOR INFRASTRUCTURE ENGINEERING STUDIES

Rapid Strengthening of Reinforced Concrete Bridges

By

Dr. Lawrence C. Bank

Dr. Michael G. Oliva

Dushyant Arora

David T. Borowicz

UTC
R64

Disclaimer

The contents of this report reflect the views of the author(s), who are responsible for the facts and the accuracy of information presented herein. This document is disseminated under the sponsorship of the Department of Transportation, University Transportation Centers Program and the Center for Infrastructure Engineering Studies UTC program at the University of Missouri - Rolla, in the interest of information exchange. The U.S. Government and Center for Infrastructure Engineering Studies assumes no liability for the contents or use thereof.

Technical Report Documentation Page

1. Report No. UTC R64	2. Government Accession No.	3. Recipient's Catalog No.
4. Title and Subtitle Rapid Strengthening of Reinforced Concrete Bridges		5. Report Date Dec 2002
		6. Performing Organization Code
7. Author/s Lawrence C. Bank, Michael G. Oliva, Dushyant Arora, David T. Borowicz		8. Performing Organization Report No. RG001140 OT064
9. Performing Organization Name and Address Center for Infrastructure Engineering Studies/UTC program University of Missouri - Rolla 223 Engineering Research Lab Rolla, MO 65409		10. Work Unit No. (TRAIS)
		11. Contract or Grant No. DTRS98-G-0021
12. Sponsoring Organization Name and Address U.S. Department of Transportation Research and Special Programs Administration 400 7th Street, SW Washington, DC 20590-0001		13. Type of Report and Period Covered Final
		14. Sponsoring Agency Code

15. Supplementary Notes

16. Abstract

In the proposed research study a new and innovative technique for rapidly strengthening reinforced concrete members with fiber reinforced plastic (FRP) strips will be demonstrated in a full-scale application on an existing bridge in the State of Wisconsin. A team of researchers from the university of Wisconsin-Madison in collaboration with the University of Missouri-Rolla, and industrial partners will strengthen an existing flat slab bridge and perform service load and ultimate load tests on the bridge to evaluate the efficiency of the proposed rapid strengthening method.

17. Key Words Reinforced, bridges	18. Distribution Statement No restrictions. This document is available to the public through the National Technical Information Service, Springfield, Virginia 22161.		
19. Security Classification (of this report) unclassified	20. Security Classification (of this page) unclassified	21. No. Of Pages	22. Price

Form DOT F 1700.7 (8-72)

Disclaimer

This document is disseminated under the sponsorship of the Department of Transportation in the interest of information exchange. The United States Government assumes no liability for its contents or use thereof. This report does not constitute a standard, specification or regulation.

The United States Government does not endorse products or manufacturers. Trade and manufacturers' names appear in this report only because they are considered essential to the object of the document.

Executive Summary

Rapid Strengthening of Reinforced Concrete Bridges

Project Summary

In this research project the use of a new method to rapidly strengthen reinforced concrete bridges with Fiber Reinforced Polymer (FRP) composite materials was investigated. In the course of the research a bridge in the city of Edgerton, Wisconsin was strengthened and tested to failure. The potential to use the method as a rapid and temporary means of upgrading load-capacity deficient bridges in the State was studied. Upgrading an under-capacity rated bridge may postpone the replacement of the bridge if it has a low Sufficiency Rating (i.e., below 50). Such an option is desirable to local governments that have budget constraints and need to replace many older deficient bridges. The purpose of this research was to study the Mechanically Fastened-Fiber Reinforced Polymer (MF-FRP) method of rapid bridge strengthening by applying it to a structurally deficient bridge in the State of Wisconsin and conducting laboratory tests at the University of Wisconsin-Madison.

Background

An innovative technique for repairing reinforced concrete beams (or slabs) by attaching FRP strengthening strips to the underside of the concrete beam using powder actuated fasteners and mechanical anchors has been developed at the University of Wisconsin-Madison under funding from the US Army Corps of Engineers. The method is known as the Mechanically Fastened (MF) Fiber-Reinforced Polymer (FRP, or the MF-FRP method, to distinguish it from the traditional Externally-Bonded FRP (EB-FRP) method. This method relies on mechanical attachment of the FRP strip, and is a rapid procedure that uses simple hand tools, lightweight materials, and unskilled labor. Unlike the conventional method of adhesively bonding FRP strips to the concrete surface, this method does not require surface preparation and allows for immediate use of the strengthened structure.

In this project the MF-FRP method was applied for the first time in the field to an existing bridge structure, which was subjected to both service and ultimate load testing to determine the in-situ performance of the strengthening system. In addition, a laboratory study was conducted on concrete beams representative of the bridge cross-section to obtain more detailed information on the behavior of the MF-FRP strengthening system.

The research was conducted as part of the Wisconsin Highway Research Program by the University of Wisconsin-Madison in collaboration with the Federal Highway Administration University Transportation Center (UTC) at the University of Missouri-Rolla. In addition, the research was coordinated with ongoing research at the University of Wisconsin-Madison with the US Army Engineer Research and Development Center (ERDC) in Vicksburg, MS, which funded additional related studies at their laboratories. The research team worked closely with the Wisconsin Department of Transportation (WisDOT) Bridge Division, Maintenance Division, and the District 1 office. Support in the field for the implementation of the strengthening system and with the load testing on the bridge in the city of Edgerton was provided by the Rock County

Department of Transportation. Local authorities from the city of Edgerton as well as private consultants including K. Johnson Engineers, TN & Associates, and McClure Engineering Associates assisted with the research. The research was also coordinated with the structural designer of the replacement bridge Forth and Van Dyke, and with Concrete Structures, the replacement bridge contractor.

Process

The research process consisted of selecting an appropriate bridge for the strengthening, evaluating the capacity of the bridge, designing a strengthening system, installing the strengthening system, conducting laboratory tests, testing the strengthened bridge, and determining the cost and the performance of the strengthening system. The research was conducted from November 2001 to August 2003, a period of 22 months. From November 2001 to July 2002 design studies and site investigations were conducted.   In August 2002 the bridge was strengthened.   From September 2002 to March 2003 laboratory testing was conducted and theoretical analysis completed. From April to June 2003 preparations were made for failure testing of the bridge and the testing was completed.   From July to August 2003 the results of the failure testing were evaluated and reporting was completed. The research was compatible with the research goal of the Structures Technical Oversight Committee of the WHRP to "consider other research programs for evaluation of innovative materials and ideas."

Bridge (P-53-702) on old Stoughton Road in Edgerton Wisconsin over Saunders Creek

The data collected during the research consisted of materials and structural performance data as well as materials cost and manpower data. During the service load and ultimate load testing of the strengthened bridge (P-53-702) on old Stoughton Road in Edgerton Wisconsin over Saunders Creek (shown above), structural data was taken by electronic and manual data acquisition systems and included, strain measurements in the concrete and the FRP materials, deflection measurements of the bridge, and photographs and video recordings of the testing. Structural data also included accurate geometric measurements of the bridge and recordings of the condition of the bridge elements (slab, abutments, barrier). Materials testing included measurements of the strength of the concrete, steel and FRP materials recovered after the failure testing on the bridge. Materials and manpower data collected included the cost of all materials

used in the project to strengthen the bridge and the man-hours needed to install the strengthening system. In the laboratory, structural and material data collected during the beam load testing included strain and deflection data as well as properties of the materials used (concrete and FRP).

Findings and Conclusions

The major finding of this research was that the MF-FRP method could be used to strengthen an existing deteriorated bridge. The method is easy to use in the field and the level of strengthening can be predicted in advance using conventional analytical methods. The strengthening can increase the load rating of the bridge, which may alleviate the need for total replacement of the bridge. The Inventory Rating of the bridge studied in this research was increased from an HS17 rating to HS25 rating, a 29% increase in moment capacity, for a unit cost of materials and manpower of $12.72/ft^2. Based on 10 months of in-service data the materials appeared to be durable and the strengthening system appeared to be sound.

A cost-benefit analysis relative to other bridge strengthening methods was not in the scope of the research and was not conducted.   The total cost of strengthening the Edgerton Bridge was $7,995 which can be compared to the approximately $140,000 cost of the bridge replacement. The practical benefits for WisDOT and especially for local and county authorities, who own small bridges that are in need of replacement, is that they may be able to strengthen their bridges instead of replacing them. In the research, it was shown that the Edgerton Bridge could have been raised to a Sufficiency Rating of above 50 with the appropriate combination of strengthening and structural repairs.   Replacement of the bridge is not required if the Sufficiency Rating is above 50. The MF-FRP strengthening method can be used as a short-term measure to raise the Sufficiency Rating for a bridge for a few years if funding for replacement is not available.   As such it provides a method to either reduce costs or to allow for reallocation of funding to more critical projects.

Since the MF-FRP strengthening method increases the load rating of the bridge it improves safety in an indirect fashion.   If a bridge is posted and the strengthening can be used to remove the posting then additional productivity and operational efficiencies would be obtained. This would provide commensurate improvement in customer service.

The research indicates that the load rating of an existing bridge can be used as a good measure of its current capacity. Based on the existing rating a "desired rating" can be calculated using existing methods provided by AASHTO. Using this "desired rating" the required capacity for the strengthened bridge can be calculated and the strengthening system can be designed. The use of this method would require bridge designers to become more familiar with load-rating methods and with methods to design strengthening systems for bridges. This research has provided an outline of the methods and procedures needed to conduct a strengthening design with the MF-FRP method.

Since the research enables a designer to determine the trade-off between strengthening an existing bridge versus its replacement the research provides information that could impact policy-based decisions. The key policy-based decision that needs to be made is whether to

strengthen a bridge or to replace a bridge. This research provides the tools to designers that will allow a technical comparison to be made between these two alternatives.   It should be emphasized, however, that it is not only the load rating that influences the decision to replace a bridge. Many additional policy-based safety and serviceability factors enter into the decision to replace a bridge. These are reflected in the Sufficiency Rating calculation as explained in the report.

The findings of this research and other current research related to strengthening of bridges may impact existing federal regulations in the future. An alternative to the existing requirement for replacement of bridges could be envisioned whereby the owner could provide a strengthening system to avoid replacement. This would not change existing regulations but rather reinterpret existing regulations. The finding could impact all states, since all states find themselves in a situation of having numerous deficient small local bridges that are in need of replacement. The findings would be of particular interest to local governments that own many of these small older bridges, and that have budget and funding constraints. It is too early to say that these findings indicate a new best practice. Further studies and demonstrations on a wider variety of bridges are needed before widespread use of the MF-FRP strengthening technology can be made.   The State of Missouri is currently considering strengthening a number of bridges using the MF-FRP method. This should provide additional data on its performance and potential for widespread use. The emerging issue raised by this study and others like it is that strengthening of existing structures is likely to be a viable option for bridge technology in the future and that given the current budget conditions it should be investigated seriously. While this is not a "new" issue per se, this research has provided additional evidence that strengthening is possible and that FRP materials can be used effectively to accomplish this goal.

Recommendations for Action

In the short-term, it is recommended that DOTs continue to study the potential for strengthening capacity deficient bridges as an alternative to costly replacements. The Mechanically Fastened-Fiber Reinforced Polymer (MF-FRP) method is a potential cost-effective method that can be used to strengthen deteriorated concrete bridges. In order for the method to be used in the future the following are recommended.

- DOTs should designate a design engineer and a maintenance engineer in the bridge section to learn to design strengthening systems for bridges with FRP materials and to perform bridge-rating calculations for strengthened bridges.

- Further research should be conducted to determine if the MF-FRP method can be used to strengthen reinforced concrete girder bridges. An implementation on a girder bridge slated for replacement is recommended in the near future.

- Additional research is recommended to determine if the MF-FRP method can be used on prestressed concrete bridge girders. This may be useful for the rapid repair of bridges that have been damaged due to truck impacts. An initial laboratory study is recommended. This should be followed by a field demonstration.

- A study is recommended to determine the relative cost/benefits of strengthening a deficient reinforced concrete bridge with the MF-FRP method to extend the current life instead of replacing the bridge. This is especially important for bridges that are just below a sufficiency rating of 50. In this case the strengthening can be used to improve the sufficiency rating to a point where mandatory replacement is not required.

- A manual for strengthening bridges with FRP and other materials should be developed for use by DOT engineers. A set of guidelines outlining which types of bridges would be most suited to different types of strengthening methods should be prepared. The guidelines should include a method to make cost comparisons between different alternatives.

The responsibility for implementation of these recommendations lies with the DOT and, when used, bridge design consultants. As long as it is seen to be more profitable and convenient to design a new bridge to replace an old deficient bridge there will be no real impetus to strengthen bridges. More incentives should be given to design consultants and bridge contractors to consider strengthening of bridges as an alternative to replacement.

In order to educate the bridge design and construction community on the technologies available to strengthen bridges with both conventional and FRP materials, it is further recommended that a workshop and training session be held on this topic for DOT designers and design consultants. It may be possible to coordinate this activity through the University of Wisconsin Continuing Education Program.

The WisDOT contact for more information on this research activity is:

Mr. Stanley Woods
Wisconsin Department of Transportation
4802 Sheboygan Avenue
Madison, WI 53707-7965
(608) 266-8348

Contents

List of Tables

List of Figures

1   Introduction

An innovative technique for repairing reinforced concrete beams (or slabs) by attaching FRP (fiber reinforced polymer) strengthening strips to the underside of the beam using powder actuated fasteners and mechanical anchors has been developed at the University of Wisconsin-Madison under funding from the US Army Corps of Engineers (Bank et al., 2002a, 2002b; Lamanna et al., 2001). The method is known as the Mechanically Fastened (MF) Fiber-Reinforced Polymer (FRP), or the MF-FRP method, to distinguish it from the traditional Epoxy-Bonded FRP (EB-FRP) method (ACI 440.2R, 2002; FIB, 2001, Teng et al., 2001). This method relies on mechanical attachment of the FRP strip, and is a rapid procedure that uses simple hand tools, lightweight materials, and unskilled labor. Unlike the conventional method of adhesively bonding FRP strips to the concrete surface, this method does not require surface preparation and allows for immediate use of the strengthened structure. Bonded repair methods have been used in a number of full-scale bridge strengthening projects (e.g., Alkhrdaji et al, 2000; Nanni, 1997). The conventional bonding method requires time consuming grinding, sand blasting, priming and smoothing of the concrete surface to make it suitable for bonding the strip. In addition, the bonded strip "must not be disturbed for a minimum of 24 hours following the application of the adhesive" (Sika, 1999).

Even with FRP bonded systems a number of authors have recommended that in order to prevent a catastrophic brittle failure of the strengthened beam by strip detachment, mechanical anchorage should be provided at the strip ends (Spadea et al., 1998, Garden and Holloway, 1998). Anchorage is usually provided by anchor bolts or cover plates. Anchorages have been used with epoxy-bonded steel plates (Hussain et al., 1995). In addition to being rapid and easy to install, the MF-FRP method provides the necessary anchoring mechanism as part of the procedure, since it is based entirely on mechanical fastening systems. Moreover, the multiple small fasteners used in the MF-FRP method, in contrast to large diameter bolts typically used for anchorages, distribute the load uniformly over the FRP strip and reduce stress concentrations which can lead to premature failure.

In the current study the MF-FRP method was used to strengthen an existing, deficient and aging highway bridge in the city of Edgerton, Wisconsin. The objective of the research was to apply the technology developed in prior research studies to demonstrate the potential of the MF-FRP method. The research consisted of identification of the bridge, determining the capacity of the existing bridge, designing the strengthening system, installing the strengthening system, and conducting service load and ultimate load tests. In addition, a laboratory study was undertaken to determine the behavior of MF-FRP beams strengthened in an identical fashion to the in-situ bridge.

The report provides a detailed account of the all the tasks undertaken in the research and provides conclusions as well as recommendations for further study and implementation.

2 Objectives and Scope

Objectives

The primary objective of the research was to study the MF-FRP (Mechanically Fastened-Fiber Reinforced Polymer) method of rapid bridge strengthening by applying it to rapidly strengthen a load-capacity deficient and aging bridge in the State of Wisconsin. The potential to use the method as a rapid and temporary means of upgrading load-capacity deficient bridges in the State was studied. Upgrading an under-capacity rated bridge may be able to be used to postpone the replacement of the bridge if it has a low Sufficiency Rating (i.e., below 50). Such an option is desirable to local governments that have budget constraints and need to replace many older deficient bridges.

In order to accomplish the primary objective the following intermediate objectives were identified:

1. To establish criteria for a deficient bridge in the Wisconsin bridge inventory that was slated for demolition and replacement to be used as the "test-specimen" for the research.

2. To work with the Wisconsin Department of Transportation (WisDOT) to identify a bridge slated for replacement in the 2002-2003 cycle for use in the research.

3. To obtain permission from the bridge owner to conduct the research study on the bridge and to coordinate the plans for the research study with the bridge owner, the WisDOT, and the bridge contractor to conduct the research.

4. To determine the in-situ capacity of the existing bridge from current inspection reports, historical data, site inspections and theoretical calculations.

5. To conduct design studies to determine the amount of strengthening required to increase the Inventory Rating of the bridge to HS25.

6. To obtain pultruded FRP strengthening strips from a local supplier according to specifications developed in prior research studies.

7. To develop a plan for attaching the FRP strip to the underside of the bridge in collaboration with local county maintenance personnel and environmental authorities.

8. To supervise the attachment of the FRP strips to the underside of the bridge using mechanical fasteners.

9. To determine the cost of strengthening the bridge in terms of manpower and materials.

10. To conduct service load tests on the bridge to assess the degree of composite action.

11. To design, fabricate and test in the laboratory four full-scale beams representative of the bridge cross-section in order to understand the behavior of the MF-FRP strengthened beams and to develop control data for the in-situ load testing.

12. To conduct an environmental study on the effects of 10 months (August 2002 – June 2003) of exposure and service loading on the MF-FRP strengthened bridge to determine if any deterioration of the FRP strip or the attachment had occurred.

13. To conduct an ultimate load test to failure on the strengthening bridge to determine the performance of the MF-FRP strengthening system on the bridge.

14. To report the findings of the research and provide recommendations for the use of the MF-FRP method for rapid strengthening of reinforced concrete highway bridges in the State of Wisconsin.

Scope

In the interests of time and funding, the scope of the bridge study and the laboratory study were limited to the following:

Bridge Study

1. A bridge of the 1920-1940 era that was slated for demolition and replacement the 2002-2003 cycle.

2. A simply-supported, single-span, flat slab bridge similar to one found in many local and county bridges that are in need of replacement.

3. A bridge with a span of 20 to 30 ft and two lanes wide to keep material costs reasonable.

4. A bridge with a below HS20 inventory load rating.

5. A bridge that was easily accessible from the underside and would not require extensive scaffolding or traffic control while the strengthening work took place.

6. A reinforced concrete bridge with a significant amount of deterioration such that the use of an epoxy-bonded FRP system would not be feasible.

7. A bridge that could be tested to failure.

Laboratory study

1. Four beams each weighing less than 5 tons (10,000 lbs), which is the capacity of the test facility at UW-Madison.
2. One control beam and three strengthened beams each with different strengthening details.

3. Three monotonically loaded beams and one cyclically loaded beam.

4. Tensile and open-hole tensile mechanical tests of the FRP strips and recovered FRP strips.

## 3	Background Review

Over the past four years research has been conducted to evaluate the MF-FRP method with support from the US Army Corps of Engineers. The following studies have been conducted:

1) In 1998 Small-scale tests were conducted to determine the load capacity of a FRP strip-to-concrete mechanically-fastened connection (Lamanna, 2002). Testing was carried out on a variety of different types of fasteners and strips, and on fasteners driven into pre-drilled holes and into concrete without pre-drilled holes. It was determined that the capacity of the connection is a function of the depth of fastener embedment in the concrete, the bearing strength and edge distances of the FRP strip, and the strength and aggregate properties of the concrete. For the types of concrete, strengthening strips, and fasteners used in the study, the lower bound design capacity per fastened-connection was recommended as 500 lbs for connections without a pre-drilled hole and 1000 lbs for connections with a pre-drilled hole.

2) In 1999 a preliminary investigation into the feasibility of the MF-FRP method of strip attachment was first conducted on 35 small-scale reinforced concrete beams (Lamanna et al. 2001a). The beams measured 6 x 6 x 48 in. and were tested in four-point bending on a span of 42 in. A variety of fasteners and fastener layouts were considered with a number of different FRP strips. The strengthened small-scale beams showed increases in yield and ultimate moments up to 36% and 30%, respectively, over the unstrengthened control beams (Lamanna et al., 2001). Strengthened beams showed a ductile failure mode.

3) In 2000 the effect of increasing the scale of the MF-FRP method was investigated. Fifteen large-scale reinforced concrete beams were tested. The purpose of this testing was to examine the effect of different types of FRP strips, fasteners, and fastener layouts on large-scale beams. The large-scale beams had the dimensions of 12 x 12 x 144 in. and were tested in four-point bending on a span at the Corps of Engineers laboratories in Vicksburg, MS (Bank et al., 2002a, Lamanna et al., 2001b). The influence of the type and number of FRP strips, and the influence of fastener type and spacing were studied. Based on the results of this study a "prototype FRP strip was developed" for strengthening with the MF-FRP method. The strip is a hybrid strip consisting of a combination of E-glass rovings, carbon tows and E-glass mats in a vinylester resin.

4) In 2001 an analytical model was developed to predict the moment-curvature relationship for reinforced concrete beams strengthened using the MF-FRP method (Bank et al., 2002 a; Lamanna, 2002). The model utilizes equilibrium, strain compatibility, and the constitutive properties of the materials. In addition to predicting the failure modes of steel yielding, concrete crushing, and FRP strip rupture, the moment-curvature model also predicts FRP strip detachment by fastener failure. In all cases the model predicts ultimate strengths similar to those reached using the Whitney stress block model when modified for the inclusion of the FRP strip. Predictions of the model were shown to compare well with the results of the large-scale beam tests (Bank et al., 2002a; Lamanna et al., 2001b). The computer program, which is known as FASTFLEX®, is available from the University of Wisconsin. It can also be used for design of strengthening systems.

5) In 2001 a series of full-scale bridge T-beams strengthened with the MF-FRP method were tested at the Corps of Engineers laboratories (Bank et al., 2002b, Borowicz, 2002; Vlazquez et al., 2002). The T-beams were 29 ft long and had a 60 x 8 inch top flange and a 22 x 12 inch web section. They were reinforced with 5 # 9 grade 60 main longitudinal bars in the bottom of the web and # 4 stirrups at 12 in o.c. The flange was reinforced with a double layer of # 4 bars at 12 in o.c. in both directions. Beams were fabricated at the Corps of Engineers with 5000 psi concrete. Three different levels of tensile reinforcement were used, identified by the number of #9 main bars, A3, A5 and A8. For each reinforcement level 3 different strengthening levels were used – no strengthening, one FRP strip and two FRP strips. A termination length of 18 inches was used in all beams. All beams had the FRP strips fastened with Hilti X-ALH power actuated fasteners in two rows spaced at 2 inches and spaced at 2 inches along the length. In the A3 and A5 controls it was not possible to achieve ultimate failure of the beams due to the large displacement required. Only the A8 beam reached its ultimate load. All the strengthened beams failed due to strip delamination prior to achieving compressive failure in the concrete. Beams showed increases of between 10 and 20% in strength at yield and at ultimate load. Figure 3.1 shows the moment versus displacement data for all nine tests.
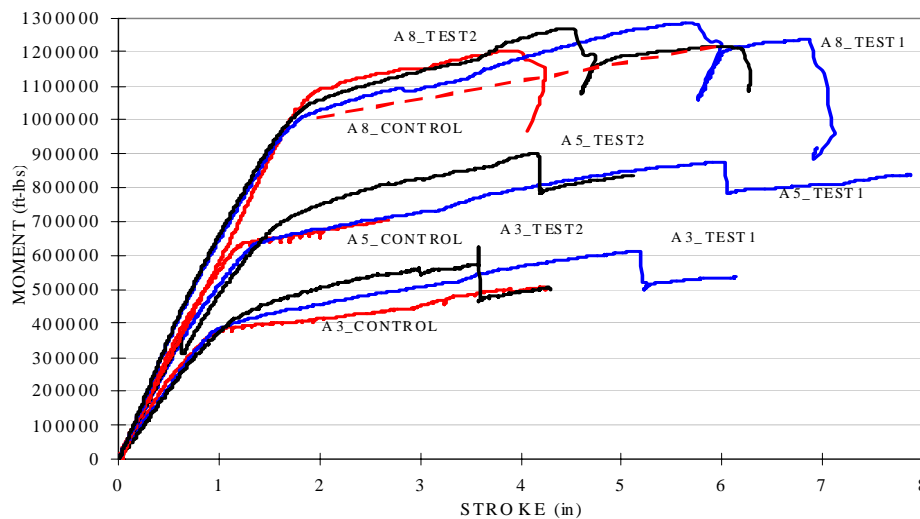
Figure 3.1. Moment-stroke data for 2001 T-beam tests

6) In 2002 a series of 10 tests on large-scale beams with dimensions of 12 x 12 x 144 in. (identical to those used at the Corps of Engineers in 2001) were tested at the University of Wisconsin to investigate the effect of shear span, end-delamination and fatigue loading on the behavior of the MF-FRP strengthening method (Borowicz 2002). Figure 3.2 shows the effect of varying the shear span (and hence the number of fasteners) on the load carrying capacity of the strengthened beams. Figure 3.3 shows the effect of varying the number of strips and also the repeatability of the behavior of the strengthened beams.
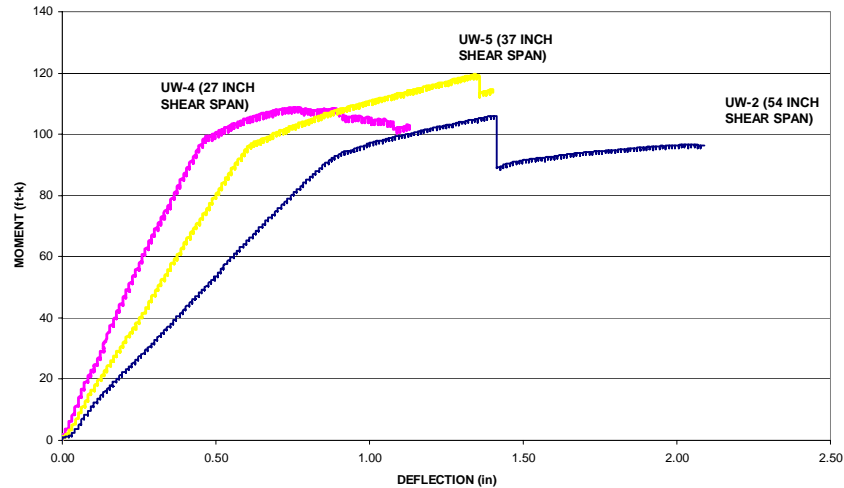
Figure 3.2. Effect of shear span on capacity of MF-FRP strengthened beams
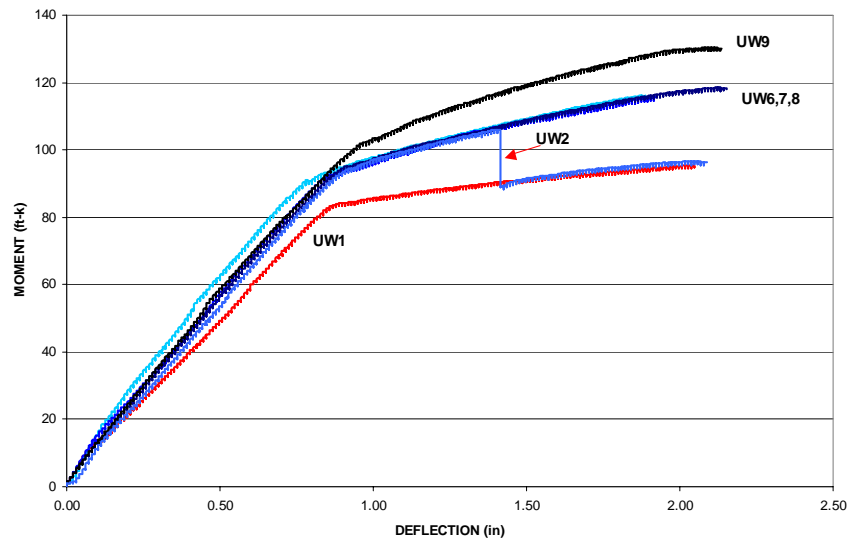
Figure 3.3.   Unstrengthened beam (UW1) versus beams strengthened with one (UW6, 7,8) and two (UW9) FRP strips.

The results of this series of tests indicated that end-termination distance and shear span play a significant role in the capacity and failure mode of the MF-FRP strengthened beams. The results of the fatigue testing showed that the MF-FRP strip did not delaminate under cyclic loads.

7) In 2002 a second phase of large scale T-beams were tested at the US Army Corps of Engineers. Six beams were tested in this series – 5 subjected monotonic loading to failure and one subjected to 2 million cycles of fatigue loading. The monotonic beams were tested in 4 point bending with two actuators having a 5 ft moment span. The fatigue beam was tested in three point bending with a single actuator at midspan cycled at 2 Hz from 10k to 30k. The

beams were strengthened with either one, two or three 4 inch wide by 1/8 in thick pultruded FRP strips, sold under the tradename of SafStrip™ and produced by Strongwell in Chatfield, MN, USA and attached with Hilti ALH fasteners embedded approximately 1.5 inches into the concrete. Other parameters studied included the "termination length" and the use of drilled expansion anchors at the strip ends to prevent end-delamination failures.   The testing showed that significant strengthening of full-size T-beams could be achieved using the method. In this series increases in capacity over unstrengthened control beams of over 25% were obtained at large deflections (2.5 inches). All beams failed due to strip end-delamination at a large deflection (> 4 inches). Ultimate compression failure of the control beam was seen at 10 inches of midspan deflection. Two 2.5 inch long by ½ diameter expansion anchors were seen to significantly delay end-delamination of the strips and to increase both the deflection and load at failure. Shorter termination lengths (3 inches versus 18 inches from the support) also increased strengthening by delaying end-delamination as anticipated. The use of multiple FRP strips (in unbonded layers) did not yield significant increases in capacity of the strengthened beams over single strips due to premature end-delamination failures and the inability of the fasteners to transfer load into the outer strips. Figure 3.4 shows the test data for the five monotonically loaded beams. The beam subjected to the fatigue loading sustained the full 2 million cycles with no degradation of the strengthening system nor change in stiffness of the beam (Bank et al., 2003)
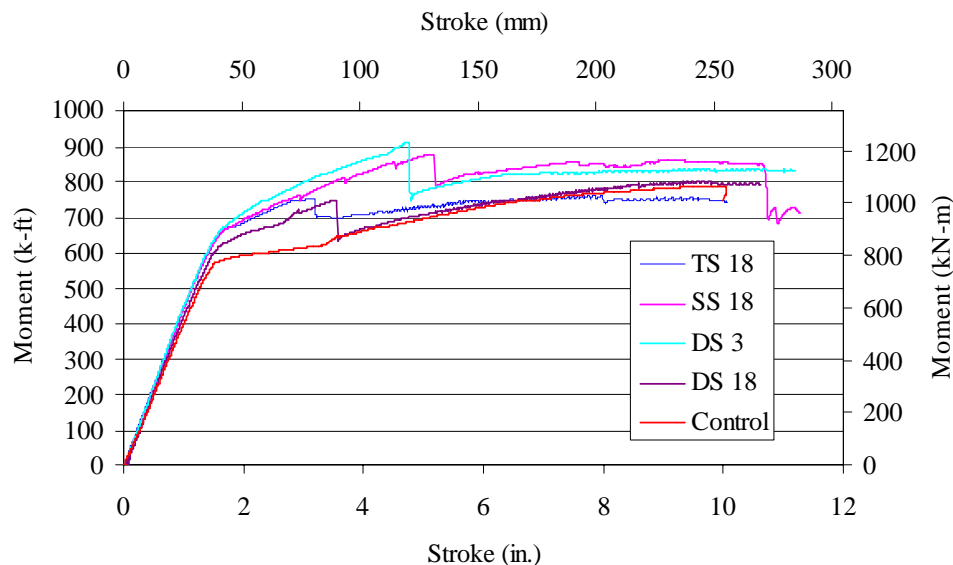
Figure 3.4. Results of 2002 T-beam tests

8) In 2002 a study was conducted to optimize the mechanical and physical properties of the FRP strip for use in the MF-FRP method (Gulbrandsen, 2002). Seven different strips with varying constituents and fiber architectures were designed by the University of Wisconsin and manufacture red by Strongwell in Chatfield, MN. Based on the results of tension and bearing tests an "optimal" strip was recommended for production for the MF-FRP method. The strip was subjected to extensive characterization and guaranteed design properties in accordance with ACI 440.2R (2002) procedures were developed (Bank et al., 2003; Arora, 2003). These "optimal" SafStrip™ strips were used to strengthen the Edgerton Bridge.

**4	Full-scale Implementation of the MF-FRP System**

Introduction

As part of the proposed research to investigate the constructibility and performance of the MF-FRP system on existing deteriorated bridge structures, a capacity deficient reinforced concrete flat slab bridge built in 1930 was strengthened and tested to failure. The full-scale application of the proposed system on an existing bridge in the State of Wisconsin was conducted to demonstrate the performance of the MF-FRP system. A procedure was developed in collaboration with the Wisconsin Department of Transportation (WisDOT) to identify a structurally deficient bridge in the Wisconsin Highway Bridge Inventory. A schedule for the rapid strengthening of the existing bridge was developed to demonstrate the installation procedure with the aid of the county maintenance personnel.   An analysis and design of the existing bridge for retrofit was conducted to improve its load carrying capacity.

Objectives of the Application of MF-FRP System on an Existing Bridge

The objectives of this part of the research were intended to demonstrate the effectiveness of the MF-FRP system to strengthen an existing bridge and are highlighted below:

- To identify a below HS20-44 rated deteriorated reinforced concrete slab bridge in the Wisconsin Highway Bridge Inventory.

- To determine the existing Load Rating (LR) and Sufficiency Rating (SR) of the candidate bridge according to AASHTO and FHWA standard procedures.

- To design a strengthening system for the bridge using the MF-FRP strips to increase the Inventory Load Rating of the bridge to HS25 and to account for moving loads in the design procedure.

- To develop a schedule, materials, personnel and methods plan for strengthening the bridge.

- To strengthen the bridge and to conduct service load testing.

- To conduct a preliminary investigation of the durability of the in-situ strengthening system.

- To conduct ultimate load testing to determine the actual strengthening level achieved with the MF-FRP system.

Bridge Identification

To identify a candidate bridge, the research team proposed the following general method to WisDOT to select an under capacity bridge with potential for rehabilitation:

- A bridge earmarked for replacement between 2002 and 2004;

- A reinforced concrete flat slab bridge with a 20-30 ft long span with simple supports;

- A vintage bridge constructed between 1930 and 1940 with available existing plans (if possible);

- A bridge rated for loads lower than HS20-44.

Three bridges were identified from the Wisconsin bridge inventory. The descriptions and characteristics of the three bridges are provided in the next sections.

Bridge 1

Candidate bridge 1 was a 20 ft long slab bridge designated B-13-518 located northwest of the city of Dane. The bridge was located on STH 113 over Spring Creek. Figure 4.1 and Figure 4.2 show the characteristics of the bridge.

Figure 4.1. View of Bridge B-13-518

Figure 4.2. Slab of bridge B-13-518

The width of the bridge was measured to be 38.1 ft. As can be seen in the figures, no traffic barriers or guardrails were installed on the bridge. The "Sufficiency Rating" of the bridge was 41, which qualified it for replacement and it was scheduled for reconstruction as part of a

roadway project in 2003. The head clearance of the bridge was measured between 2-3 ft and the depth of the slab was 20 in. No extreme deterioration or section loss was observed in the slab, however the bridge was posted for its under-capacity. While the bridge was a suitable candidate for the project, other bridges were considered for easier access to the bridge soffit.

Bridge 2

Candidate bridge 2 was a 23 ft long slab bridge designated P-53-71 located on Marsh Road over a branch of Bass Creek in the Town of Magnolia, Rock County. The bridge was due for replacement in the 2002-2003 cycle. The letter "P" designates that bridge plans for the structure were not available. The bridge was built in 1930 and was 26.9 ft wide. In 1950 the bridge was widened utilizing four steel girders. Due to the complexity of the structural system the bridge was not investigated further.

Bridge 3

Candidate Bridge 3 was a 23 ft long flat slab bridge designated P-53-702 located on Stoughton Road over Saunders Creek in the City of Edgerton, Rock County. The bridge was originally constructed in 1930 for an H15 truck loading and was 25.9 ft wide. Figure 4.3 and Figure 4.4 show the details of the bridge.

Figure 4.3. View of roadway of Bridge P-53-702

Figure 4.4. Side view of Bridge P-53-702 over Saunders Creek

Upon preliminary assessment, the underside of the bridge looked in reasonable (but deteriorated) condition with a clearance of 4 to 5 ft. A large number of stalactites were seen on the underside of the slab and one of the edges showed some section loss. Figure 4.5 shows the underside of the bridge.

Figure 4.5. Stalactites and efflorescence seen on the underside of the slab of P-53-702

Efflorescence was seen on the edge of the bridge slab, which was around 24-28 in. thick. The creek that ran under the bridge was shallow but had a decent flow to it. The concrete guardrail that appeared to be constructed monolithically with the slab showed some spalling on the edges. The bridge was scheduled for replacement in the summer of 2003 and was considered ideal for the research study even though plans did not exist. The bridge was considered representative of structurally deficient bridges in the age group and of the type needed for the research study.   Based on the criteria developed candidate bridge 3, P-53-702, was selected for the strengthening study.

Preliminary Investigations of bridge P-53-702

Following the selection of the bridge, a detailed investigation was required to determine the properties of the constituent materials. The bridge was owned by the City of Edgerton and was maintained by the county's maintenance department. Since the owner of the bridge was other than the Wisconsin Department of Transportation, an owner approval was required prior to any investigations on the bridge could be conducted. The city officials raised concerns regarding the project, including responsibilities for additional costs and liability. The main items of concern of the City of Edgerton were the following:

- *Liability:*
  The insurance and liability for the personnel and equipment to be used in conducting the research on the bridge, including the research team from the UW.

- *Financial Responsibilities:*
  Additional costs incurred during the research project for traffic control and detour.

- *Logistics*
  The loading techniques and traffic control during the testing of the bridge.

- *Environmental Considerations:*
  Coordination with the Department of Natural Resources (DNR) on the impact on the surrounding flora and fauna needed to be considered. A purple parsnip plant, a particularly rare species, and the trout in the creek were items of concern.

- *Schedule:*
  The time frame for the installation and load testing of the bridge needed to avoid the activities scheduled in the park next to the bridge. In addition, the strengthening work had to be conducted in the DNR "construction window" from June to August to prevent damage to the creek and the adjacent watershed.

On August 5, 2002, a motion to conduct research on the bridge was brought before the Common Council of the City of Edgerton. The UW research team presented details of the project to the City Common Council. An agreement was reached between the City of Edgerton and WisDOT relieving the City of any liability and financial responsibilities related to the research. The City Council was impressed with the intended purpose of the research as it has difficulty finding funds for replacement of deteriorating bridges. After the concerns of the city were addressed by the UW and the WisDOT, unanimous approval for the research study to be conducted on the bridge was given by the Common Council.

Investigations were conducted on the ±70-year old bridge. The Bridge Inspection Report and the Load Rating Sheets of the bridge were obtained from the WisDOT maintenance department. Key information on the bridge was reviewed. Appendix A provides the Bridge Inspection Report and Load Rating Sheet for P-53-702. The main properties of the bridge as per the inspection report are listed in Table 4.1.

Table 4.1. Key Properties of Bridge P-53-702						
Span (ft)	Width (ft)	Inventory Rating	Operating Rating	Sufficiency Rating	Rate Score	Comments
23	25.9	HS 17.6	HS 29.3	32.7	64	Deep deterioration of the concrete slab. Recommended for replacement or other (action)

The Average Daily Traffic (ADT) for the bridge in 1980 was recorded at 600. The last inspection conducted on the bridge in January of 2001 recommended a re-rating of the bridge for its capacity. Other comments noted on the inspection report were "deep deterioration of the deck edges and cracks" and "spalls about the abutments at the corners." Over the years a 3 -5 in. bituminous overlay was placed on the bridge, however no record of when this was done was found. Figure 4.6 and Figure 4.7 show more details of the selected bridge.

Figure 4.6. Depth of Creek under Bridge P-53-702

<div align="center">(a)   (b)</div>
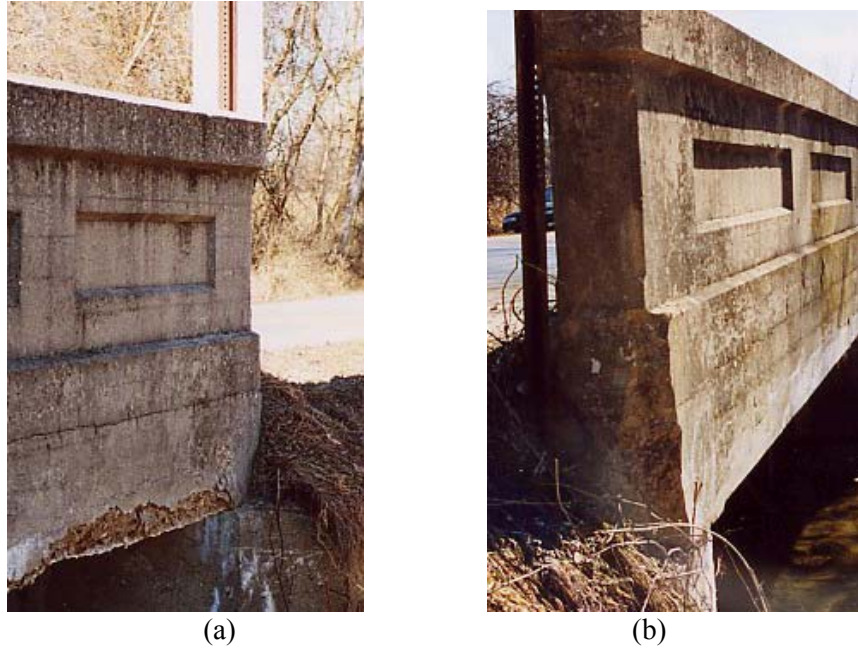
Figure 4.7. (a). Deterioration seen at one edge of the bridge (b). Barrier deterioration

Table 4.2 provides the measured properties of the bridge elements.

Table 4.2. Measured Properties of Bridge P-53-702								
Total Length	Span	Clear Span	Width	Abutment Width	h (Mid-span) est.	h (Edge)	d (Mid-span) est.	d (Edge)
(ft)	(ft)	(ft)	(ft)	(in)	(in)	(in)	(in)	(in)
24	22.75	21.33	26	16	20	28	18	26

The details of the bridge deck reinforcement and material properties were unknown due to the unavailability of the bridge plans. A historical search for plans of similar bridges built during the same time period was undertaken. Relevant literature was reviewed along with information obtained from the DOT on the load rating of the bridge. These were used to estimate the existing properties of the bridge. To determine the steel reinforcement in the selected bridge, a bridge plan for a 23 ft bridge built in 1940 was studied. In addition, properties for a 20 ft bridge built in 1956 as detailed in the revision of "Standard Plans for Highway Bridge Structures" by U.S. Department of Commerce, Bureau of Public Roads (USDC, 1956) was also studied. A design for a new flat slab bridge in accordance with the latest AASHTO LRFD specifications (AASHTO, 1998) was also conducted. Table 4.3 lists the comparison of reinforcement details obtained from the historical research and analysis of the existing bridge.

Table 4.3. Comparison of Reinforcement Properties for Bridges								
Type	Span	Width	Depth	Bar Size	Spacing	Area per ft.	Yield Strength	Shear Reinforcement
	(ft)	(ft)	(in)	(#)	(in)	(in^2)	(ksi)	
1930[*](In-Situ)	23	25.9	18.5	1 in. sq. bar	6	2.0	33[**]	Bent long. bars 4 ft from each support
1940 Standard Plan	23	28.0	18	7	4	1.8	33[**]	Bent long. bars 4 ft from each support
1956 Standard Plan	20	24	10.5	8	8.5	1.6	33[**]	Bent long. bars 4-5 ft from each support
1998 LRFD Bridge Design	23	26	24	7	4.5	1.6	60	NA[***]
[*] Selected bridge P-53-702 from Inspection Report								
[**] Expected considering the time period.								
[***] Not required if designed in accordance with AASHTO LRFD 4.6.2.3 (1998)								

Based on the above the existing steel reinforcement for the selected bridge was assumed to be 1 in. square bars at 6 in. o.c., which provided an area of 2 in^2 per foot of the bridge deck. These assumptions were correlated with visual field inspection. The location of a number of visible corroded square rebars was noted and this confirmed the assumed reinforcement details. The location of a bent longitudinal bar near the support for shear resistance was seen on the edge of the bridge that was deteriorated.

The strength properties of the concrete and the reinforcing steel were determined based on the recommendations provided by AASHTO in the *Manual For Condition Evaluation of Existing Bridges* (AASHTO, 2000.) Ultimate strength of concrete is based on the year of original construction of the bridge and shown in Table 4.4.

Table 4.4. Ultimate Strength of Concrete (AASHTO, 2000)	
Year Built	f'_c (psi)
Prior to 1959	2,500
After 1959	3,000

The research team intended to extract cores from the bridge deck to experimentally determine the concrete strength, however, this was not possible. The research team decided to evaluate the existing capacity using concrete properties of the bridge as defined in the standard procedure by AASHTO (AASHTO, 2000). Table 4.5 lists the allowable unit stresses in tension for reinforcing steel as specified by AASHTO (2000).

16

Table 4.5. Yield Strength of Steel in Tension (AASHTO, 2000)	
Type	Yield Strength (psi)
Structural or unknown grade prior to 1954	33,000
Grade 40 billet, intermediate, or unknown grade (after 1954)	40,000
Grade 50 rail or hard	50,000
Grade 60	60,000

In addition to longitudinal tension reinforcement, field inspections showed evidence of relatively small reinforcing steel bars in the transverse direction of the bridge.   It was also believed that some reinforcement near the top surface of the concrete deck was present. Figure 4.8 and Figure 4.9 show assumed sections of the bridge.
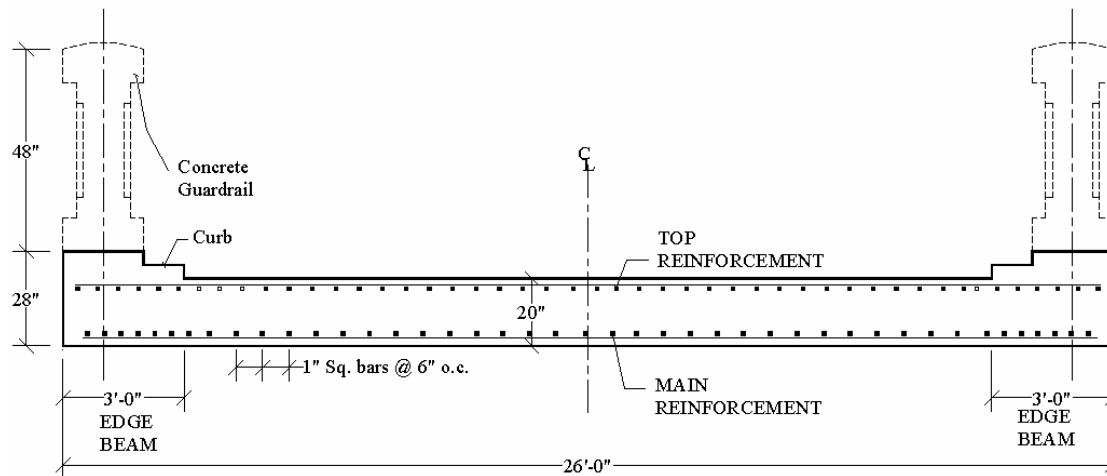
Figure 4.8. Transverse bridge section with main reinforcement running parallel to traffic
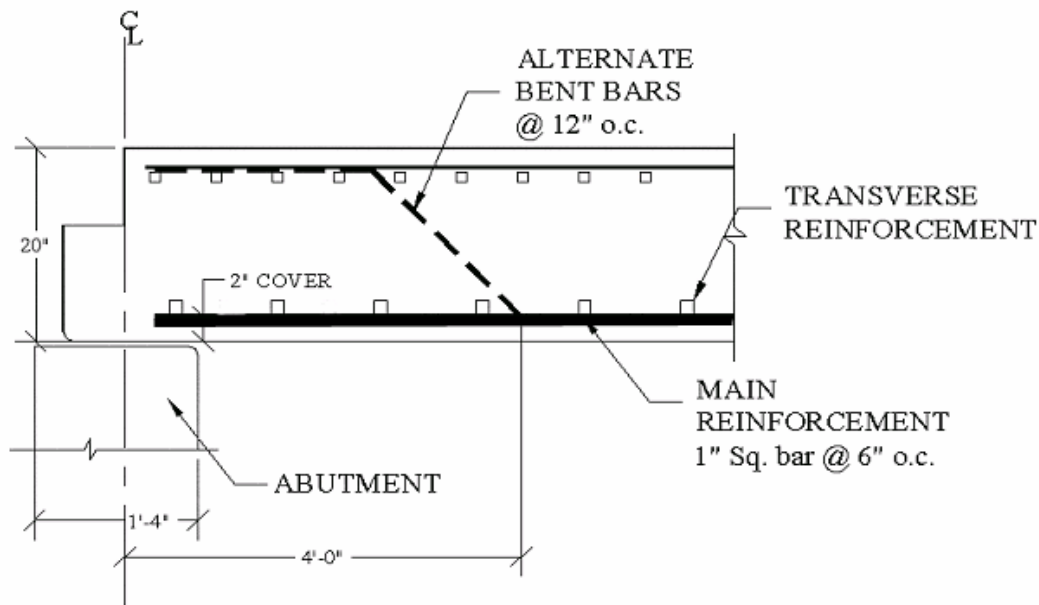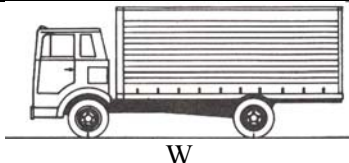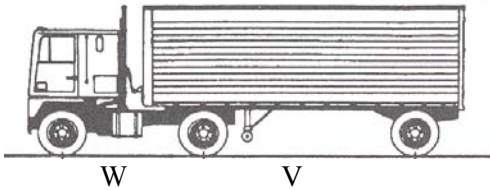
Figure 4.9. Bridge section at abutment with alternating bent bars for shear

Investigation of Design Loads on Bridges

A highway bridge must be designed for the vehicular live loads as they move across the span. The loads produced by standard trucks specified by AASHTO are used to analyze bridge structures for vehicular live loads. Since the 1930s AASHTO has specified the standard truck weights and configurations for bridge design. Since then truck loadings have evolved to better represent the increased weight of trucks. Table 4.6 shows the configurations of standard trucks specified by AASHTO (1996).

Table 4.6. Standard Truck Configurations and Weights as Specified by AASHTO (AASHTO, 1996)					
Type	Front Axle (k)	Rear Axle1 (k)	Rear Axle 2 (k)	Weight (Tons)	Description
H15-44	6	24	-	15	
H20-44	8	32	-	20	
HS15-44	6	24	24	27	
HS20-44	8	32	32	36	
HS25-44[*]	10	40	40	45	
Note: W = 14ft, V = varies between 14ft and 30 ft. [*]Denotes anticipated in future codes.					

While the H class loadings were used in the early 1930s, heavier and larger HS class trucks have since replaced the lighter and smaller trucks. According to the latest AASHTO specifications, the HS20-44 standard truck must be used to design all highway bridges. Furthermore, trends show a further increase of 25% in the weight of standard trucks indicating a standard HS25 truck may be used for design in the upcoming years.

Load envelopes corresponding to the axle loads of standard trucks as they move along the length of the span are used to analyze the maximum load effects on a bridge structure. The bridge for the project was built in 1930 and was originally designed for an H15 standard truck loading. The moment envelopes for the different types of truck loadings on the bridge are shown in Figure 4.10. A significant increase in the demand for the bridge from the original H15 load to the current demands is noted. The increased live load moment demand for the existing bridge for different standard trucks specified by AASHTO is provided in Table 4.7.
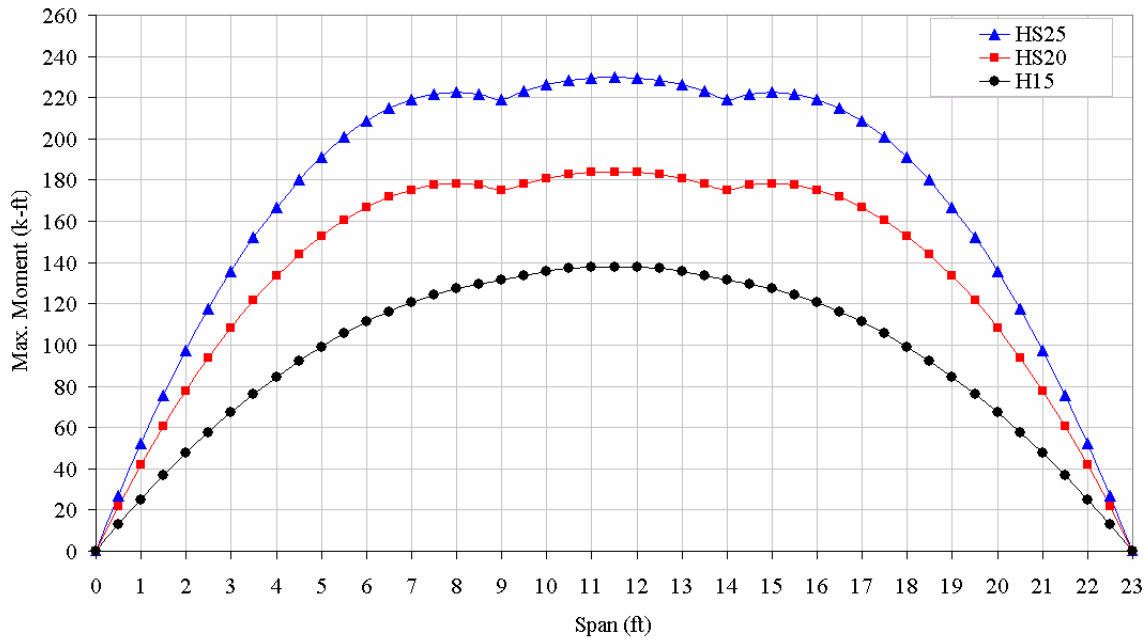
Figure 4.10. Moment envelope for the 23ft span bridge P-53-702

Table 4.7. Increase in moment for the bridge for current truck loads		
Type	Maximum Moment (Live Load)	Increase
	(k-ft)	%
H15-44	138	-
HS20-44	184	33.33
HS25-44*	230	66.67
*Denotes anticipated in future codes.		

Review of Bridge Inspection and Rating Procedures

The Federal Highway Administration (FHWA) U.S. Department of Transportation, National Bridge Inspection Standard (NBIS) establishes the requirements for the inspection and maintenance of bridges located on or over all public roads. The NBIS further establishes the requirements for inspection procedures, frequency of inspections, load ratings, qualifications of personnel, inspection reports, and preparation and maintenance of bridge inventory records (AASHTO, 2000). The NBIS standard uses the *Recording and Coding Guide for the Structure Inventory and Appraisal of Nation's Bridges* (FHWA, 2000) to record and code the structural and non-structural elements of a bridge. The *Manual for Condition Evaluation of Existing Bridges* (AASHTO, 2000) and the *Bridge Inspector's Training Manual/90*, supplement the Guide. These manuals are used by federal, state, and local agencies as the basis for Highway Bridge Replacement and Rehabilitation Programs (HBRRP) and recordings in the National

Bridge Inventory (NBI) Database. This National Bridge Inventory Database is used to evaluate and make recommendations for the nation's infrastructure.

The Wisconsin Department of Transportation (WisDOT) has established its own set of guidelines for the inspection of bridges in the State of Wisconsin. These guidelines use the *Pontis Bridge Inspection Program* for bridge inspections. The *Pontis Manual* specifies numerical values for the condition state information and actions for the various elements of the bridge. These values are used in the bridge inspection report and are used to evaluate the overall condition of the bridge. While these values are different from those used in the federal guidelines, a direct conversion can be made to the NBI ratings by the bridge inspector. The Inspection report in Appendix A for bridge P-53-702 also shows the NBI ratings.

These recordings are used to determine three major criteria or "ratings" of the bridge. These ratings are numerical values that are recorded to indicate the existing condition, strength and serviceability of the structure and are further used to determine maintenance and replacement schedules for the bridge. The three types of ratings are:

1. Condition Rating (CR)
2. Load Rating (LR)
3. Sufficiency Rating (SR)

These ratings are further subdivided into various categories that describe in detail the properties of a particular bridge. Details of each rating are described in the following sections.

Condition Rating (CR)

The condition rating of a bridge is defined as "the results of the determination of the functional capability and the physical condition of bridge components including the extent of deterioration and other effects" (AASHTO, 2000).

The observations made during the inspection of the bridge are interpreted numerically in the inspection report by assigning an environment for the physical condition of the bridge component. These environments are assigned such that they allow different values (or limit states) of deterioration for each element. The limit states have a high value to signify severe deterioration and a low value to signify minimal deterioration. For example, the concrete deck of a bridge may have a condition state of 5 representing "area of distress" (potholes etc.) > 25% of the deck area, or a condition state of 1 to represent an area of distress < 2%. The condition ratings of bridge components are provided in the inspection report.

Load Rating (LR)

According to the AASHTO specification, the *Manual for Condition Evaluation of Bridges* (AASHTO, 2000), load rating is defined as, "the determination of the live load carrying capacity of an existing bridge using existing bridge plans supplemented by information gathered from a field inspection." Bridge load ratings are a basis for determining the safety and serviceability of a bridge under usage. They are reviewed periodically and updated to reflect any

changes in the condition of the bridge. The ratings are required under federal regulations to be maintained in conjunction with inspection reports. The load ratings are used to monitor and manage the load posting, rehabilitation and replacement schedules of bridges.

The load rating is a calculated numerical value that defines the safe load carrying capacity of a bridge. Load ratings are calculated at different levels of usage. On occasions a bridge may be used to carry special vehicles and the load rating for such atypical loadings may be considered as well. Primarily, levels of rating provide an effective means of determining limitations on the bridge under service and ultimate conditions. The two levels of load rating suggested by AASHTO are *Inventory Level* and *Operating Level*. The two rating levels are described below.

Inventory Rating (IR)

The Inventory Rating corresponds to the customary design level of stresses but reflects the existing bridge and material conditions with regard to deterioration and loss of section. Load ratings based on the Inventory level allow comparisons with the capacity for new structures and, therefore, results in a live load, which can safely be used on an existing structure for an indefinite period of time (AASHTO, 2000).

Operating Rating (OR)

The maximum permissible live load, to which a bridge structure may be subjected to, corresponds to the Operating Rating of the bridge. This maximum load is generally associated with special occasions and may shorten the life of the bridge if used consistently (AASHTO, 2000).

These rating levels may be calculated using the *Allowable Stress* method (AS), *Load Factor* method (LF) or the *Load and Resistance Factor Rating* method (LRFR) to evaluate the capacity of the bridge members. The *Allowable Stress* (AS) method or working stress method is a traditional method used to calculate the structural capacity of a member under actual loadings, which are combined to produce maximum stresses in a member (AASHTO, 2000). These limiting stresses are based on the safety and reliability of the material under service conditions. The *Load Factor* (LF) method is based on factored loads, which are multiples of the actual loads experienced by the candidate structure. These factors reflect the effects of different types of loads and are used to ensure the strength of the member is maintained under uncertain loading conditions (AASHTO, 2000).

Load ratings are calculated for each of the elements of the structure and the member with the lowest rating controls the bridge rating. The following general equation is used in evaluating the load rating of a candidate structure based on the Allowable Stress Design (ASD) method or the Load Factor Design (LFD) method.

$$RF = \frac{C - A_1 D}{A_2 L(1 + I)}$$ 	 Equation 6-1a (AASHTO, 2000)

$$RT = (RF) \times W$$ 	 Equation 6-1b (AASHTO, 2000)

where,

RF: Rating Factor for the live-load carrying capacity. The rating factor multiplied by the rating vehicle in tons gives the rating of the structure.
C: Capacity of the member based on Allowable Stress Design or Load Factor Design.
D: Dead Load effect on the member
L: Live Load effect on the member
I: Impact Factor to be used with Live Load to amplify static loading to dynamic loading
A_1: Factor for Dead Load
A_2: Factor for Live Load
RT: Bridge Rating and;
W: Weight of Rating Truck.

In the above expression, the "load effect" is the effect of the applied loads on the element and is typically axial force, vertical shear force, bending moment, axial stress, shear stress and bending stress (AASHTO, 2000). Based on current load requirements specified by AASHTO for an HS20 truck an *RT < 20* or *RF < 0.56* represents an under-capacity bridge.

Sufficiency Rating (SR)

The sufficiency rating of a bridge is indicative of its sufficiency to remain in service and is calculated to determine the strength and serviceability of the bridge. The sufficiency rating of a bridge is based on the condition ratings of the bridge components and the load ratings as explained above. The Sufficiency Rating (SR) is a calculated numerical value that defines the usage of the bridge based on four factors each of which corresponds to the strength and serviceability of the bridge (FHWA, 2000). These four factors are:

1) The Structural Adequacy and Safety (S_1)
2) Serviceability and Functional Obsolescence (S_2)
3) Essentiality for Public Use (S_3) and
4) Special Reductions (S_4)

The result of numerical calculations of the four factors as a percentage are then combined using the following equation:

$$SR = S_1 + S_2 + S_3 - S_4 \qquad \text{Equation A-1 (FHWA, 2000)}$$

where,

$$0\% < SR \leq 100\%$$

The equation above yields a percentage value in which a 100 percent would represent an entirely sufficient bridge and zero percent would represent an entirely insufficient or deficient bridge (FHWA, 2000). The sufficiency rating is used to implement the maintenance, scheduling, and planning of rehabilitation of existing bridges. According to FHWA regulations the following measures are appropriate based on the SR.

$SR \leq 80\%$ Bridge qualifies for rehabilitation techniques;

$SR \leq 50\%$ Bridge qualifies for Federal funds for replacement.

Analysis and Rating Calculations for Bridge P-53-702

Following the selection and investigation of the bridge for demonstration of the MF-FRP system to strengthen existing bridges for increased flexural strength, the next part of the project was to investigate the existing flexural capacity of the bridge and to calculate its load rating.

Condition Rating for P-53-702

The Inspection Report for bridge P-53-702 provided the Condition Rating (CR) of various bridge components reflecting their level of deteriorated physical condition. Table 4.8 shows the Condition Ratings for the bridge elements. It should be noted here that a rating of "4" for *Poor Condition* is similar to a rating of "3" for *Serious Condition* except for the absence of fatigue cracks in steel rebar or shear cracks in concrete and can be improved upon if improvements in strength are shown.

Table 4.8. Condition Rating for Key Components for Bridge P-53-702		
Component	Condition Rating (NBI)	Description
Concrete Slab	3	*Serious Condition*: loss of section, deterioration, spalling or scour, have seriously affected primary structural components. Local failures are possible. Fatigue cracks in steel or shear cracks in concrete may be present.
Superstructure	3	
Substructure	5	*Fair Condition*: all primary structural elements are sound but may have minor section loss, cracking, spalling or scour.

The effects of fatigue in the reinforcing steel can be reduced if the stresses in the steel are reduced. The addition of FRP strips on the bridge soffit will decrease the stresses in the steel. Since the condition rating influences the Sufficiency Rating (SR) (inherent in factors S_1, S_2, and S_3) of the bridge the potential improvement in the SR was calculated for the proposed retrofit in what follows.

Load Rating for P-53-702

According to available records the load ratings for the bridge were last conducted in 1979. The rating calculations are shown in Appendix A. Due to the uncertainty over the rating procedures adopted for load ratings in 1979, it was not possible to determine the exact methodology used at the time. Furthermore, current practice is to use the Load Factor method of rating for all bridges except for prestressed girders and must be used to re-rate all bridges (WBM, 1994).

The load rating of the existing bridge was conducted using the load rating equation given by AASHTO (AASHTO, 2000). The procedure to calculate the Inventory (IR) and Operating Load Rating (OR) levels essentially represents the calculation of the capacity of the bridge in the service and ultimate conditions. The rating procedure requires the placement of the rating truck at critical locations on the bridge span that will create the maximum load effects. The location of the critical sections are found from envelopes as the live loads are moved across the bridge span as discussed previously. The calculated load effects (for example dead and live load moments) are then distributed to the bridge elements, which are subsequently analyzed for their existing capacity.

Table 4.9 shows the calculated Rating Factors for the bridge for its existing capacity and for an increased rating factor for HS20 and HS25. The calculations for the bridge Load Ratings and the improved Inventory ratings of HS20 and HS25 are provided in the following sections.

Table 4.9. Rating Factors for Bridge P-53-702			
Level	Existing	Future	
	HS17	HS20	HS25
Inventory	0.49	0.56	0.69

Sufficiency Rating for P-53-702

The Sufficiency Rating for the bridge P-53-702 provided by the WisDOT was 32.7%, which qualifies it for replacement with Federal funds. Calculations based on the FHWA criteria result in a SR of 36.83% (see Arora, 2003 for details). The difference between the calculated and the reported value is small and is attributed to the lack of accurate information on some non-structural conditions of the bridge. The effect of increasing the Inventory Rating from HS17 to HS25 on the Sufficiency Rating was calculated for a variety of scenarios. Table 4.10 shows a summary of SR rating levels for the bridge for these scenarios. It can be seen that if the Inventory rating of the bridge is improved from HS17 to HS25, the Sufficiency Rating of the bridge may also be improved. However, increasing the load rating alone will not improve the sufficiency rating that significantly. If, however, in addition to improving the load rating, repairs are carried out together with the strengthening to improve the deck condition rating, the bridge life may be improved beyond the 50% mark that qualifies it for replacement.

Table 4.10. Summary and Comparison of Ratings

#	Scenario	Sufficiency Rating	
		Calculated	Reported*
0	Existing bridge	36.83 %	32.70 %
1	Increase Inventory Rating (HS17 to HS25)	40.45 %	36.30 %
2	Increase Inventory Rating (HS17 to HS25) + Increase NBI Condition Rating of Item # 59 (Superstructure) from 3 to 4**	52.65 %	51.60 %
3	Increase Inventory Rating (HS17 to HS25) + Increase NBI Condition Rating of Item # 59 (Superstructure) from 3 to 4** + Increase NBI Condition Rating of Item # 58 (Deck) from 3 to 4***	54.67 %	53.70 %
4	Increase Inventory Rating (HS17 to HS25) + Increase NBI Condition Rating of Item # 58 (Deck) from 3 to 4***	42.49 %	38.40 %
* As provided by WisDOT ** Superstructure: Serious to Poor *** Deck: Serious to Poor			

Capacity of Existing Bridge P-53-702

The existing capacity "C" of the bridge was calculated using the analytical model specified by AASHTO (2000). For a concrete flat slab subjected to live load effects on a unit width, the flexural capacity of the bridge is calculated using strain compatibility, internal force equilibrium and the constitutive relationships of the materials. The Whitney stress-strain model for concrete is used, while an elastic-perfectly plastic model for steel reinforcement in tension is used. The strength properties for the constituent materials as specified by AASHTO (2000) were used to calculate the exiting flexural capacity of the bridge. The capacity of a unit (12 in.) slab section for the bridge was calculated using the properties in Table 4.11.

Table 4.11. Section Properties Used to Calculate the Existing Capacity of Bridge P-53-702

Width	Depth	Area of Steel	Depth to Tension reinforcement	Concrete Strength	Yield Strength
b	h	A_s	d_s	f'_c	f_y
(in)	(in)	(in^2)	(in)	(psi)	(psi)
12	20	2*	18.5	2,500	33,000
* For 1 in. square bar @ 6 in. o.c.					

Figure 4.11 shows the stress-strain distribution and the internal force equilibrium for a unit section of the existing slab. Note that the contribution of the compression steel is ignored.
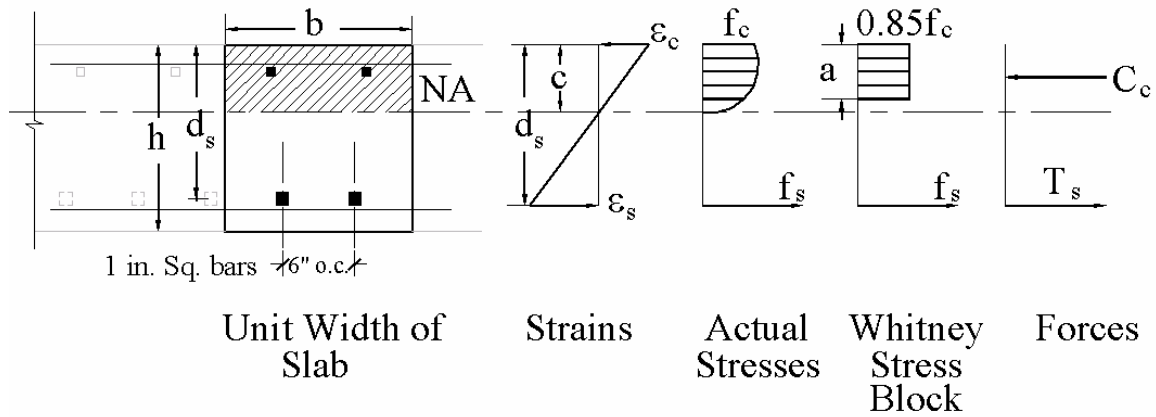
Figure 4.11. Internal force distribution for calculating capacity of existing slab

The nominal moment capacity of the unit section of the existing slab was determined from,

$$M_n = A_s f_y \left(d_s - \frac{a}{2} \right)$$

where,

$$a = \frac{A_s f_y}{0.85 f_c' cb}$$

The ultimate capacity of the slab is calculated with a strength reduction factor $\phi = 0.9$ for flexure as,

$$C = M_u = \phi M_n$$

Table 4.12 gives the calculated nominal and ultimate capacities of the bridge section.

Table 4.12. Predicted Nominal and Ultimate Capacities for Bridge P-53-702			
Nominal Capacity M_n		Ultimate Capacity M_u	
(k-in/ft)	(k-ft/ft)	(k-in/ft)	(k-ft/ft)
1135.5	94.6	1022	85.2

Dead Load on Existing Bridge P-53-702

The Dead Load (DL) moment for a unit (12 in.) width of the bridge was calculated using the unit weight of concrete and a 3" overlay to be 18.9 k-ft/ft (Arora, 2003).

27

Live Load Distribution for Bridge P-53-702

The AASHTO load rating equation can be modified to calculate the ratings based on the flexural demand of the bridge. The rating factor for the flexural rating of a bridge can be written in terms of the effective width (E) as,

$$RF = \frac{C - A_1 M_{DL}}{A_2 \dfrac{M_{LLHS20}}{E}(1+I)}$$

where the rating of the bridge is given as,

$$RT = (RF) \times W$$

and,

M_{DL}:	Dead Load Moments
M_{LLHS20}:	Live Load Moments for HS20 (184 k-ft)
E:	Effective width used to distribute the live load moment (ft)
C, I, A_1,A_2:	as before.

The AASHTO specifications (AASHTO, 1996; AASHTO LRFD, 1998) and the Wisconsin Bridge Manual (WBM, 1994) suggest the use of "effective strip" models to determine the live load distribution. AASHTO LRFD (1998) defines the effective strip (*E*) as "the artificial linear element, isolated from the deck for the purpose of analysis, in which extreme force effects calculated for a line of wheel loads, transverse or longitudinal, will approximate those actually taking place in the deck." The effective strip (*E*) is essentially the equivalent rectangular width of uniform stress that represents the non-linear stress distribution of the live load on the entire lane. Table 4.13 lists the different effective strip widths calculated using different specifications.

Table 4.13. Equivalent Strip Width Calculation for Bridge P-53-702		
AASHTO 1998 One Lane[*]	$E_1 = 10in + 5\dfrac{in}{ft}\sqrt{(S \times W)} < 7ft$	$\dfrac{E_1}{2} = 5.0\,ft$
AASHTO 1998 Two Lanes[*]	$E_2 = 84in + 1.44\dfrac{in}{ft}\sqrt{(S \times W)} \le \dfrac{12.0W}{N_L}$	$\dfrac{E_2}{2} = 4.9\,ft < 6ft$
AASHTO Standard Spec. 1996	$E_3 = (4\,ft + 0.06 \times S)$	$E_3 = 5.38\,ft < 7ft$
Wisconsin Bridge Manual	$E_4 = (4\,ft + 0.06 \times S) < 7ft$	$E_4 = 5.38\,ft < 7ft$
[*] Denotes per Axle and are therefore divided by 2 to obtain per wheel line.		

28

The effective width was also back calculated based on the given WisDOT inspection report rating of HS 17.6 as follows,

$$E_5 = \frac{RFA_2 M_{LLHS20}(1+I)}{C - A_1 M_{DL}}$$

For M_{LLHS20} = 184 k-ft, M_{DL} = 18.9 k-ft/ft, RF = 0.49, C = 85.2 k-ft/ft, I = 0.3, A_1= 1.3, A_2 = 2.17 gives,

$$E_5 = 4.2 \text{ ft}$$

To maintain consistency with the existing rating (i.e., HS 17.6) the effective width distribution factor (E) calculated using the original ratings was used in further calculations to design the strengthening system. It should be noted here that this value is not the same as any of those shown in Table 4.13. However, it is within the same range as those in Table 4.13 and was felt to be the most appropriate value for use in the strengthening design. Table 4.14 provides the uniform live load effects calculated for various trucks using this equivalent width.

Table 4.14. Live Load Moments per Foot Width of Slab for P-53-702				
Type	Maximum Live Load Moment	Distribution Factor (E)	Maximum Unit Live Load Moment	Diff
	(k-ft)	(ft)	(k-ft/ft)	%
H15-44	138	4.2	32.9	-
HS20-44	184	4.2	43.8	33.1
HS25-44*	230	4.2	54.8	66.6
*Denotes anticipated in future codes.				

The maximum live load moments per unit width are then factored and combined with the dead load moments per unit width to calculate the moment capacity required for HS20 and HS25 trucks. As discussed previously, the Load Factor (LF) method has been adopted to evaluate the Inventory rating of the bridge. The safety factors as used in the rating calculations are used here. Table 4.15 provides the summary of the design moments required per unit width of the slab for various standard trucks and compares them with the design moments used originally to design the bridge based on standard H15 truck.

Table 4.15. Design Moments per unit Width of Slab for Bridge P-53-702						
Type	LL Moment (M_{LL})	DL Moment (M_{DL})	Load Factor Design (LFD) Moments **	Diff. From H15	Allowable Stress Design (ASD) Moments ***	Diff. From H15
	(k-ft/ft)	(k-ft/ft)	(k-ft/ft)	%	(k-ft/ft)	%
H15-44	32.9	18.9	117.4	-	61.7	-
HS20-44	43.8	18.9	148.1	26.1	75.9	23.0
HS25-44*	54.8	18.9	179.2	52.6	90.2	46.2
* Denotes anticipated in future codes						
** Using a Dead Load Factor of 1.3 and Live Load Factor of 2.17 plus Impact = 0.3						
*** Using a Dead Load Factor of 1.0 and Live Load Factor of 1.0 plus Impact = 0.3						

Note that the calculated design moment using the Load Factor method for the H15 truck loading may not be the moment used originally to design the bridge in 1930. The ASD design methodology was probably used. This may reduce the actual design moment for the bridge. In such a case the design factors A_1 and A_2 may more likely to be 1.0 each. Therefore, 61.7 k-ft/ft is most probably the original design moment value for the bridge. Table 4.16 provides a comparison between the required design moment (per unit width) from Table 4.15 and the nominal capacity of the unit width of the bridge for the LFD method.

Table 4.16: Comparison of Design Moments with Existing Capacity of P-53-702				
Type	Ultimate Design Moments (M_u)	Nominal Design Moments (M_n)	Existing Nominal Capacity	Diff. From H15
	(k-ft/ft)	(k-ft/ft)	(k-ft/ft)	%
H15	117.4 (61.7)[**]	105.7 (61.7)[**]		--
HS20-44	148.1	133.3	94.6	40.1
HS25-44[*]	179.2	161.3		70.5
[*] Denotes anticipated in future codes				
[**] Denotes for ASD method				

A significant increase in the nominal moment is seen to be needed to increase the capacity of the existing bridge. Figure 4.12 graphically shows an approximate behavior of the existing unit width of the bridge slab using a Moment-Curvature model, which includes strain hardening of tension steel and a non-linear stress-strain distribution for concrete (Lamanna, 2002). The existing nominal capacity is compared with limits of required nominal design capacity for various standard trucks given in the above table.
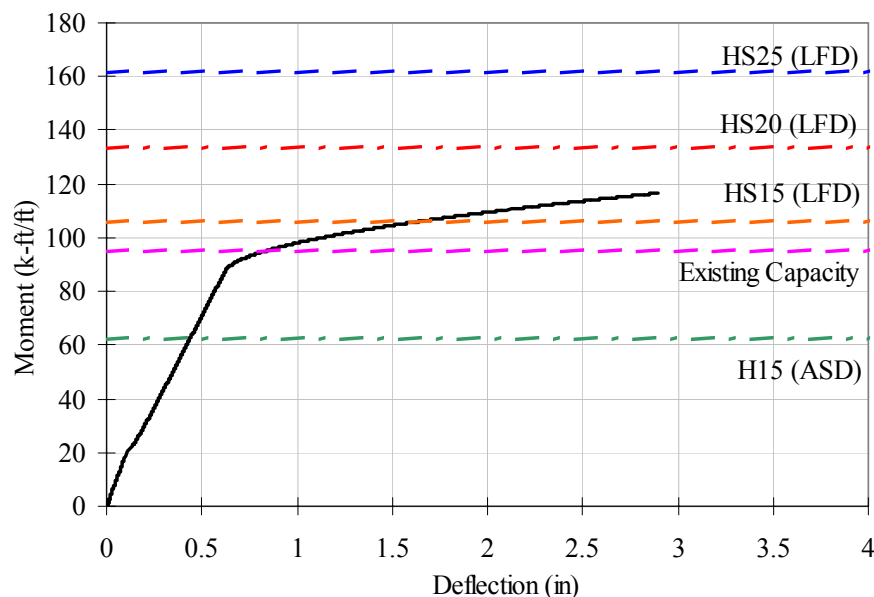
Figure 4.12. Comparison of flexural capacity of the bridge with required moments for different trucks

Strengthening Required for Increased Rating

To increase the Load Rating of the selected flat slab bridge from HS17 to HS25, the analytical model used to determine the existing capacity of the slab was modified to design the strengthening system. The methodology used to calculate the existing Inventory Rating for the bridge using Equation AASHTO equations (AASHTO, 2000) was modified to calculate the increased flexural capacity of the bridge slab from the Inventory Rating of HS17 to HS25. The required Rating Factor (RF) for the increased ratings is calculated as follows,

$$RF_{REQ} = \frac{RT_{REQ}}{W_{HS\,20}}$$

and the required capacity "C" of the section for the required Rating Factor was then calculated from,

$$C = RF_{REQ}\left(A_2 M_{LL}\left(1+I\right)\right) + A_1 M_{DL}$$

where,

$C = M_u$ = Required Ultimate Capacity of the section and M_{DL}, M_{LL}, I, A_1, A_2 as before for LFD method.

The required nominal capacity was then calculated as,

$$M_{n,REQ} = \frac{C}{\phi}$$

Results of the calculations are given in Table 4.17. It can be seen that a 29% increase in the existing capacity of the unit width of the bridge is required to increase the Inventory rating of the bridge from HS17 to HS25.

Table 4.17: Summary of Required Moment Capacity for Increase in the Rating Level for Bridge P-53-702					
Rating Level	Existing Rating (Rating Factor)	Improved Rating (Rating Factor)	Existing Nominal Capacity (k-ft/ft)	Required Nominal Capacity (k-ft/ft)	Increase in Capacity (%)
Inventory	HS 17.6 (0.49)	HS 20 (0.56)		104.3	10.2
		HS 25 (0.69)	94.6	122.1	29.0
Operating	HS 29.3 (0.81)	HS 33 (0.93)		104.3	10.2
		HS 41 (1.15)		122.1	29.0

Design of the MF-FRP Strengthening System

Preliminary analytical investigations were required to estimate the number of FRP strips and fasteners for the existing bridge slab corresponding to the increase in the Inventory Rating from HS17 to HS25. The objectives of this task were:

- To conduct a preliminary design for the strengthening of the existing bridge slab for the required flexural capacity using existing models for the MF-FRP system.

- To conduct parametric studies to account for varying properties that may exist in the existing bridge and to assess their influence on the design.

- To find the optimal configuration to produce the increase in capacity with a desirable failure mode.

- To finalize the MF-FRP system design of the bridge based on the parametric studies.

In previous research, an analytical Moment-Curvature (M-C) model was developed to predict the flexural behavior and ultimate capacity of the MF-FRP strengthened section (Lamanna, 2002). This model was used to design the strengthening system for the existing bridge slab. The M-C model is an incremental model that predicts the elastic and post yield behavior of the section and includes tension strain hardening. A Strength Model was also developed using material relationships similar to the M-C model to predict the ultimate strength of the section without the affects of strain hardening. The strength model assumes full composite action between the FRP strip and the concrete section with a non-linear concrete stress-strain model as used in the M-C model. A conventional Whitney Model was used for the unstrengthened section analysis.

As explained previously, the required design nominal moment of 122 k-ft per unit width of the bridge slab, corresponding to an Inventory Rating of HS25 requires a 29% increase in the existing flexural capacity of the bridge slab. These nominal design moments were used to design the strengthening system for the bridge using the MF-FRP system.

The preliminary design was conducted with two reinforcement ratios to determine the number of FRP strips required for the strengthening. The FRP reinforcement ratio is defined as,

$$\rho_{frp} = \frac{A_{frp}}{b \times d_{frp}}$$

where,

ρ_{frp}: FRP Reinforcement Ratio
A_{frp}: Area of FRP Reinforcement
b: Width of Cross section (12 in.)
d_{frp}: Depth of FRP Reinforcement (20.0625 in.)

A unit width of the slab section with one FRP strip (i.e., one FRP strip @ 12" o.c.) with a FRP reinforcement ratio of 0.21% and an FRP reinforcement ratio of 0.12% corresponding to a 20 in. spacing of the FRP strips were considered. Since FRP strips are prefabricated with a cross section 4" x 1/8", the reduced area of FRP reinforcement for a unit width of section is conveniently accommodated by the increased spacing.

Figure 4.13 shows the two design reinforcement ratios used for the preliminary design and the parametric study.
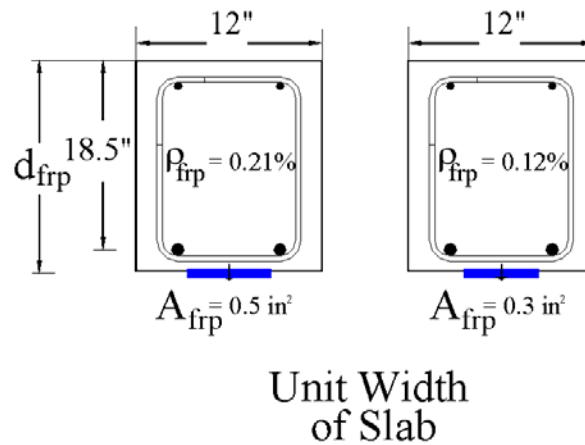
Figure 4.13. Designs for preliminary analysis and parametric studies

Parametric Design Studies

In addition to the FRP reinforcement ratio, concrete strength, tensile reinforcement strength, and the number of fasteners required were varied in the parametric design studies for the MF-FRP system.

Concrete Strength

The actual concrete compressive strength of the section may be different from the 2500 psi assumed for the calculation of the existing capacity of the bridge slab. A number of previous studies suggest that concrete strength for bridges built around the same time may be as high as 8,000 psi. (Shahrooz et al, 1994). Therefore, concrete compressive strengths of 2,500 psi, 4,000 psi, and 6,000 psi were considered in the parametric study.

Yield Strength of Tensile Reinforcement

Yield strength of steel in tension-controlled slab sections may range from 33 ksi for bridges built prior to 1954 to 60 ksi for conventional Grade 60 steel (AASHTO, 2000). Table 4.18 provides a comparison of areas of steel for different yield strengths.

Table 4.18: Comparison of Areas of Steel Reinforcement for Different Yield Strengths		
Original Reinforcement	Yield Strength	12 in Wide Section
	(ksi)	(in^2)
1- 33ksi sq. bar @ 6" o.c. (2in^2 per ft)	33	2
	40	1.65
	60	1.1

The modulus of elasticity of the steel reinforcement was assumed constant at 29 x 10^6 psi for the different steels.

Fastener Spacing

The strength and failure mode associated with the strengthened MF-FRP section is highly dependent on the number of fasteners used to attach the FRP strips. Previous tests conducted on the strength of the connections have limited the amount of shear force per fastener to 1000 lb (Bank et al., 2002a). The force per fastener in the FRP strip is calculated in the Moment – Curvature model and is checked against the 1000 lb limit (Bank et al., 2002a). While an extensive model for the fastener spacing is needed for the effects of moving loads, due to the schedule of the bridge strengthening, a simple analysis for the maximum moment at the most critical location (here the midspan) was considered for the strengthening.

Results of Parametric Studies for Preliminary Design

Table 4.19 and Table 4.20 show the results of the parametric study for the two reinforcement ratios. For the parametric studies the modulus of the strip was taken as 8,900 ksi and the open-hole strength taken as 85.4 ksi based on previous testing (Bank et al., 2002a). The beam span was taken as 23 ft. The analysis was conducted for a beam in 4-point bending with a shear span of 11.3 ft and a constant moment span of 0.3 ft to provide a worst-case scenario (i.e., a "concentrated load" at the midpoint). 44 X-ALH fasters were used in the shear span – a single row at 3 in. on-center spacing. A design load of 1000 lbs per fastener was used. No end anchors were assumed in the modeling.

Table 4.19: Results of Parametric Study for 0.21% FRP Reinforcement Ratio Design							
		Whitney	Strength Model		Moment-Curvature		
Yield Strength	Area	Unstrengthened	Strengthened	Failure Mode	Unstrengthened	Strengthened	Failure Mode
(psi)	(in²)	(k-ft)	(k-ft)		(k-ft)	(k-ft)	
Concrete Strength 2500 psi							
33000	2.0				117.0	165.0	
40000	1.65	94.6	154.8	Conc. Comp.	114.0	164.0	FRP Rupture
60000	1.1				109.0	162.0	
Concrete Strength 4000 psi							
33000	2.0				131.0	172.0	
40000	1.65	97.3	161.4	Conc. Comp.	126.0	170.0	FRP Rupture
60000	1.1				118.0	166.0	
Concrete Strength 6000 psi							
33000	2.0				147.0	175.0	
40000	1.65	98.8	166.4	Conc. Comp.	140.0	173.0	FRP Rupture
60000	1.1				127.0	169.0	
Note: All Calculations used E_{frp} = 8.9 ksi, f_{frp} = 85.4 ksi, 44 fasteners in shear span, Shear Span = 136 in., Span = 276 in. Load per fastener = 1000 lb.							

Table 4.20: Results of Parametric Study for 0.12% FRP Reinforcement Ratio Design							
		Whitney	Strength Model		Moment-Curvature		
Yield Strength	Area	Unstrengthened	Strengthened	Failure Mode	Unstrengthened	Strengthened	Failure Mode
(psi)	(in²)	(k-ft)	(k-ft)		(k-ft)	(k-ft)	
Concrete Strength 2500 psi							
33000	2.0				117.0	142.7	
40000	1.65	94.6	132.0	Conc. Comp.	114.0	140.8	FRP Rupture
60000	1.1				109.0	137.5	
Concrete Strength 4000 psi							
33000	2.0				131.0	147.3	
40000	1.65	97.3	138.0	Conc. Comp.	126.0	145.2	FRP Rupture
60000	1.1				118.0	141.4	
Concrete Strength 6000 psi							
33000	2.0				147.0	149.6	
40000	1.65	98.8	139.2	Conc. Comp.	140.0	147.5	FRP Rupture
60000	1.1				127.0	143.6	
Note: All Calculations used E_{frp} = 8.9 ksi, f_{frp} = 85.4 ksi, 44 fasteners in shear span, Shear Span = 136 in., Span = 276 in. Load per fastener = 1000 lb.							

The results show a small variation in ultimate moment for the strengthened section for the different concrete strengths used. In addition, the yield strength of the steel reinforcement does not affect the ultimate capacity of the section since the area of the steel was scaled so that E_sA_s remained constant. The unstrengthened capacity predicted by the Moment-Curvature model shows considerable change and is attributed to the strain hardening of reinforcing steel. The two models for the strengthened sections, however, predict different failure modes. The Moment-Curvature model predicts FRP rupture as the primary failure mode for all designs, while the strength model predicted concrete compression as the primary failure mode. The reason for the difference is a cause for concern and requires further study, however, the strains in the concrete for the M-C model at FRP rupture were found to be close to concrete compression failure of 0.0038 (more than the typical 0.003 used in the Whitney model).

Final Design for Bridge P-53-702

The strengthening of the bridge P-53-702 with the MF-FRP system for an improved Inventory Rating of HS25 may be achieved with one strip attached every 12" o.c. using 40 fasteners spaced equally at 3 in. o.c. on each side of the midspan and 2 anchor bolts on each end of the FRP strip. Since no material safety factors and strength reduction factors for the preliminary design were used, 12 in. FRP strip spacing would provide strengthening greater than the required 29%. Table 4.21 shows the final design for the bridge.

Table 4.21. Final Design for Bridge P-53-702					
Whitney	Strength Model		Moment-Curvature		
Unstrengthened	Strengthened	Inc.	Unstrengthened	Strengthened	Inc.
(k-ft)	(k-ft)	%	(k-ft)	(k-ft)	%
94.6	154.8	63.6	117.0	165.0	41.0

Figure 4.14 shows the behavior of strengthened unit section of the bridge slab as modeled by the Moment-Curvature model and provides a 41% increase as compared to the unstrengthened section. Note that the unstrengthened section capacity is approximately the same as calculated using the Whitney stress block.
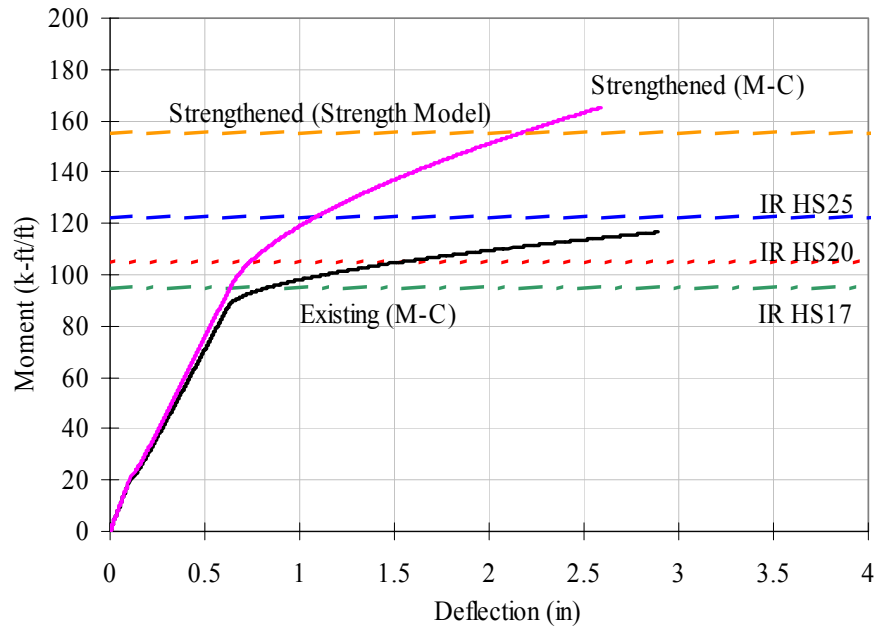
Figure 4.14. Predicted behavior of strengthened unit width of bridge slab

The final design for the MF-FRP system for the bridge is shown in Figure 4.15.
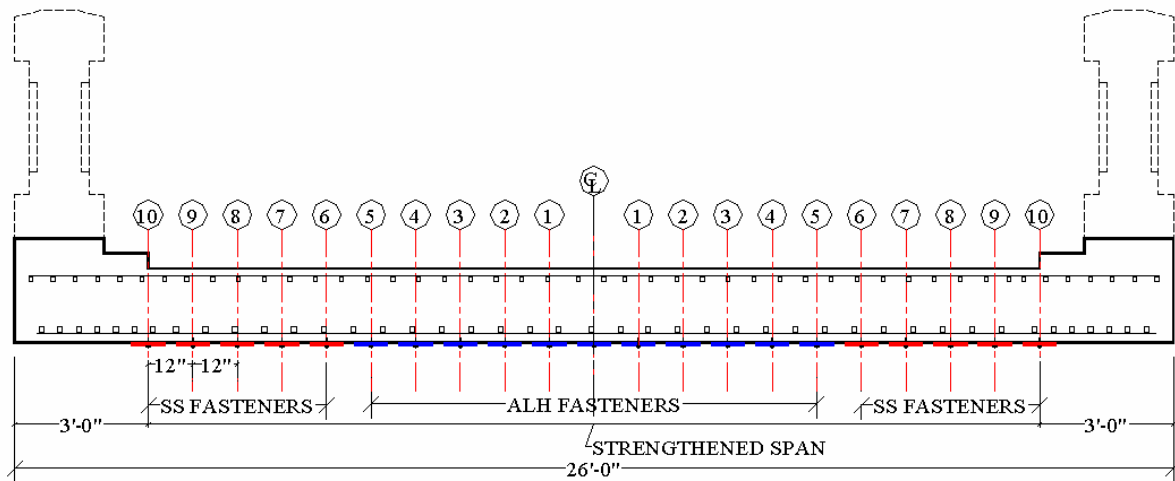
Figure 4.15. Final design layout of the FRP strips on the bridge

A total of 21 strips are required to be attached to the bridge deck. 11 strips were designed to be attached using galvanized steel X-ALH fasteners, and 10 FRP strips using stainless steel X-CR-SS fasteners to observe the environmental effects on the fasteners.

37

Installation of MF-FRP System

A plan for the installation and testing of the bridge was developed to address issues such as site access, material transportation, strengthening procedure, instrumentation and data collection. A schedule of the project was developed to accommodate local DOT personnel, scheduled area activities near the bridge, and the window period provided by the DNR. It was an objective of the research team to conduct the strengthening in a two-week period. Table 4.22 shows the schedule of the 10-day field installation and testing plan.

Table 4.22. Schedule for Field Application and Testing			
Week	Day	Date	Proposed Activity
I	1	8/19/02	Site Access, Setup and Clean up of underside
	2	8/20/02	Mark layout of FRP strips and Instrumentation setup for Service Load Testing
	3	8/21/02	Reserve Day
	4	8/22/02	Service Load Test I (Control)
	5	8/23/02	Demonstration of MF-FRP system and certification for local DOT personnel
II	6	8/26/02	Application of FRP strips
	7	8/27/02	Application of FRP strips
	8	8/28/02	Instrumentation setup for Service Load Testing
	9	8/29/02	Reserve Day
	10	8/30/02	Service Load Test II (Strengthened) and cleanup

For the field application and service load testing of the bridge a plan was devised to distribute the activities between the UW-research team and the WisDOT. Table 4.23 details the distribution of responsibilities between the two teams.

Table 4.23. UW and WisDOT Roles and Responsibilities		
Description	UW Responsibilities	WisDOT Responsibilities
Site Access and Setup	Material for setup and clean up	Personnel to aid UW team
Load Test I	Instrumentation and Setup	Preloaded trucks and personnel for traffic control
Application of MF-FRP	Materials and equipment	Personnel to assist with application
Load Test II	Instrumentation and Setup	Preloaded trucks and personnel for traffic control

The research engineers from UW and the DOT supervised the field installation and load tests. A staff engineer from the US Army Corps of Engineers, Vicksburg, MS, also was on hand to witness the second service load test on the bridge. Table 4.24 shows the DOT man-hours utilized and the tasks completed. Table 4.25 shows the project material and estimated labor costs.

Table 4.24. Schedule for Field Application and Testing			
Week	Day	Activity	Man-hours
I	1	Setup, Clean up underside and Mark Layout	7.5
	2	Instrumentation	NA
	3	Instrumentation	
	4	Service Load Test I (Control) Certification of DOT personnel for PAFS system (One strip attached)	6
	5	Attached 9 strips	18
II	6	Attached 10 strips (10-15 min. attachment time per strip)	12
	7	Instrumentation	NA
	8	Instrumentation	
	9	No Work	
	10	Attach 1 strip for demonstration and Service Load Test II (Strengthened) and cleanup	18
Total			61.5
Total hours for MF-FRP installation only			30
Total labor cost for MF-FRP installation at $60/hr (est.)			$1,800

Table 4.25. Costs for the Strengthening of P-53-702			
Material	Unit Cost	Quantity	Cost ($)
FRP Strips (Strongwell Inc.) (21 Strips 23 ft long ea.)	$ 9 / ft	483 ft	4,347
X-ALH Fasteners + booster + neoprene coated washer (80 per strip, 11 strips)	$ 0.50 ea.	880	440
X-CR SS Fasteners + booster (80 per strip, 10 strips)	$ 1.15 ea.	800	920
Steel Anchor Bolts (4 per strip, 11 strips)	$ 1.14 ea.	44	50
Stainless Steel Anchor Bolts (4 per strip, 10 strips)	$ 4.70 ea.	40	188
Misc. Supplies	$ 10 / Strip	21	210
Total materials cost	$9.84/ft^2	26 x 24 = 625 ft^2	$6,155
Total Labor cost for installation	$2.88/ft^2	625 ft^2	$1,800
Total bridge strengthening cost	**$12.72/ft^2**	**625 ft^2**	**$7,995**

Material and Equipment for Strengthening

Table 4.26 shows the material and equipment used during the strengthening of the existing bridge.

Table 4.26. Materials and Equipment Used for the Strengthening of the Bridge		
Material	Type Used	Description
Fastening System	Hilti Powder Actuated Fastening System DX A41 and DX 460 (shown here)	
Pre-Drilling System	Hilti Type TE 6-A Rotary Hammer	
Charge for Fastening System	Hilti 0.27 in. caliber boosters for fastening system with selected power level as per ANSI (1995) guidelines	
Fastener Selection	Hilti Type X-ALH 47 P8 (w/ R-18 5/8 washer) and X-CR44-P8-S12	
FRP Strip	Strongwell FRP Safstrip™	
Expansion Anchors	Hilti Type KBII CS ½ in. x 2-3/4 in. KBII SS ½ in. x 2-3/4 in.	

Table 4.27 shows the protective gear that was recommended for use during the installation of the MF-FRP system.

Table 4.27. Protective Gear Used During the Application/Installation of the MF-FRP System			
Face Shield	Gloves	Hard Hat	Ear Protection

Installation Procedure

The process used to install the MF-FRP system on the bridge was as follows:

Strip Preparation

The FRP strips supplied by the manufacturer were in 100 ft long rolls. The strips were cut to the desired length of 21'-2" using a circular saw with a masonry blade. A hacksaw with a masonry blade was used for field cuts if necessary. Figure 4.16 shows the roll of FRP Strip used for the project as supplied by the manufacturer.

Figure 4.16. Roll of 100 ft long FRP strips as supplied by the manufacturer

Mark Center of Strip

The centerline of the pre-cut strip was marked. A horizontal and vertical grid was marked on the FRP strip using a permanent marker to locate the center of the strip and the spacing of the fasteners required by the design (3 in. o.c.).

Pre-Drill Holes in the Strip

The marked grid was then predrilled with a 3/16 in. masonry drill bit at fastener locations.

Setup For Application

        A working platform was set up under the bridge. Wooden planks were supported on 4x4 lumber placed near the abutments. This was done to maintain an unrestricted flow in the creek. Figure 4.17 shows the setup of the working platform.

Figure 4.17. Working platform under the bridge

Surface Preparation

        The concrete substrate was cleaned of any residual matter that would have hindered the application of the FRP strip. A spatula and a wire brush were used to scrape the soft calcium stalactites from under the bridge deck. Figure 4.18 shows the soft calcium stalactites on the concrete substrate. Figure 4.19 shows the cleanup using a spatula.

Figure 4.18. Soft calcium stalactites seen on the concrete substrate

Figure 4.19. Surface preparation of the concrete prior to application of FRP strips

Layout of FRP Strips

Using chalk powder and a permanent marker, the desired locations for the FRP strips were marked on the concrete surface.

Suspend FRP Strip on Substrate

The FRP strip was then suspended along the underside of the concrete slab at the appropriate location. Duct tape was used to temporarily position the FRP strip in its desired location. In addition, the strip was manually held in position until the first few fasteners were installed. Working from midspan of the bridge towards one support, the strip was moved into its proper position. Measurements were taken at regular intervals along the length of the strips to ensure the required spacing between the strips was maintained.

Secure Strip at Midspan

Pre-drilling into the concrete substrate was done through the drilled hole in the FRP strip. A 3/16 in. Hilti type DX-Kwik masonry bit was used with a rotary hammer drill. Figure 4.20 shows the pre-drilling at the midspan while the FRP strip is temporarily held up against the soffit.

Figure 4.20. Pre-drilling into the concrete substrate at the midspan

Power Level for Fastening System

The charge selection for the fastening system was first determined by tests on the surface where the FRP strips were to be attached without predrilling. Starting with lowest power level and booster type, a fastener was driven into the concrete with an attached washer. The power level was then increased to fully embed the fastener and attach the washer snug against the concrete surface. If the highest power setting was not enough to fully embed the fastener, the procedure was then repeated with a higher-level booster.

Attach Fastener

The selected fastener was then inserted with the attached washer into the PAF gun, leaving the fastener point protruding out. The gun was placed perpendicular to the strip and was pressed to unlock the safety mechanism of the gun. The gun was then "fired" to insert the fastener. Figure 4.21 shows the fastening of the FRP strip at the midspan while it is temporarily held in place. Figure 4.22 shows a properly secured fastener at the midspan.

Figure 4.21. Fastening of the FRP strip at the midspan

Figure 4.22. Properly installed ALH fasteners at the midspan

After the midspan fasteners were secured, the next sets of fasteners were installed with alternate pre-drilling and fastening sets of four fasteners at a time. After four to eight fasteners were installed the position of the FRP strips became fixed. The procedure then continued rapidly with a single person or two people drilling and attaching fasteners towards one end of the strip. When one half of the strip was secure the fastening was then resumed from the midspan towards the direction of the other support. Alternate drilling and fastening was done simultaneously to speed up the process. Figure 4.23 shows the simultaneous drilling and fastening of the FRP strip after the strip was securely fastened at the midspan.

Figure 4.23. Simultaneous drilling and fastening of the FRP strip

Placement of End Anchors

The strips were predrilled at the locations of the anchor bolts using the rotary hammer drill with the nominal diameter of the anchor bolt. The hole was then cleaned before the anchors bolts were inserted. Once the anchor was inserted in the drilled hole, the anchors were hammered into place (taking care not to damage the FRP strip). The anchor bolts were then tightened using a socket wrench. Figure 4.24 shows the installed end anchors near the support ends.

Figure 4.24. Installed end anchor next to the abutment

The completed strengthening of the bridge is shown in Figure 4.25 and Figure 4.26.

Figure 4.25. 12 in. Strip spacing between FRP strips

Figure 4.26. Bridge P-53-702 strengthened using MF-FRP system

Observations During Strengthening

The field installation of the MF-FRP system was similar to that experienced during prior laboratory fastening procedures. However, a number of unique challenges were posed during the field installation. The following difficulties were observed:

It was cumbersome to position the FRP strip at the proper location. At times three to four people were required to temporarily hold the strip at the location before a few fasteners were installed. While the installation of the fasteners along the length of the span (80 fasteners @ 3in. spacing) took not more than 15 minutes, the positioning of the strip took an additional 15 minutes, and this slowed down the rate of installation. Occasionally, instances occurred where the fastener did not fully penetrate the concrete substrate. This was seen when a fastener encountered an obstruction in the substrate. Improper embedment of the fastener was seen. This ranged from incomplete embedment of the fastener to no embedment at all. Incomplete embedment was observed when the fastener encountered the following obstructions:

1. Large Aggregate
2. Pocket of poor consolidation or deteriorated concrete

3. Existing rebar

Figure 4.27 shows a missing fastener.
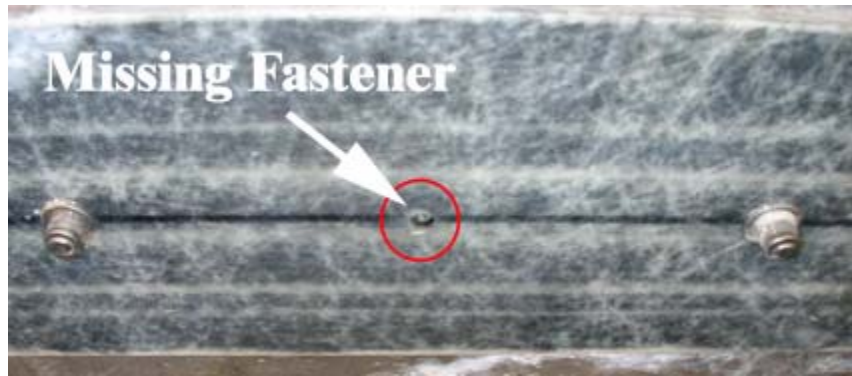
Figure 4.27. Missing fastener due to pocket of poor consolidation in the concrete

In cases where improper embedment was seen a lower power level was used to reinsert the partially embedded fastener. Extreme caution was used to ensure the fasteners were not over driven. To do this the power level was set to low so that no damage to the strip was caused. In cases when no embedment was seen and the fastener completely came out of the predrilled hole, no further attempts to reinsert the fastener were made. Figure 4.28 shows an overdriven fastener. Such situations should be avoided.

Figure 4.28. Over-driven fastener in the FRP strip

In a situation where the row of fasteners was anticipated to achieve improper embedment the FRP strip was slightly re-positioned. Figure 4.29 shows the position of the FRP strip in close proximity to a local damaged area. The strip was moved a few inches to avoid the damaged area.

Figure 4.29. Relocated FRP strip near existing local damaged area

Local damage in the existing concrete substrate did not cause a problem with the fastening of the FRP strip. Figure 4.30 shows an existing damaged area in the bridge with the exposed steel reinforcement.

Figure 4.30. Existing damaged area in the bridge with the exposed steel reinforcement

Furthermore, locations of localized out-of-plane variations did not affect the fastening procedure. Figure 4.31 shows a location where the original formwork had produced out-of-plane variations.

Figure 4.31. FRP strips fastened over original formwork lines

Service Load Testing

Service load testing of the bridge was conducted to determine if the MF-FRP system was performing appropriately and had increased the flexural capacity of the bridge. The objectives of the tests were to investigate and gather control data on the in-situ strength of the bridge before and after the strengthening.

Testing Procedure

The methodology adopted for the service load test was to conduct static diagnostic load tests on the bridge. Figure 4.32 shows the service load tests on the bridge.

Figure 4.32. Service load tests on bridge P-53-702

The static diagnostic load method used is a non-destructive test method and has been the method of choice for various studies conducted on bridges (Saraf, 1998; Chajes et al., 1997; Stallings et al., 2000). The method employs the positioning of a truck with known configuration

and weight at critical locations on the bridge with the response determined by measuring strains in the materials. Strain readings measured in the concrete and the FRP strips were used to verify the composite behavior of the strengthened slab.

A three-axle truck with known wheel configurations was used for the service load testing of the bridge. It was calculated that a truck loaded between 50,000 and 60,000 lbs would produce acceptable response without causing any damage to the bridge. The truck was provided by Rock County DOT and was weighed prior to each load test. Figure 4.33 shows the wheel and axle spacing of the truck used. Table 4.27 provides the distribution of the weight.
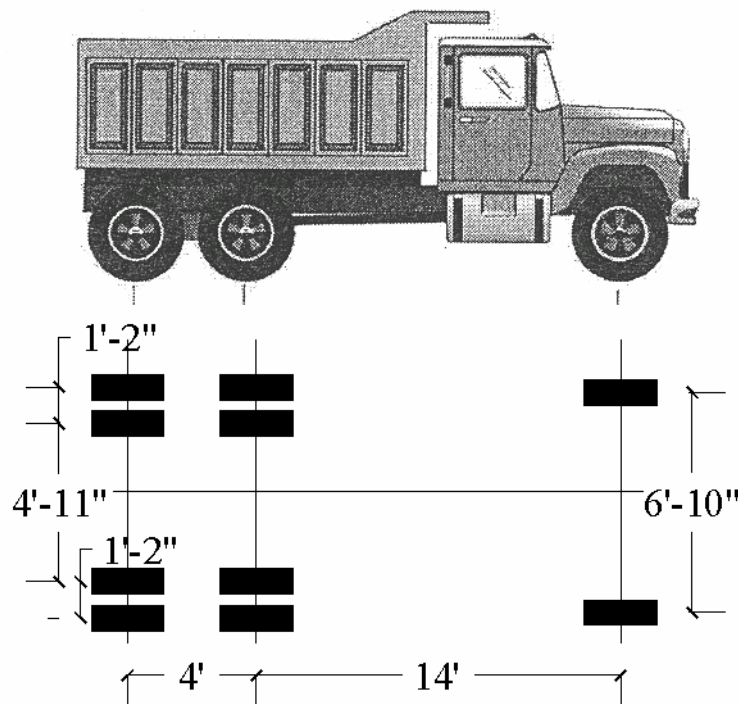
Figure 4.33. Wheel spacing for the truck used for service load testing

Table 4.27. Weights Distribution for the Truck Used for Service Load Testing			
Truck #	Front Axle (kips)	Rear Axles (kips)	Total Weight (Tons)
1021 WisDOT	12.9	37.8	25.4

Instrumentation and Load Cases

For the service load testing, strain gages and LVDTs were attached to measure the structural behavior of the concrete slab. Strain gages were also placed on the FRP strips to measure the strains and to confirm the composite action of the strengthened slab. Figure 4.34 shows the locations of the strain gages attached on the underside of the concrete and the FRP

strips. Designations C, E, W, S, and F correspond to Concrete, East, West, South, and FRP respectively.
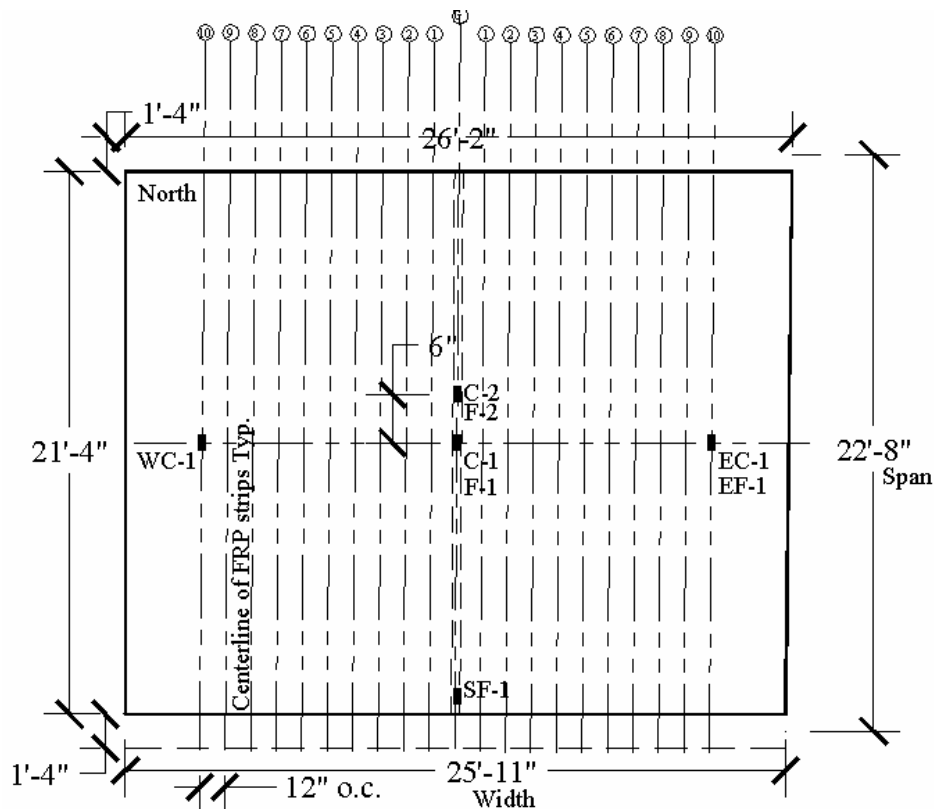
Figure 4.34. Layout and location of strain gages on the bridge slab

The strain measurements were made at various locations for different load cases using a portable data acquisition system. Due to the lack of a direct current source at the location of the bridge, a generator was used to power the data acquisition system. During the initial load testing, the data acquisition system could not be stabilized due to the unstable power source. Therefore, manual strain indicators and switch boxes were used to measure the strains at various locations of the slab. Dial gages (0.0001 inch resolution) were used in place of the LVDTs to measure the deflections of the bridge.

On the day of the second load tests, rain affected some of the strain gages placed on the concrete surface. While, careful precautions were taken to shield the strain gages from direct contact from water, some of the strain gages were affected due to seepage seen through the vertical cracks in the slab. While some of the strain gage readings were consistent with those measured during the first series of tests, others were inconsistent and decreased the reliability of the results.

The load cases for both series of service load tests were conducted using the same truck, which was weighed for each series of tests. The load cases used are shown in Figure 4.35.
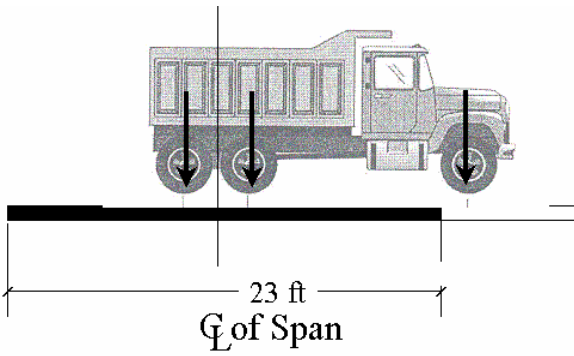
Load Case I: **Rear axles centered at Midspan of the bridge.**
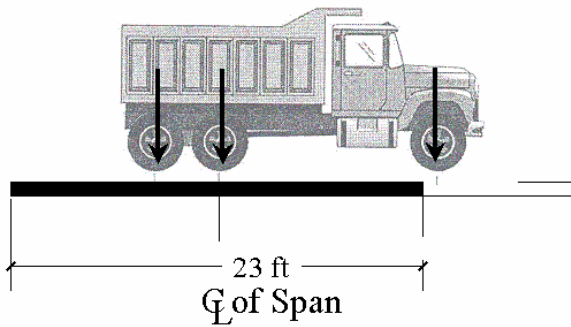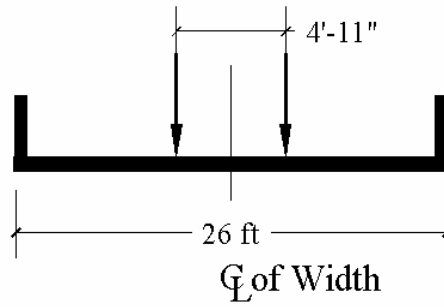
Load Case II: **Front rear axle centered at Midspan of the bridge.**
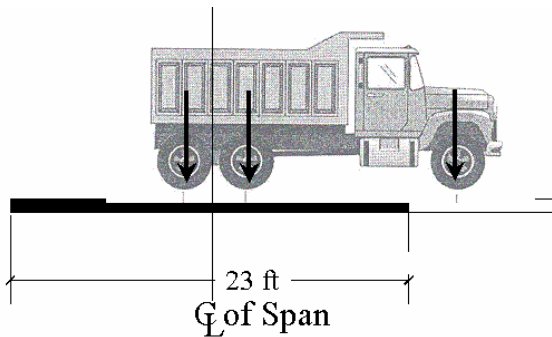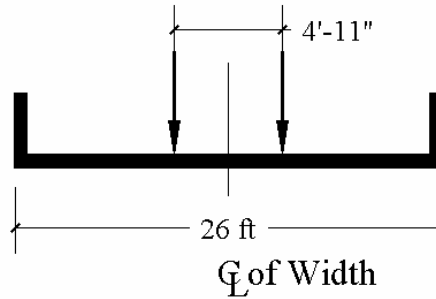
Load Case III: **Rear axles centered on Eastern edge of the bridge.**
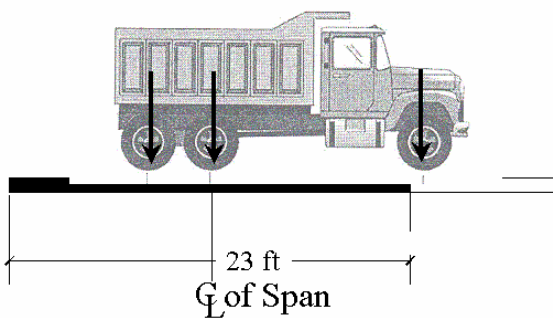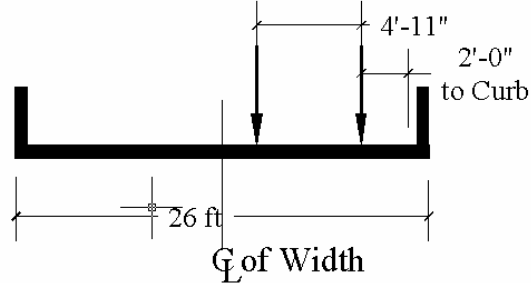
Load Case IV: **Front rear axle centered on Eastern edge of the bridge.**
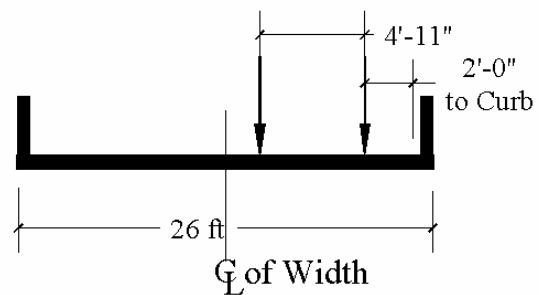
Figure 4.35. Load case for service load tests

The load cases were considered to represent the most extreme loading conditions possible. Because of the transverse symmetry of the structure, only one lane was tested. Figure 4.36 shows Load Case I on the bridge after strengthening.

Figure 4.36. Load Case I on bridge P-53-702

Results of Service Load Tests

Table 4.28 and Table 4.29 summarize the strain readings for the service load tests conducted on the bridge.

Table 4.28. Strains for Service Load Test I (unstrengthened)			
Load Case	WC-1	C-1	EC-1
	(με)	(με)	(με)
I	13	15	13
II	2	16	5
III	7	9	13
IV	-9	10	30

Table 4.29. Strains for Service Load Test II (strengthened)							
Load Case	WC-1	C-2	F-1	F-2	Centerline	EC-1	EF-1	East
	(με)	(με)	(με)	(με)	Avg.	(με)	(με)	Avg.
I	5	3	26	12	13.7	-5	11	3
II	6	13	14	7	11.3	29	-	29
III	2	1	-	-	1.0	-6	18	6
IV	1	8	13	5	8.7	30	13	21.5

Figure 4.37 and Figure 4.38 show the strain distributions of all the four load cases for the two series of tests. For the strengthened case, the average of the concrete strains and FRP strip strains were plotted.
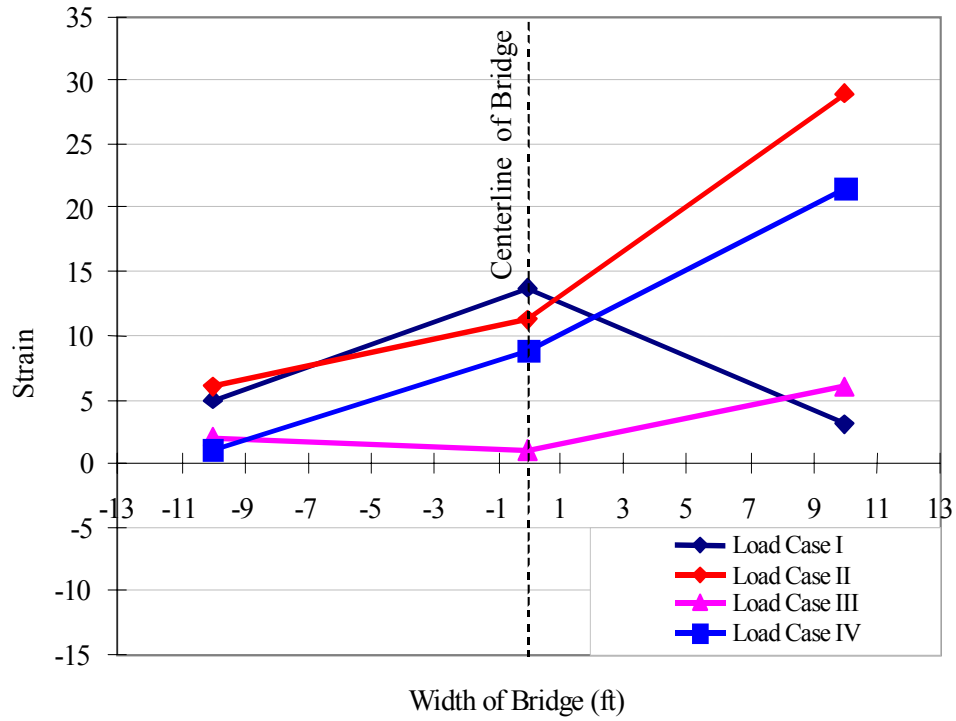
Figure 4.37. Strain distribution for service load tests (Unstrengthened)
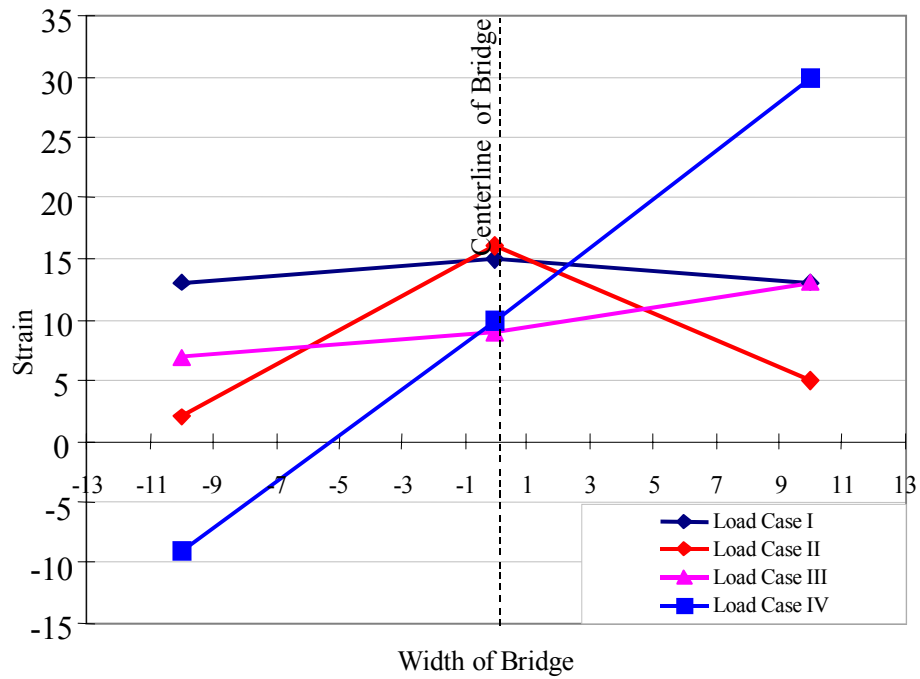
Figure 4.38. Average strain distribution in concrete and FRP for service load tests (Strengthened)

55

Discussion of Results of Service Load Tests

The largest average strain reading measured was 30με for load case 2 at the East end of the bridge. 90% of the strain measurements were below 30με. While such small strain readings may be inconclusive, some general trends were observed. The somewhat symmetrical distribution of the strain in the bridge is observed for the first two load cases (I and II). Figure 4.39 shows the plot of the strain distribution for the two series of tests, before and after the retrofit of the bridge for Load Case I.   The reduction in strains is attributed to strengthening.
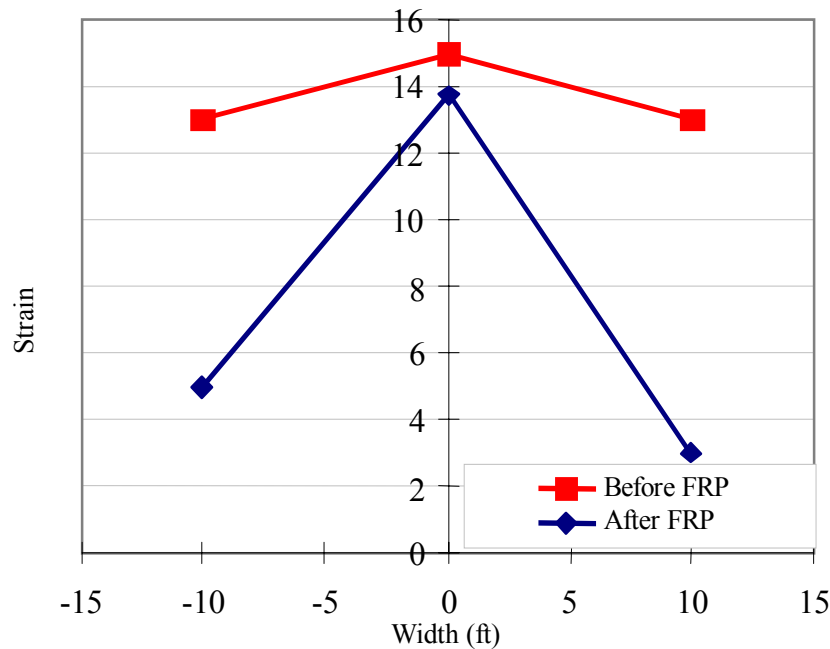
Figure 4.39. Strain distribution for Load Case I

While as much as a 77 % reduction in the strain is observed on the east end of the bridge, only a 9% decrease in the concrete strain at the middle was observed. The highest measured strain in the FRP strip for Load Case I was 26με corresponding to a stress in the FRP strip of 231 psi. The corresponding average stress in the FRP strip at the middle was 169 psi.

The unsymmetrical distribution seen in Load Case II after strengthening was peculiar and is difficult to explain. Similar unsymmetrical behavior has been seen in research studies conducted on existing bridges (Stallings, et al, 2000). Therefore, Load Case II was not considered in later analysis.   For Load Case III and IV, the unsymmetrical behavior is logical due to the offset loading of the truck. Figure 4.40 shows the strain distribution for Load Case III measured before and after the strengthening of the bridge.
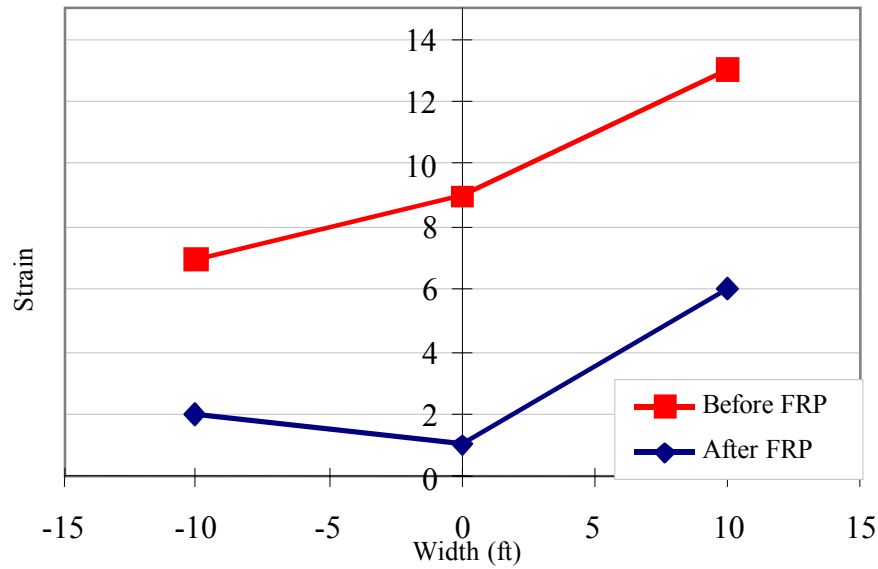
Figure 4.40. Strain distribution for Load Case III

A 54% difference in the strains measured near the load point at the east end was seen. A larger 88% strain difference was seen at the center of the bridge for the strengthened section. Figure 4.41 shows the strain distribution for load case IV.
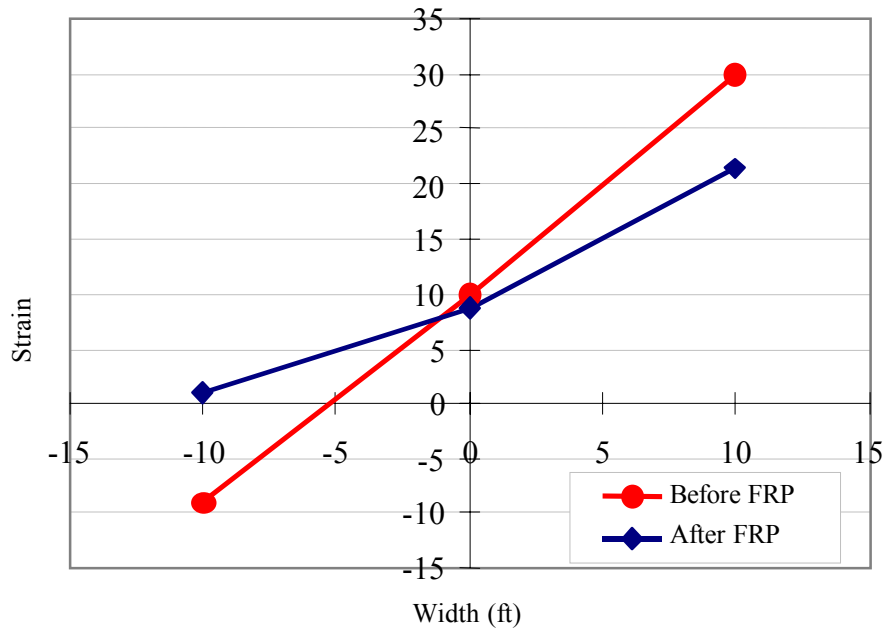
Figure 4.41. Strain distribution for Load Case IV

The strain distribution for the Load Case IV shows a 20% reduction in the concrete substrate strain in the middle of the slab, and a 28% reduction at the east end of the bridge where the load was located. The measured strain in the FRP strip was 13 µε corresponding to a stress

in the FRP strip of 115 psi. At the west end, a negative strain corresponding to compression is seen in the concrete slab. This may be attributed to some negative bending observed in the west end, when the load was located on the opposite end. After strengthening, a positive strain corresponding to tensile stress in the concrete substrate was seen.

While the results of the service load tests produced some trends that were expected, the strain measurements were probably not significant enough to draw any definitive conclusions related to stiffness or strength increase. Strain data does, however, suggests the composite behavior of the FRP strips with the concrete slab. The reduction in concrete substrate strain and the strain measured in the FRP strips strongly suggest the transfer of stresses to the FRP strip. Due to the low levels of load it was not possible to detect any deflection of the bridge with the equipment used.

Conclusions of MF-FRP Implementation Study

The first-ever full-scale implementation the MF-FRP system on an existing bridge structure proved that the method is easy to apply in the field, is economical, and can be designed using existing AASHTO procedures to increase the load rating of a bridge structure. The following specific observations and conclusions related to the full-scale field implementation can be made:

- The total cost of materials and labor for the MF-FRP strengthening was $7,995.00. The unit cost for the 625 ft^2 bridge was $12.72/ft^2. This is a highly economical strengthening system when compared with existing epoxy-bonded systems.

- Department of Transportation maintenance workers that had no prior training with the use of FRP composite materials easily installed the FRP strips in the field using commercial fasteners and tools.

- The FRP strips were attached to a cracked and spalled concrete substrate without any difficulty and with minimal surface preparation (and no surface repair). An epoxy-bonded FRP strip would not have been able to be attached in these conditions.

- The increase in moment capacity needed to increase the inventory load rating of the bridge from HS17 to HS25 was determined using standard AASHTO procedures. In order to determine the existing live load design capacity of a unit width strip of the bridge the effective width was back calculated from the reported HS17 load rating.

- The analysis and design of the MF-FRP strengthening system was preformed using a moment-curvature model and a simplified strength model. Parametric studies were conducted to assess the influence of different existing concrete and steel strengths. It was found that these parameters did not have a large effect on the design when the steel area was scaled for equivalent axial stiffness (EA).

- The final design of the strengthening system was in keeping with recommendations developed from prior laboratory testing. These included the use of a single row of fasteners

at 3 inch spacing along the length, the use of two anchor bolts at each end of the strip, and the use of a single FRP strip at 12 inches on center spacing across the bridge.

- Both galvanized steel and stainless steel fasteners could be used. No difference in the installation procedure was found for the different fasteners. Stainless steel fasteners are two to three times more expensive than galvanized steel fasteners and their use needs to be justified based on further environmental durability studies.

- Service load testing was conducted with a 50k vehicle. The results of strain readings before and after the strengthening indicate that the MF-FRP system is carrying some load. However, due to the very low level of load used for the service load testing, final conclusions could not be reached at this stage regarding strength and stiffness increases provided by the MF-FRP system. The results of the ultimate load testing described in following sections were used to demonstrate this aspect of the MF-FRP system.

5   Laboratory Testing of MF-FRP Strengthened RC Beams

Overview

In an effort to demonstrate the performance of the MF-FRP system and to obtain data for comparison with the strengthened bridge, laboratory specimens were fabricated and tested. Unstrengthened and strengthened beams were tested using similar methods and materials to those used in the bridge strengthening. The results of the tests were compared to assess the effects of strengthening on the beams and to evaluate the bridge strengthening design.

Objectives of Laboratory Tests

The objectives for laboratory testing program were:

- To fabricate beams representative of the Edgerton bridge.

- To strengthen the beams with the MF-FRP system using the same materials and methods used for the Edgerton Bridge strengthening.

- To conduct laboratory tests of the beams to obtain the complete load-deformation behavior of the beams.

- To conduct cyclic loading on one of the beams to simulate repeated loading on the bridge.

- To investigate the effect of the strengthening on the ductility and failure modes of the beams.

- To obtain unstrengthened "control" data for the in-situ ultimate load testing of the bridge.

Methodology

A plan was developed to fabricate four beams with the same height, reinforcement ratio and similar concrete strength to the selected bridge. For the laboratory specimens, a 24 in. wide section of the bridge was considered ideal to represent a section of the unstrengthened bridge. However, a 24 in. x 20 in. x 24 ft beam was beyond the handling capabilities of the laboratory and therefore a 20 in. x 20 in. x 24 ft beam was chosen to represent the properties of the bridge. The tensile reinforcement for the 20 in. wide representative beam was calculated to be 1.83 sq. in. for grade 60 rebars having a nominal yield strength of 60 ksi. An area of 1.80 in^2 provided by three # 7 bars was used for the laboratory beams. The existing concrete strength of the bridge slab used in the load rating analysis was 2,500 psi as specified by AASHTO (2000). A 2,500-psi concrete was not possible to obtain. However, the parametric study conducted on various concrete strengths showed that higher concrete strengths could be used without a significant effect on the ultimate strength of the section. Therefore a concrete strength of 4,000 psi was selected for the fabrication of the laboratory specimens.

The design for the strengthened bridge section called for one FRP strip fastened per foot width of the bridge to provide sufficient strengthening. Two FRP strips were used for the 20 in.

wide section for the laboratory beams. This slightly higher FRP reinforcement ratio was not expected to qualitatively affect the test results and could be accounted for quantitatively in calculations. Figure 5.1 shows a graphical comparison between the properties of the bridge cross-section and the cross-section of the laboratory beams.
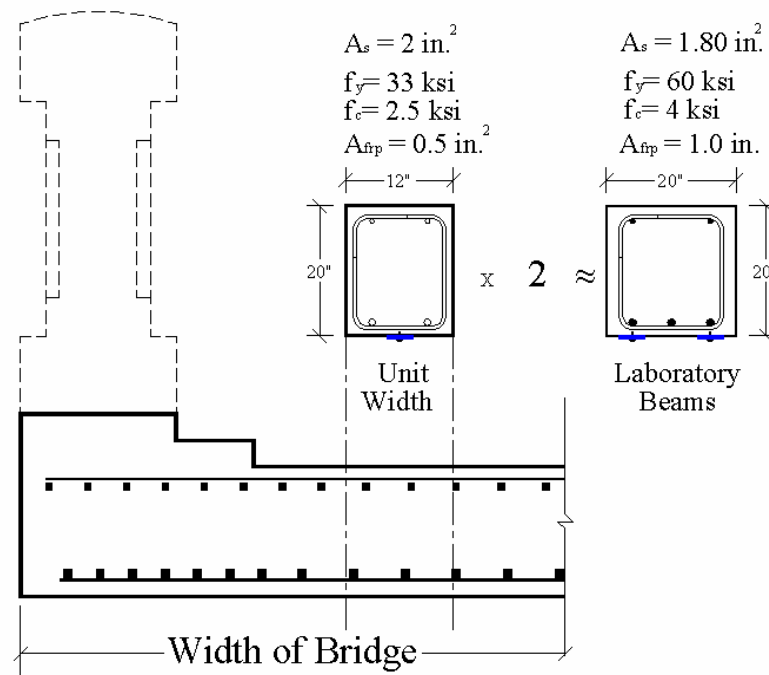
Figure 5.1 Comparison between properties of bridge and laboratory beams

Fabrication of Laboratory Specimens

Four laboratory beams with nominal measurements of 20 in. x 20 in. x 24 ft were detailed in accordance with ACI 318-99. The beams were fabricated at the Structures and Material Testing Laboratory (SMTL) at the University of Wisconsin-Madison. As explained previously, shear reinforcement for the bridge slab was provided at the ends by means of bent bars. For the laboratory beams, shear reinforcement was provided by stirrups to ensure that flexural failure of the beams would occur. Figure 5.2 illustrates the reinforcement of the beams.
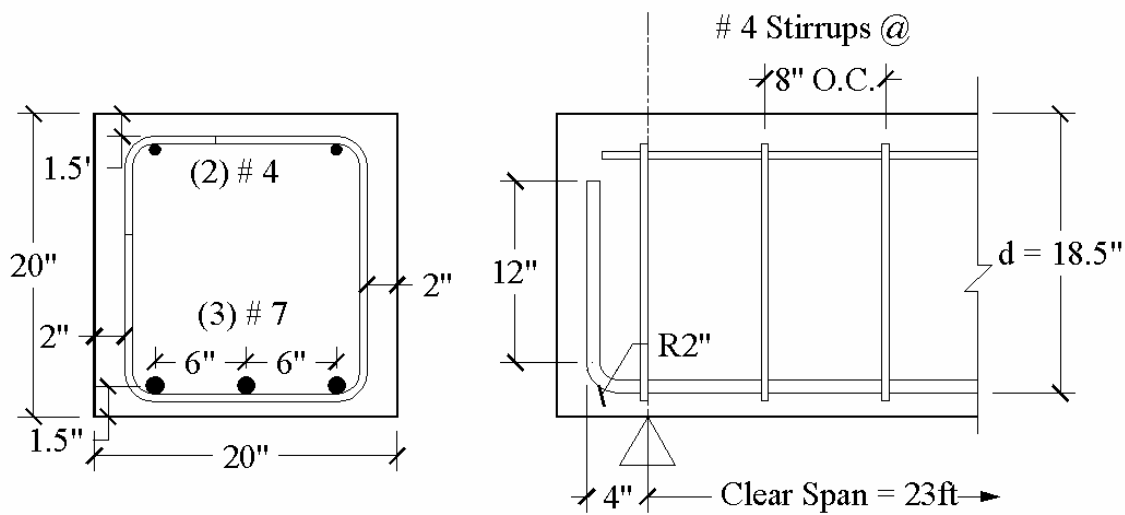
Figure 5.2. Steel reinforcement in laboratory beams

Concrete

A standard Grade "A-FA" mix as specified by the *Standard Specifications for Highway and Structure Construction* (WisDOT, 1996) was used for the construction of the beams. The selected grade limits the composition and proportion of the constituent materials. Table 5.1 provides a comparison between the concrete mix properties as recommended by the specifications and the mix delivered for the construction of the beams. A local vendor supplied 11 cubic yards of the concrete with a specified strength of 4000 psi for the construction of the four beams and concrete cylinders. An initial slump of 3 in. was specified for the mix with a slump of 7 in. at the time of the pour. This was achieved by adding a superplasticizer to increase the workability of the concrete.

Table 5.1. Concrete Mix Properties				
	Recommended A-FA (*WI. Specification.* 1996.)		Used Mix 339 A-FA 4000 psi	
	kg/m^3	lb/yd^3	kg/m^3	lb/yd^3
Type I Portland Cement	285	479	267	450
Class C Fly Ash	65	109	89	150
Total Aggregate	1815	3055	1816	3060
Water Cement Ratio	0.57		0.6	
Air Entraining Agents	As per State DOT. Approval		6.9 oz	
Water Reducers	As per State DOT. Approval		18 oz.	
Superplasticizers	As per State DOT. Approval & Manufacturer		72 oz.	

Formwork and Rebar Cages

The 24 feet long beams were cast in formwork built from ¾ in. plywood and 2"x 4" lumber obtained from local vendors. The steel reinforcement was tied together to form a cage

outside the formwork and was lifted into place. All four beams were poured on the same day. Figure 5.3 shows the tied reinforcement cage inside the formwork and Figure 5.4 shows the casting of the beams. Consolidation of the concrete was achieved using vibrators prior to finishing. During the casting of the first beam, the concrete formwork began to "bow out" due to lateral pressure because of inadequate lateral ties on the formwork. As a result the cross section of one of the beams was larger than the nominal 20 in. Each beam was provided with lifting hooks. Figure 5.5 shows the finishing of the top surface and the lifting hooks. Table 5.2 gives the identification scheme used for the four beams and explains their intended purpose.

Table 5.2. Laboratory Test Beams	
Beam	Purpose
C-1	Determine the flexural behavior of the unstrengthened (control) beam.
FRP 1	Determine the flexural behavior of a strengthened beam (2 FRP strips) with galvanized steel X-ALH fasteners.
FRP 2SS	Determine the flexural behavior of a strengthened beam (2 FRP strips) with stainless steel X-CR fasteners.
FRP 3	Determine the flexural behavior of a strengthened beam with 3 FRP strips and assess the performance under cyclic loading.

Figure 5.3. Formwork and reinforcement cages

Figure 5.4. Concrete casting

Figure 5.5. Finishing of the concrete

Properties of FRP Strips

The FRP strips, the powder actuated fasteners, and the end-anchors used to strengthen the laboratory beams were identical to those used in the strengthening of the Edgerton Bridge. The FRP strips were manufactured by Strongwell (Chatfield, MN). They were designed by researchers at the University of Wisconsin-Madison (Bank et al., 2002a). The FRP strips were tested at the University of Wisconsin for ultimate tensile strength, open-hole tensile strength, longitudinal tensile modulus, and longitudinal bearing strength as per ASTM standards D3039, D5766 and D5961, respectively. Full details of the testing can be found in Gulbrandsen (2002). Five coupons were tested in the tensile tests and ten coupons were tested in the bearing tests. The results of the tests are shown in Table 5.3.

Table 5.3. Properties of FRP strips used in laboratory beams					
Ultimate Strength (ksi)			Open-hole Strength (ksi)		
Mean	SD	COV	Mean	SD	COV
122.4	11.2	9.2	92.8	7.1	7.6
Bearing Strength (ksi)			Modulus of Elasticity (ksi)		
Mean	SD	COV	Mean	SD	COV
38.2	4.0	10.5	8,893	765	8.6

Properties of the Fasteners

The geometric and material properties of the Hilti fasteners used to attach the FRP strips to the laboratory beams are shown in Table 5.4. These were identical to the fasters used in the Edgerton Bridge strengthening.

Table 5.4. Fasteners used in Laboratory Beams				
Type	Material	Shank Diameter	Length	Picture
		mm (in)	mm (in)	
X-ALH-47	Zinc Plated Hardened Steel	4.5 (0.177)	47 (2.875)	
X-CR-44	SS CrNiMo Alloy HRC 52	4.0 (0.158)	44 (1.75)	
KBII CS	Carbon Steel	12.7 (0.5)	70 (2.75)	
KBII SS	Stainless Steel			

Laboratory Strengthening Procedure

The procedure used to attach the FRP strips to three of the laboratory beams was similar to that used in the strengthening of the bridge. The charge and power level for the Hilti DX A41 tool were chosen. The strengthening of the beams was done in-place with the beams supported on large concrete blocks that provided a clearance of 2-3 ft. The fastener locations were marked on the strengthening strip and the strip was predrilled using a 0.188 in. drill bit. The FRP strips were positioned and held in place by the means of carpenter's clamps and duct tape. Pre-drilling of the concrete to approximately 0.5 in. depth was done through the 0.125 in. FRP strip at the intended fastener locations. The fasteners were then inserted into the Hilti DX A41, lined up at the drilled locations, and driven directly through the composite strip into the concrete. A total of 80 fasteners corresponding to an equal spacing of 3 inches along the length were used to fasten each strip.

Only a small amount of surface pre cracking was observed upon attachment of the FRP strip. Two end anchors at each support end were used for all three beams. The termination lengths and the anchor locations are illustrated in Figure 5.6. Figure 5.7 shows the end of one of the beams.   Table 5.5 shows the dimensions and details of the four laboratory beams.
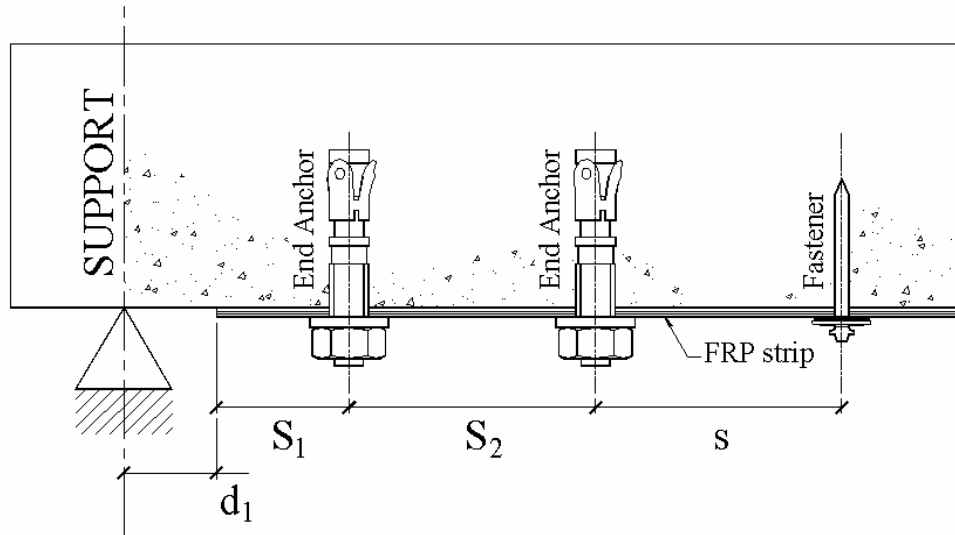
Figure 5.6. End condition for strengthened beams

Figure 5.7. End anchor bolts and end fastener for FRP2 SS

Beam	Width	Height	Concrete Strength	Dist. to FRP	Area of FRP	Fastener & Anchor Type (Diameter, Length)	Cross-section
	b	h	f'c	d_{frp}	A_{frp}		
	(in.)	(in.)	(psi)	(in.)	(in^2)		
C-1	20	19.75	5960	-	-	-	(2) # 4 (3) # 7
FRP 1	20	20.25	6015	20.3	1.0	X-ALH-47 (0.177,1.85) KBII CS (1/2 x 2-3/4)	(2) # 4 (3) # 7 4" 4"
FRP 2 SS	20	20.25	6015	20.3	1.0	X-CR-44 (0.158,1.75) KBII SS (1/2 x 2-3/4)	(2) # 4 (3) # 7 4" 4"
FRP 3	20-25 Varies	20.25	5970	20.3	1.5	X-ALH-47 (0.177,1.85) KBII CS (1/2 x 2-3/4)	(2) # 4 (3) # 7 4" 6" 6" 4"
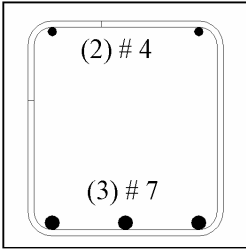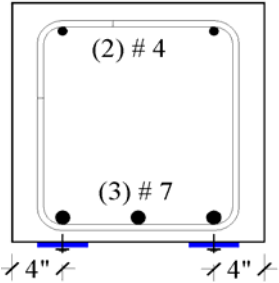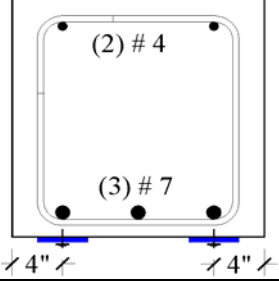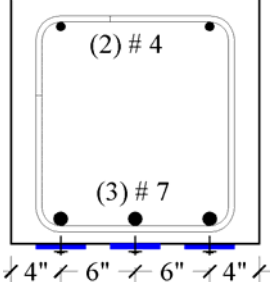
<div align="center">Table 5.5. Geometric Details of Laboratory Beams</div>

Note: All beams with Area of Steel A_s = 1.8 in^2; Distance to steel d_s = 18.5 in.; fastener spacing s = 3 in. 80 fasteners per FRP strip; d_1 = 1 in, S_1 = 2 in.; and S_2 = 3 in..

Figure 5.8 shows the relative positions of the FRP strips for beam FRP 3 strengthened with three FRP strips.

Figure 5.8. FRP 3 beam strengthened with three FRP strips

The stainless steel fasteners used for the bridge and the beams were Hilti type X-CR-44. These fasteners have a smaller shank diameter and length compared to the X-ALH fasteners. In addition, the stainless steel washers available with the X-CR fasteners did not have neoprene backing as was provided on the X-ALH fastener washers. Figure 5.9 shows a close-up photograph of the two types of fasteners (with washers) used for fastening the FRP strips. During the fastening of the FRP strips for FRP 2SS, it appears that the stainless steel washers may have damaged the FRP strips because they did not have the neoprene backing like the X-ALH fasteners.

Figure 5.9. X-ALH-47 with neoprene backed washer (left) and X-CR-44 with washer (right)

Laboratory Testing Procedure

The beams were tested in the University of Wisconsin Structures and Materials Testing Laboratory (SMTL) in four-point bending with a constant moment span of 30 in. The 14-day and 28-day concrete strengths were obtained from tests on cylinders and also subsequently on the day of the tests. The control beam was tested first followed by the strengthened beams. Figure 5.10 provides a schematic of the test setup.
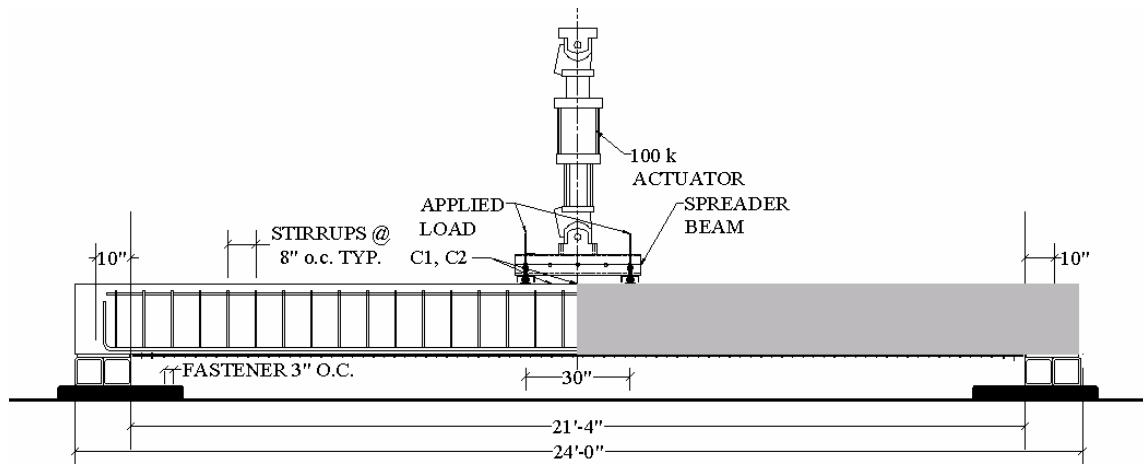
Figure 5.10. Test setup for laboratory beams

A 100 kip servo hydraulic MTS actuator with an MTS TestStar IIs controller was used to load the beams. The actuator was attached to a spreader beam, which distributed the loads evenly to produce a 4-point bending configuration. The beams were supported on heavy steel sections with gypsum grout bearing supports. Similar to the bridge span all the beams had a span of 256 in. and 10 in. bearing at each support end. Figure 5.11 and Figure 5.12 show a beam prior to testing.

Figure 5.11. Laboratory beam in test frame

Figure 5.12. Close-up of spreader beam used for loading

Instrumentation of Beams

An HP 3582A data acquisition system and a LabVIEW™ software program were used record the data for the tests. All the tests were run under displacement control of 0.1 in./min. Strain gages were used to measure the strain in concrete and the FRP strips at different locations. For the control beam, only 2 concrete strain gages C1, C2 were used at the top of the beam in the moment span. For the strengthened beams, an additional 8 strain gages (F1 - F8) were used on the FRP strips at various locations. Figure 5.13 shows the location of the strain gages on the FRP strips on the beams.
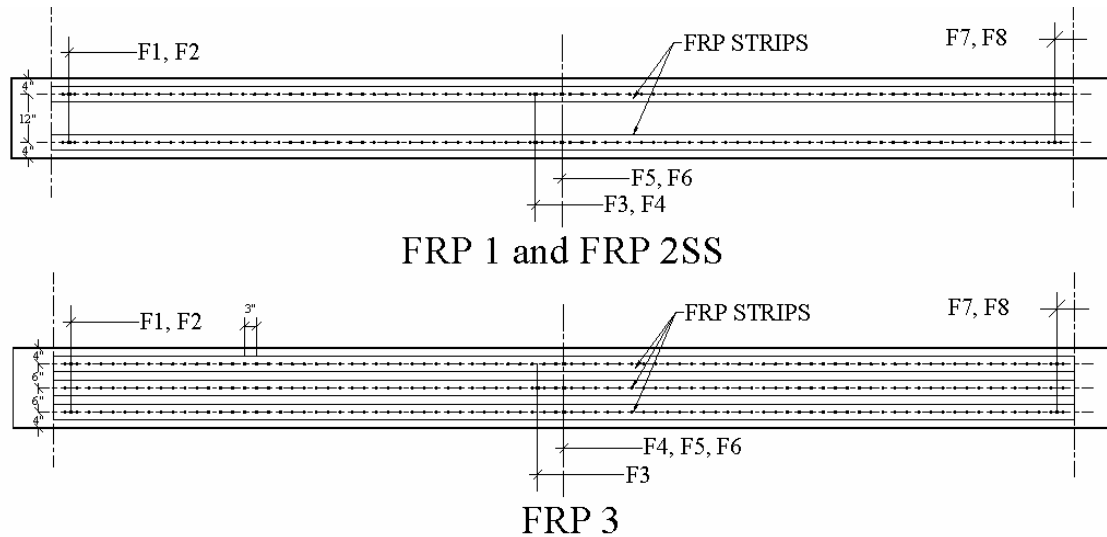
Figure 5.13. Location of FRP strain gages on laboratory beams

Two linear string potentiometers, one on either side of the beam, measured the relative displacement at one of the load points. This was done to detect any twisting of the beams due to rotation of the load cell. The string potentiometer readings for the displacement at the load point were used for comparison with the displacement of the stroke of the actuator. Figure 5.14 shows the plot of the actuator stroke and the average strain potentiometer readings for beam FRP 1.
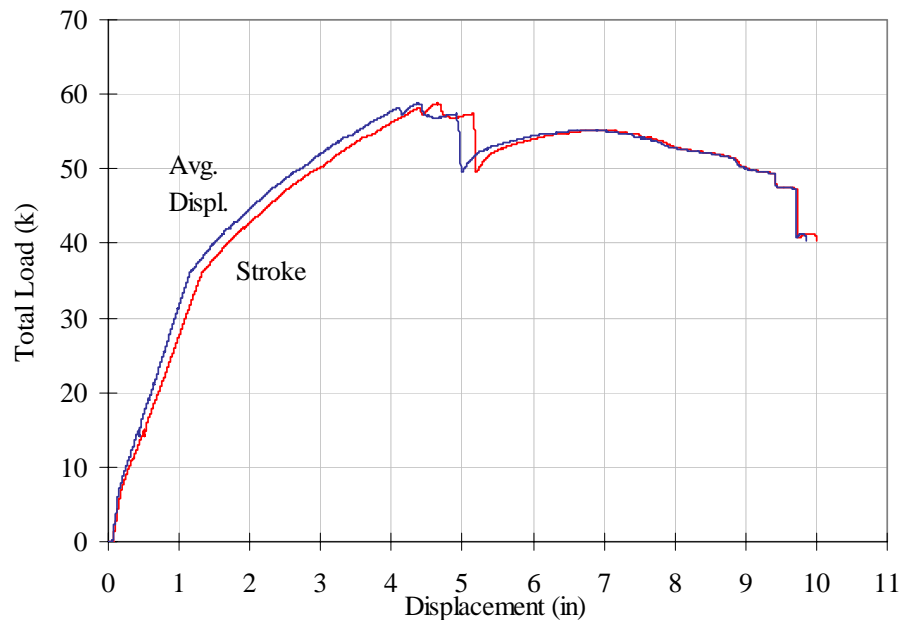
Figure 5.14. Comparison between stroke and average of the two strain potentiometers for FRP 1

The average difference in displacement between the two readings was 14% at yield and this difference in the displacement increased with the increase in the load. The difference was attributed to the flexibility of the test frame and the location of the devices. It was concluded that the difference in displacement would affect the strengthened beams more than the control beam because of higher load applied to the strengthened beams. Since the primary objective of the tests was to obtain the ultimate strength of the beams the stroke (midspan deflection) was plotted in what follows for the sake of convenience. As a result, the stiffness of the beams may be higher than apparent in the results but relative to one another they are comparable.

All beams, except for FRP 3 were tested under monotonic load. The beams were loaded up to 1000 lbs, a load level below the calculated concrete cracking load of 2000 lbs, and loading was then halted. This was done to check all the data obtained for the load, strain, and displacement. The loading was then resumed. Beyond the cracking load it was halted again at 20,000 lbs to measure and mark cracks on the beams. The next time the loading was halted was at 40,000 lbs after the yielding of the beam, and the cracks were again marked. After this the beam was loaded to failure.

FRP 3 beam was tested under cyclic loading to assess the performance of the fasteners and the FRP strip under repeated loadings in the elastic and inelastic ranges. The beam was loaded up to 20,000 lbs (below yield) and then for 10 cycles at the rate of 1in./min with a mean load of 11,000 lbs and amplitude of 9,000 lbs. The test was then resumed at 11,000 lbs under displacement rate of 0.1in/min. until the yielding of the steel reinforcement. The cyclic loading was then repeated at 40,000 lbs. (beyond yield). 10 more loading cycles were applied at the rate of 1 in/min. with a mean load of 21,000 lbs and amplitude of 19,000 lbs. Thereafter, the loading was resumed with the monotonic loading of 0.1 in/min until failure of the beam occurred. Figure

5.15 and Figure 5.16 show the loading cycles for the beam FRP 3.
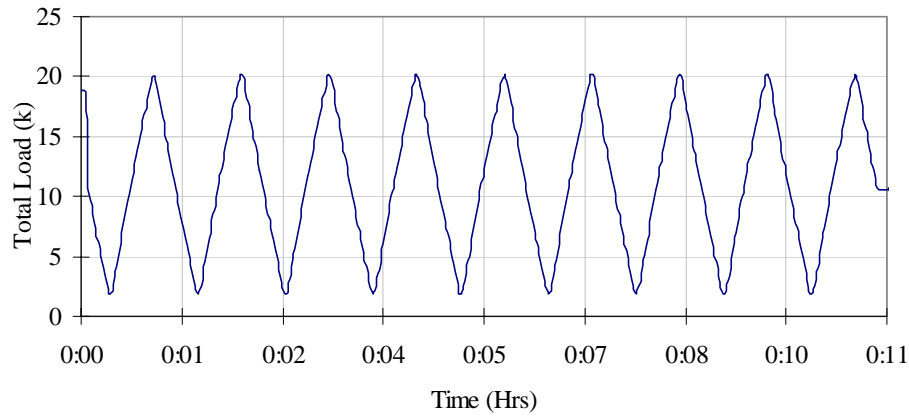
Figure 5.15. Loading cycles for beam FRP 3 in the elastic range
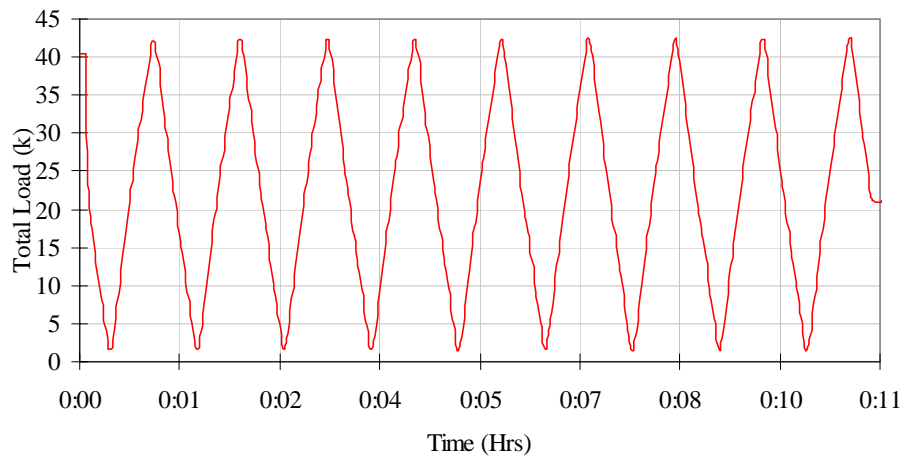
Figure 5.16. Loading cycles for beam FRP 3 in the inelastic range

Laboratory Tests Results

A summary of the test results is given in Table 5.6. Figure 5.17 shows the load versus displacement and moment versus displacement for the beams. The displacement measured at the load point δ and the total load P were plotted for each beam. In addition, the moment M, calculated by multiplying half the total load by the shear span *"a"* of each beam was also plotted for the moment versus displacement behavior of each beam.

Table 5.6. Summary of Laboratory Test Results								
Beam	Yield Moment (k-ft)	% Inc.	Ultimate Moment (k-ft)	% Inc.	Moment @ L/64 (k-ft)	% Inc.	Failure Mode at Ultimate	Secondary Failure Mode
C-1	143.6	-	208.7	-	177.2	-	Concrete crushing after yielding of tension steel	-
FRP 1	169.8	18.2	277.2	32.8	265.1	49.6	Concrete crushing after yielding of tension steel	Fastener Pullout
FRP 2SS	177.0	23.2	286.9	37.5	273.9	54.6	Concrete crushing after yielding of tension steel	FRP Rupture
FRP 3	180.0	25.2	329.9	58.1	302.7	70.8	Concrete crushing after yielding of tension steel	Anchorage Failure
% Increase =			$\dfrac{\text{Strengthened - Control (Unstrengthened)}}{\text{Control (Unstrengthened)}}$					x 100
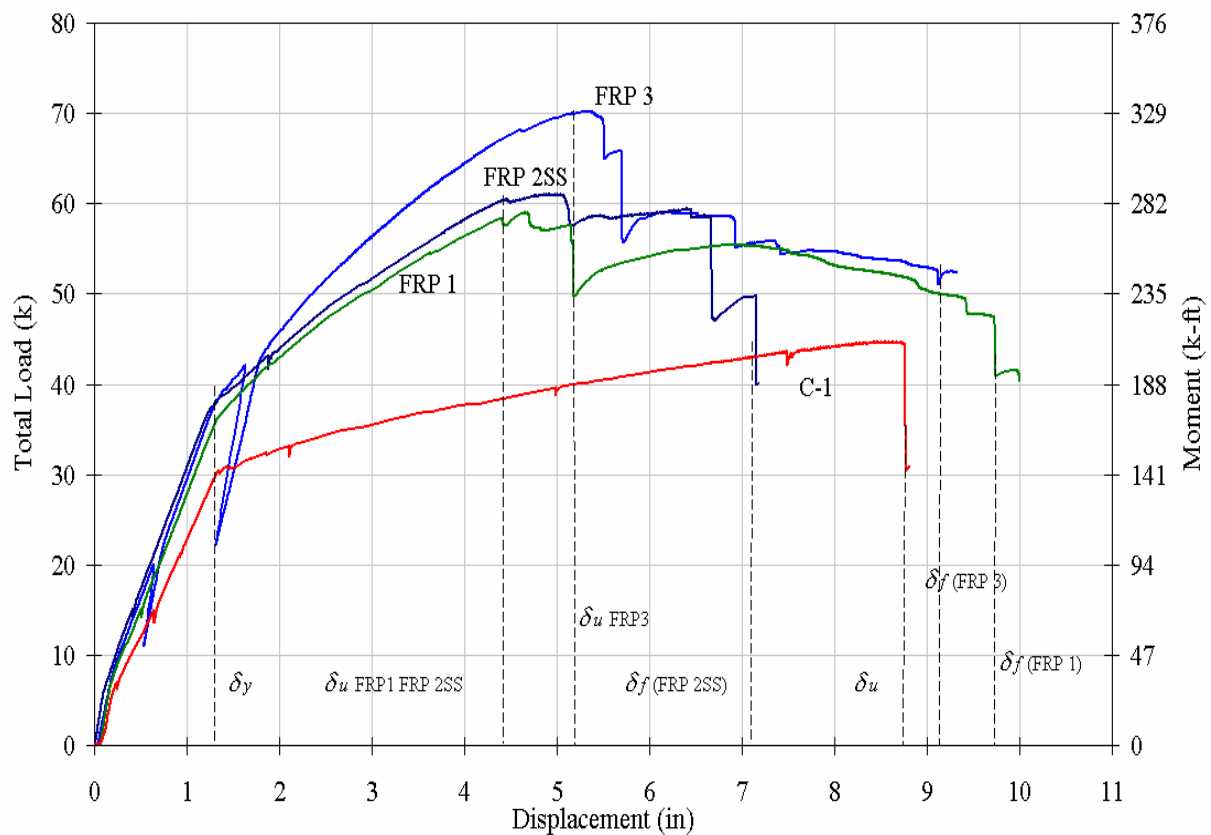
Figure 5.17. Load/Moment versus displacement curves for beams

74

Analysis and Discussion of Laboratory Tests

The yield load P_y and the corresponding moment M_y for each beam was taken at δ_y, the deflection at which the stiffness deviated from its initial linear regime. The moment at a displacement of 4 inches corresponding to a point close to the ultimate failure of all the strengthened beams at a ratio of L/64, which is well beyond typical design limits of L/360. The ultimate load P_u and the calculated moment M_u was the largest the beam reached at the deflection δ_u. The displacement at which the load carrying capacity dropped dramatically after failure of the strips is designated as δ_f.

Ductility ratios were calculated to evaluate the ductility of each beam. An "ultimate" ductility ratio ϕ_{ult} corresponding to the displacement at ultimate load and a "final" ductility ratio ϕ_f corresponding to the displacement at FRP failure of the strengthened beams were calculated as follows,

$$\phi_{ult} = \frac{\delta_u}{\delta_y} \tag{5.1}$$

$$\phi_f = \frac{\delta_f}{\delta_y} \tag{5.2}$$

Table 5.7 provides a summary of the loads, displacements and calculated ductility ratios.

Table 5.7. Load, Displacement and Ductility Results									
Beam	P_y	δ_y	P_u	δ_u	δ_f	ϕ_{ult}	Diff.	ϕ_f	Diff.
	(k)	(in)	(k)	(in)	(in)		%		%
C-1	30.5	1.38	43.6	8.80	8.80	6.4	-	6.4	-
FRP 1	36.0	1.35	58.0	4.74	9.73	3.5	-45.3	7.2	12.5
FRP 2SS	37.6	1.28	60.9	4.85	7.16	3.8	-40.6	5.6	-12.5
FRP 3	38.2	1.33	69.9	5.31	9.32	4.0	-37.5	7.0	9.4

The ultimate failure mode observed in all the beam tests was concrete crushing following yielding of the tensile steel rebar. Concrete crushing occurred when the concrete at the top of the beam in the moment span crushed in compression. This is the typical ultimate failure mode of a conventional reinforced concrete flexural member. All the strengthened beams exhibited the same initial failure mode but at a significantly higher load than the control beam. A secondary failure mode was seen in all strengthened beams at a much higher displacement when a load drop occurred due to failure of the FRP strengthening system. Observations made during the testing and the detailed results for each beam are given in the following sections. A discussion is also presented comparing the results of different tests.

<u>Beam C-1</u>

The control beam C-1 was tested to obtain the unstrengthened capacity of the Edgerton Bridge section and also to obtain the basis for comparison with the strengthened beams. The load and moment versus displacement curve for the control beam is shown in Figure 5.18.
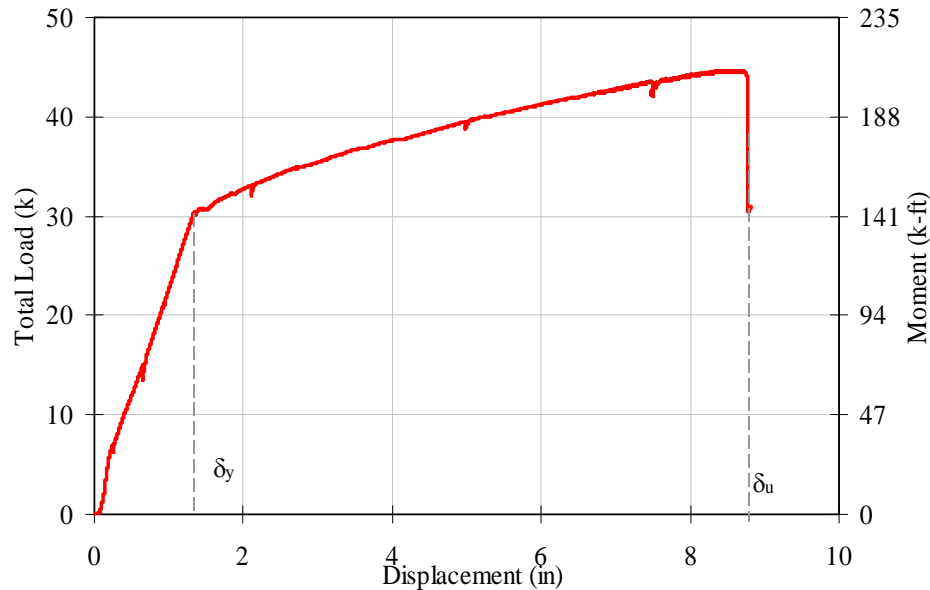
Figure 5.18. Load/Moment versus displacement for beam C-1

The C-1 beam yielded at 30.5 kips corresponding to a moment of 143.6 k-ft. The ultimate moment of the control beam occurred at a load of 43.6 kips corresponding to a 208.7 k-ft moment. A 30% increase in the post-yield strength of the control beam is attributed to strain hardening of the steel reinforcement and progressive and continuous movement of the neutral axis of the beam. The 4-point bending applied to the control beam produced flexural and some shear cracks in the beam. After the cracking load flexural surface cracks began to appear in the constant moment region of the beam. With increasing load, the flexural cracks increased in width and started to travel up towards the top of the beam. At the point of yield, cracks were visible and began to open up. Beyond yield, the cracks were significantly larger. Some local crushing was seen near one of the load points. The beam failed due to concrete compression in the moment span. No further increase in load was observed after concrete compression. Figure 5.19 shows the compression failure of the beam in the moment span.
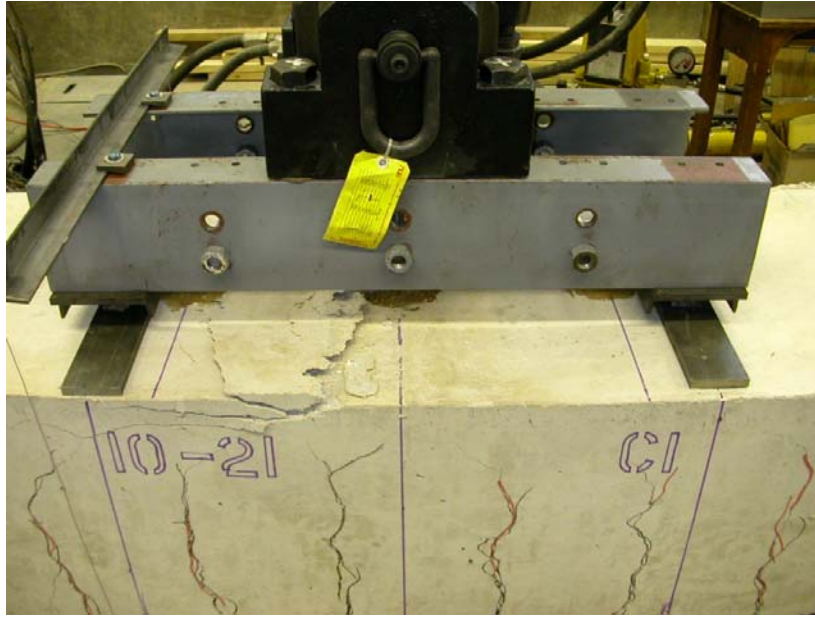
Figure 5.19. Concrete compression failure in the moment span in beam C-1

Figure 5.20 shows the moment vs. strain plot for the control beam showing concrete compression failure close to –0.3% (-0.003 in/in).
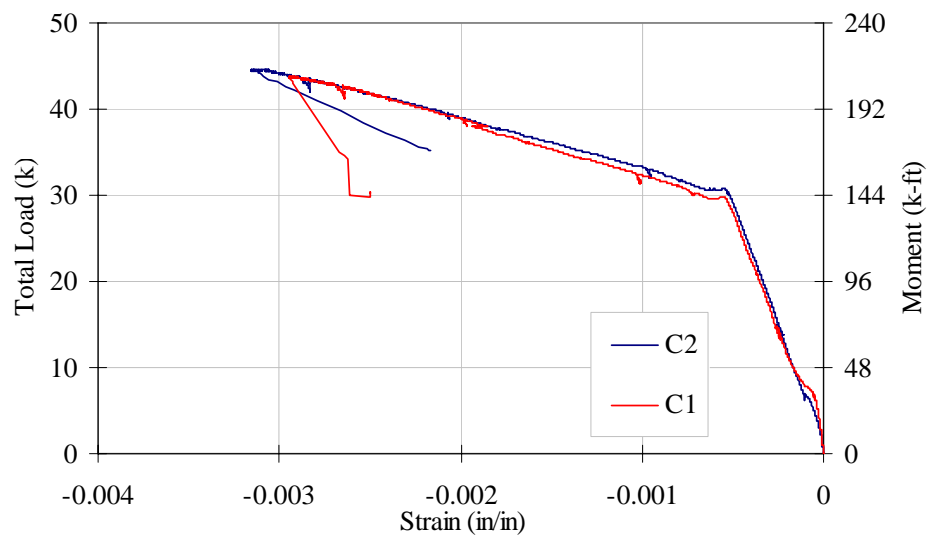
Figure 5.20. Moment vs. concrete strain for beam C-1

Beam FRP 1

Beam FRP 1 was strengthened with 2 FRP strips. The objective was to observe the increase in strength of the beam in addition to the deformability and the failure modes of the strengthened beam. Figure 5.21 shows the total load/moment versus displacement behavior of FRP 1.
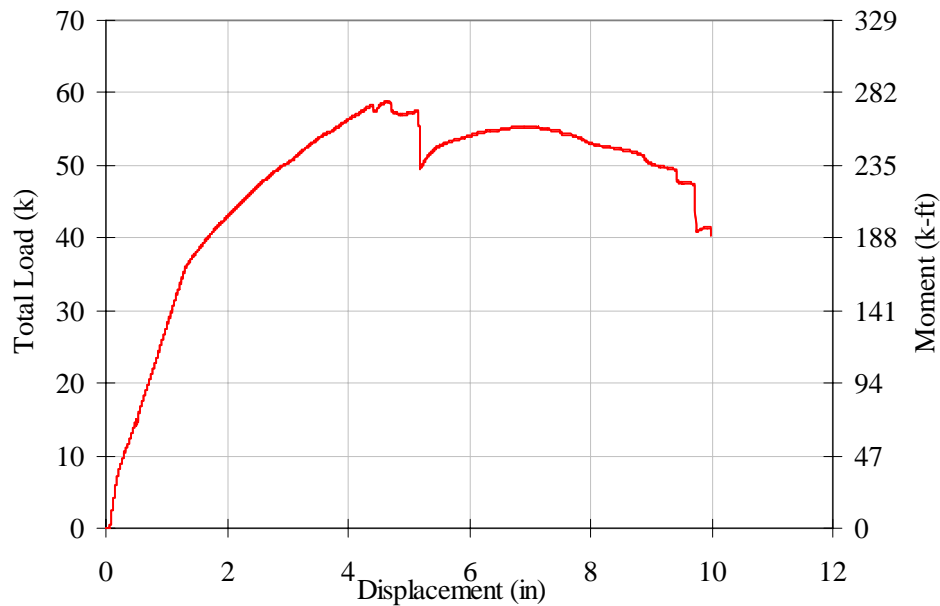
Figure 5.21. Load/moment versus displacement for beam FRP 1

During the initial loading of the strengthened beam flexural cracks, which traveled upwards as the loading increased, were seen in the moment span. At the point of yield, the cracks in the moment span were visibly larger. Beyond the yielding of the concrete, the beam continued to gain strength until concrete compression failure occurred near one of the load points. At first, local crushing was observed which eventually developed into the entire top of the beam failing due to concrete compression. A load drop was seen at this point. Figure 5.22 shows the concrete compression failure in the moment span.

Figure 5.22. Concrete compression failure of FRP1

The loading was continued after concrete compression failure and a nonlinear load increase was seen. The load seemed to stabilize for a period of time until a decrease in the load was seen. The behavior was similar to the "pseudo-ductile" behavior seen in "over-reinforced"

78

concrete beams. The beam ultimately collapsed when the fasteners near the load point pulled out. Beam FRP 1 yielded at 36 kips corresponding to a moment of 169.8 k-ft and the ultimate moment was seen when the beam failed by concrete compression at a load of 58.8 kips, corresponding to a moment of 277.2 k-ft. The strengthened beam showed an increase of 18% in the yield strength and 32.8% in the ultimate capacity over the control beam. In addition to the improved capacity, FRP-1 showed significant ductility. Even after concrete crushing, a significant level of load was sustained by the beam. Figure 5.23 shows the comparison between the control beam C-1 and the strengthened beam FRP 1.
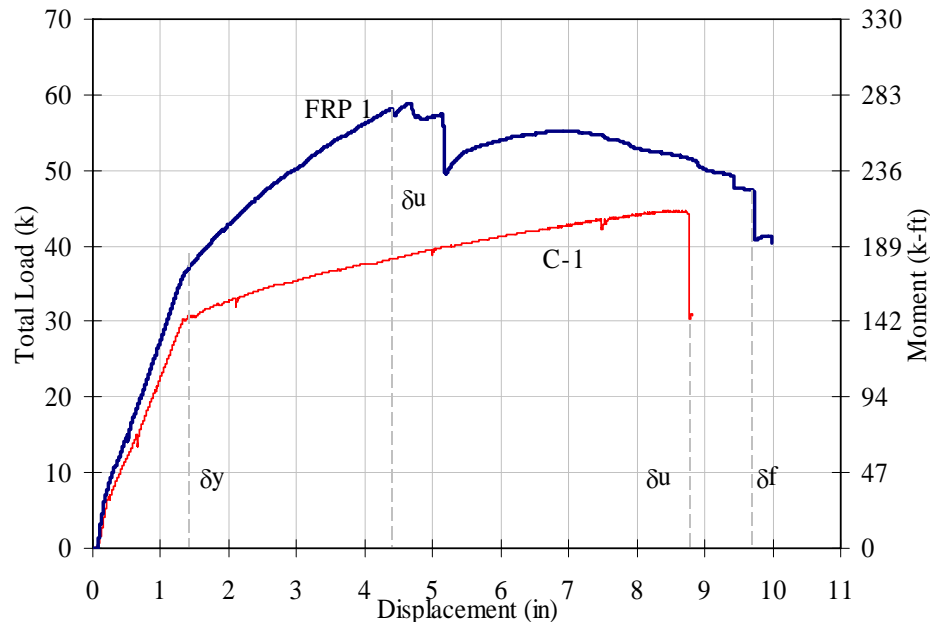
Figure 5.23. Comparison between FRP 1 and C-1

Figure 5.24 shows the moment versus strain distribution of the beam. The strain distribution clearly indicates the composite behavior of the section and that strain is effectively transferred into the FRP strip. Strain gage C2 shows concrete compression failure at - 0.5% near the load point, while the gage C1 in the middle shows concrete compression at - 0.3%. The maximum strain seen in the FRP strip was 0.8%. At the ends of the beam negative strain corresponding to compression in the FRP strip near the support is seen. A general discussion on the strain distribution in all the beams is given at the end of this section.
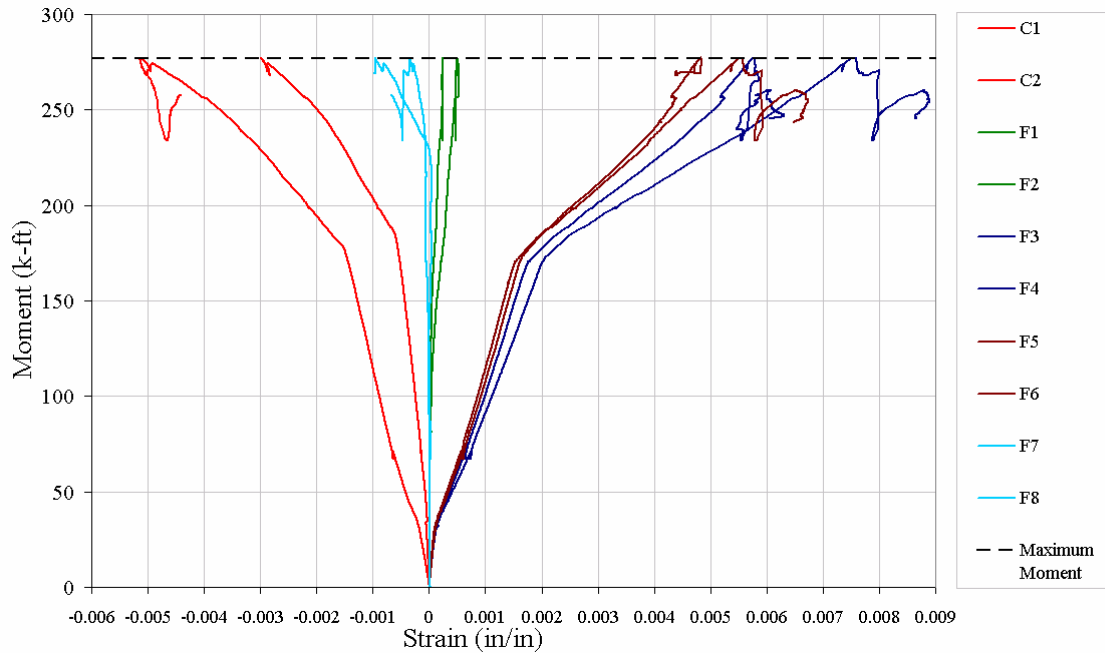
Figure 5.24. Strain distribution for beam FRP 1

The failed beam was turned upside down to study the failure mode of the FRP strips. The FRP strips showed a sustained bearing failure at the ends of the strips near the locations of the supports. Figure 5.25 shows the bearing failure of one of the FRP strips at the end.

Figure 5.25. Bearing failure at the end of an FRP strip in beam FRP 1

This bearing failure was seen to decrease towards the center of the beam. A shear-out failure of the FRP strips at one of the ends of the beams was seen. In the middle of the span, under one of the load points, fastener failure due to pullout was seen. A concrete "tooth" failure was also noted. Figure 5.26 shows this failure.

Figure 5.26. Secondary failure mode of beam FRP 1 due to fastener pullout

This failure mode occurred after the beam carried a significant load for a period of time after concrete compression failure was observed. Figure 5.27 diagrammatically illustrates the failure mode under the load point.
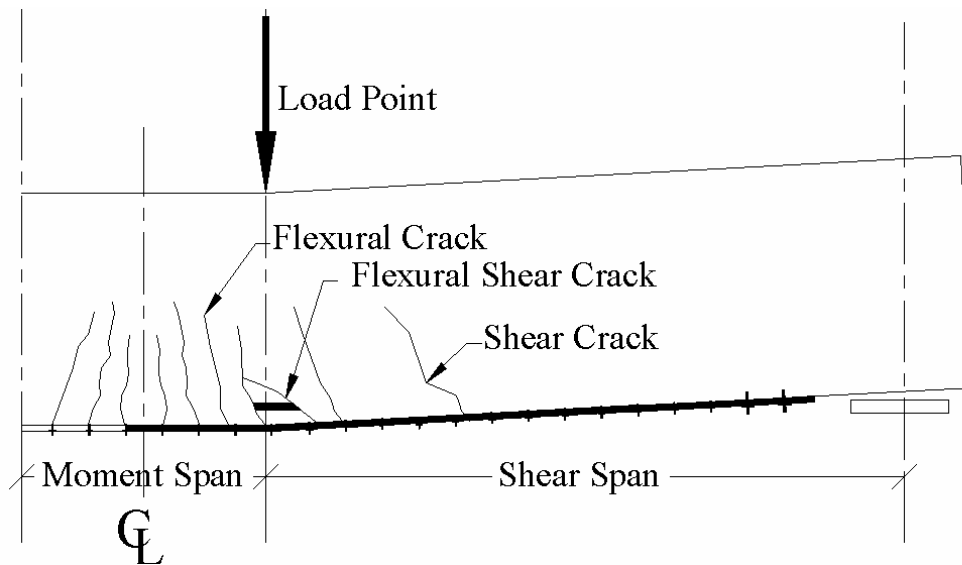
Figure 5.27. Concrete "tooth" failure due to flexural shear crack under the load point

The concentrated load produced both vertical flexural cracks in the moment span and diagonal shear cracks in the shear span. After concrete compression failure was observed, the downward progression of the neutral axis caused vertical flexural cracks in the moment span to deviate diagonally. Similar failure modes have been observed for bonded FRP systems resulting in premature delamination of the concrete cover (Teng et al, 2001; Sebastian, 2001). However,

81

it must be noted here that the FRP strip in this case remained attached to the concrete throughout the load history of the beam. Figure 5.28 shows the variation of the maximum strain versus the depth of the concrete beam with increasing applied moment. A downward progression of the neutral axis is observed at the ultimate moment of 277 k-ft where concrete compression failure occurred.
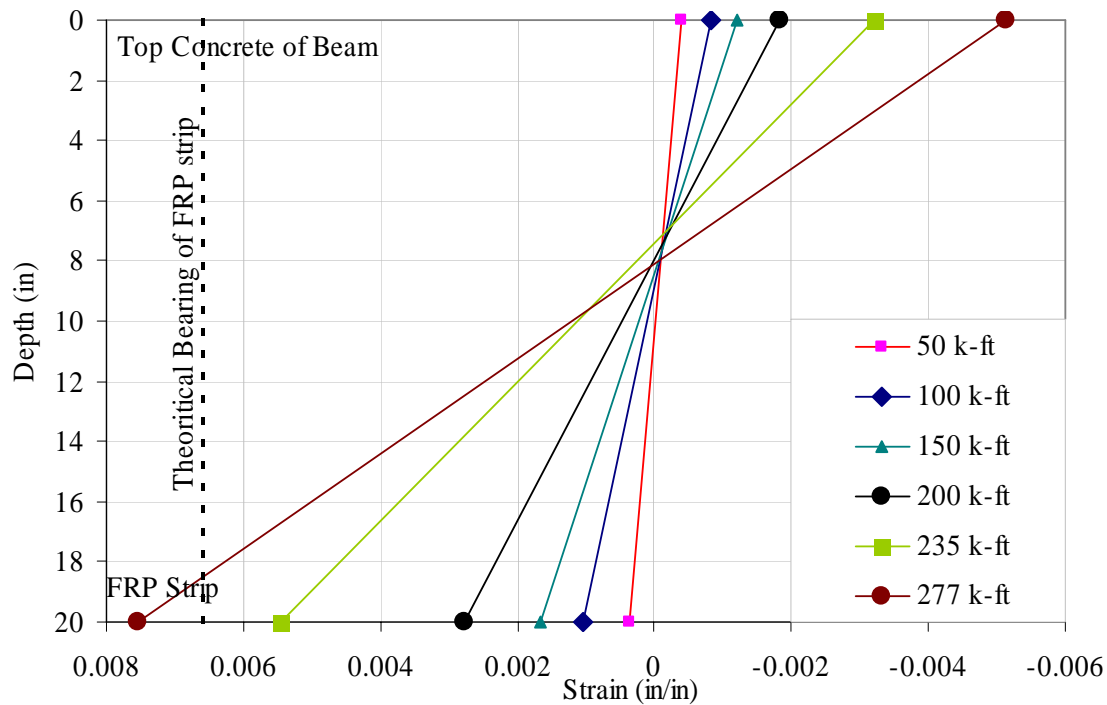
Figure 5.28. Variation of strain through the depth of beam FRP 1

Beam FRP 2SS

This configuration of the strengthened beam was used to observe the strengthening effect of 2 FRP strips attached with Hilti type X-CR SS (Stainless Steel) fasteners. Half of the bridge was strengthened using stainless steel fasteners and anchors, which provide increased corrosion resistance under aggressive environments. Data for strengthening using stainless fasteners was needed. Figure 5.29 shows the total load/moment versus displacement behavior of FRP 2SS.
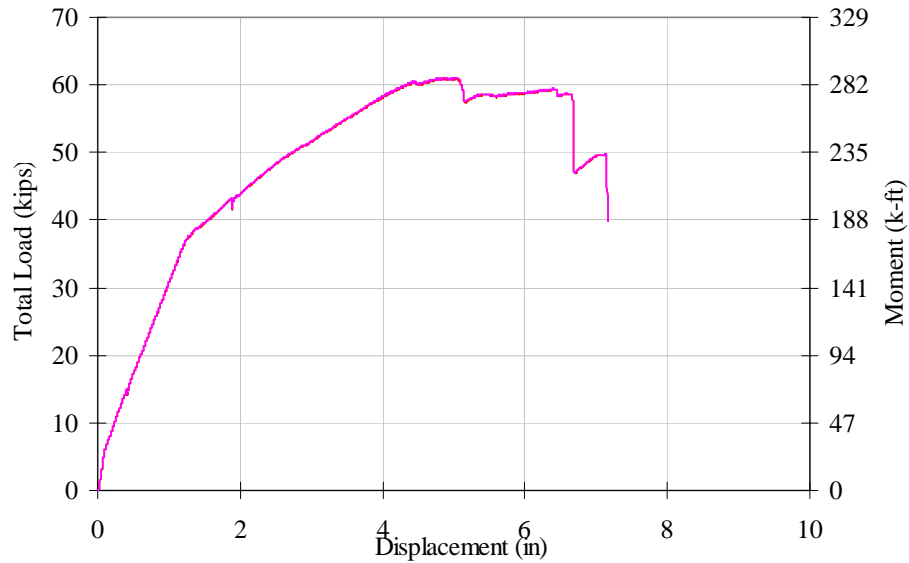
Figure 5.29. Load/Moment versus displacement for beam FRP 2SS

The crack pattern for the beam was similar to beam FRP 1. Flexural cracks became visible in the midspan after the cracking load was reached. As the beam approached yield, flexural cracks outside the moment span began to "bend over" and become flexural-shear cracks. The ultimate strength of the beam was achieved when the concrete failed in compression in the moment span. Figure 5.30 shows the concrete compression failure mode. The loading was continued after the concrete compression failure and the load seemed to stabilize for a period of time until a secondary load drop was seen.
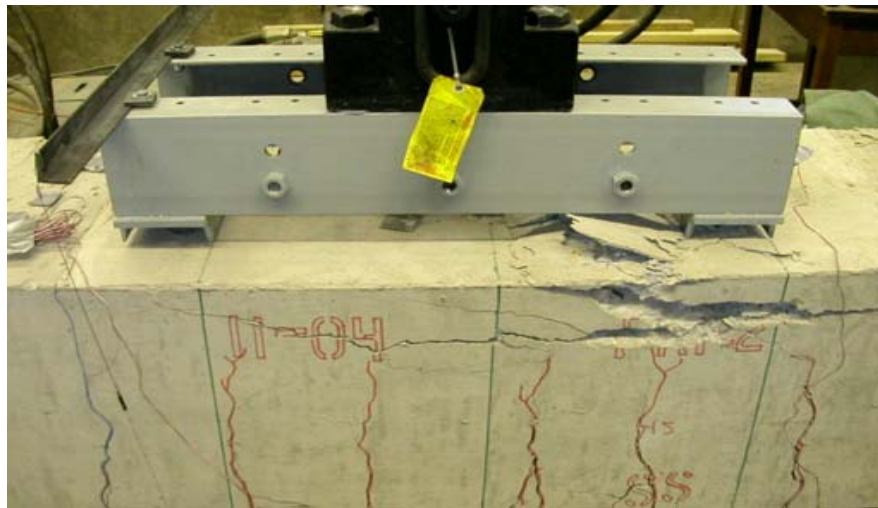
Figure 5.30. Concrete compression failure in beam FRP 2SS

The load at yield was 37.8 kips corresponding to a moment of 177 k-ft. The ultimate load of 60.9 kips was obtained corresponding to a moment of 286.9 k-ft. The yield strength

increase was 23.3 percent while the ultimate strength increase was 37.5 percent. An overall increase in stiffness, strength and ductility was seen. Figure 5.31 shows the comparison between beam FRP 2SS and the control beam C-1.
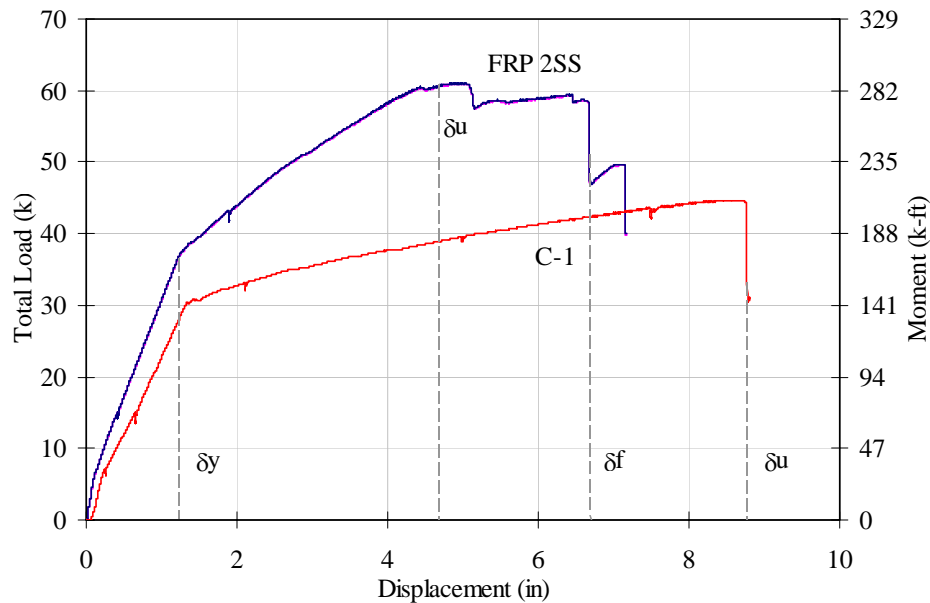
Figure 5.31. Comparison between FRP 2SS and C-1

After the failure of the beam, it was turned over to study the behavior of the FRP strip. Similar to FRP 1, slotting or bearing of the strip near the fasteners was clearly visible. Figure 5.32 shows the bearing failure of the FRP strip at the fasteners.

Figure 5.32. Bearing failure seen at fasteners in beam FRP 2SS

The FRP strips, however, showed no slotting at either end of the beam. Figure 5.33 shows one of the ends of the strip. Similar behavior was seen on the other end of the FRP strip.

Figure 5.33. FRP strip at the end for beam FRP 2SS (post failure)

The secondary failure mode seen was attributed to the rupture of the FRP strip. This can be seen in Figure 5.34, which shows a "splintered" strip.

Figure 5.34. Rupture of FRP strip in beam FRP 2SS

A horizontal splitting shown in Figure 5.35 was observed. While the location of the rupture could not be pinpointed it was clear that it occurred near one of the load points.

Figure 5.35. Horizontal splitting of the FRP strip in FRP 2SS

It appears that the FRP splitting rupture was due to damage caused by the stainless steel washers. Figure 5.36 shows the splitting initiating at a fastener location.
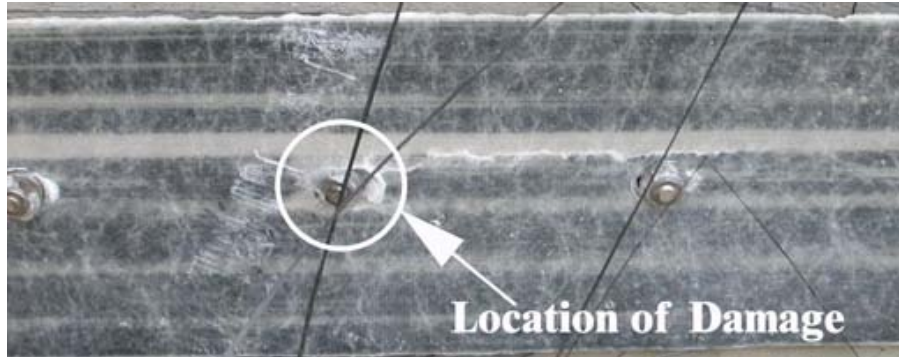
Figure 5.36. Horizontal splitting at a fastener location

It is believed that at the time of the installation of the stainless steel fasteners, the stainless steel washer damaged the FRP strip due to the lack of a neoprene backing.   Under high tensile loads, once bearing in the FRP strip was initiated, the embedded washer in the FRP strip created horizontal failure plane in the strip. This mechanism is illustrated in Figure 5.37.
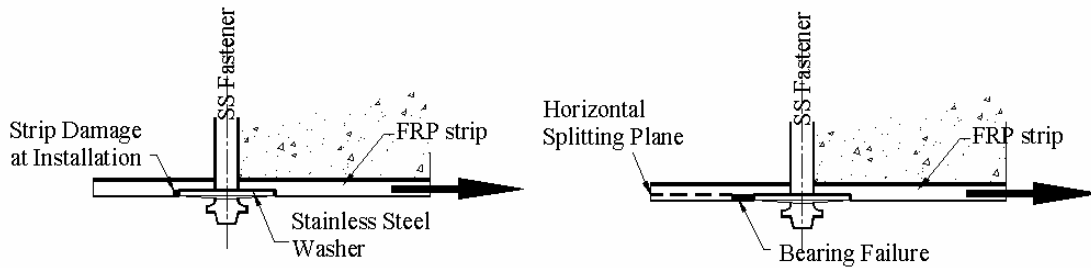
Figure 5.37. Failure mechanism at location of the stainless steel fastener

Figure 5.38 shows the strain distributions in FRP 2SS.   The strain distribution is similar to beam FRP 1. Figure 5.39 shows the variation of the maximum strains versus depth of concrete beam with increasing applied moment.
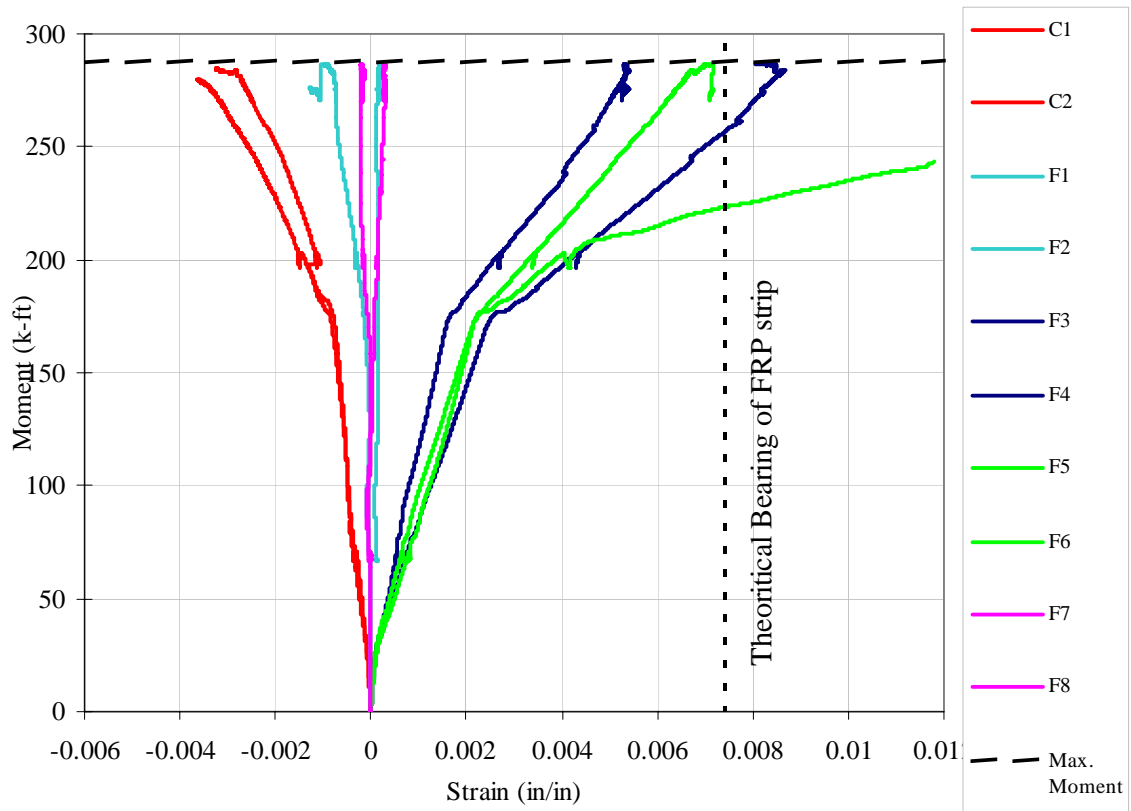
Figure 5.38. Strain distributions for FRP 2SS
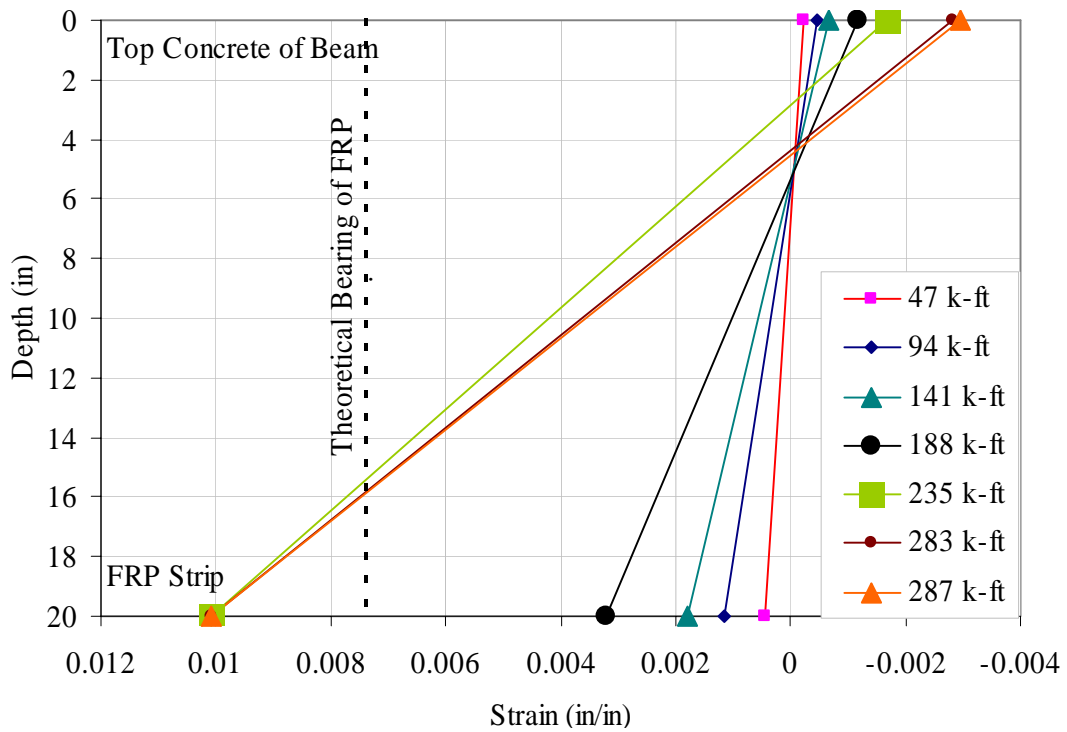
Figure 5.39. Variation of FRP strain through the depth of the beam FRP 2SS

87

The movement of the neutral axis is clearly seen in the Figure 5.39. Initially, the upward movement of the neutral axis is seen. At the ultimate moment of 287 k-ft concrete compression failure occurred and the neutral axis dropped down. In comparing the results of the two strengthened beams, FRP 1 and FRP 2SS, similar trends are seen. Figure 5.40 shows the moment versus displacement behavior of the two strengthened beams with the control beam.
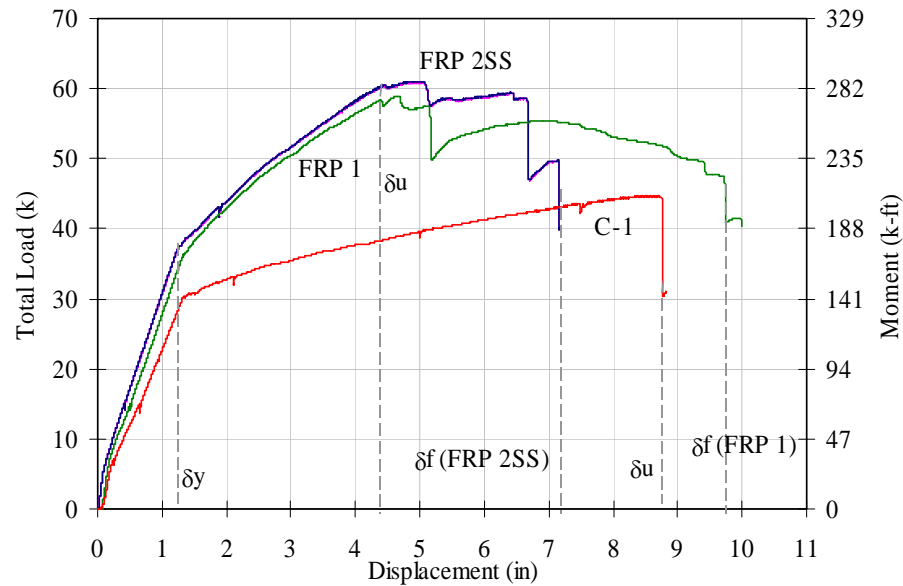
Figure 5.40. Comparison between beams FRP 1, FRP 2SS and C-1

The two strengthened beams failed in concrete compression at almost identical displacement. While the FRP 2SS showed a slightly greater increase in capacity, its final ductility was reduced as compared with FRP 1. At the final stage, the ductility ratio for FRP 2SS was calculated at 5.6, while FRP 1 showed a ductility ratio of 7.0.

Beam FRP 3

Beam FRP 3 was strengthened with three FRP strips to examine the effects of increased FRP reinforcement. In addition the objective of the test was to observe the effects of cyclic loading on the strengthening system. Figure 5.41 shows the load versus displacement behavior of the beam.
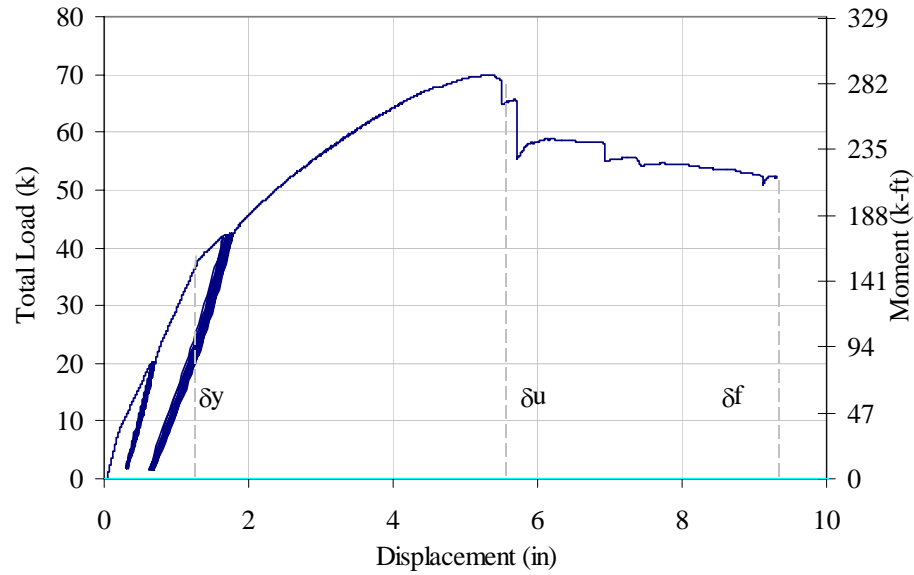
Figure 5.41. Load/Moment versus displacement for beam FRP 3

The two breaks in the load history correspond to the cyclic loadings. Figure 5.42 shows the small decrease in the stiffness for the elastic cyclic loading. Figure 5.43 shows a similar behavior during the cyclic loading applied after the yielding of the steel reinforcement.
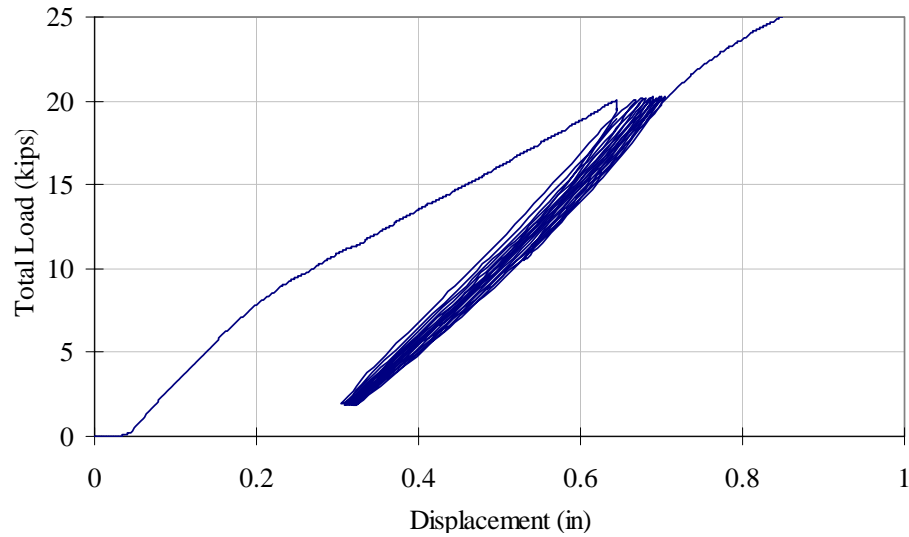
Figure 5.42. Load vs. Displacement plot for elastic cyclic loading on FRP 3
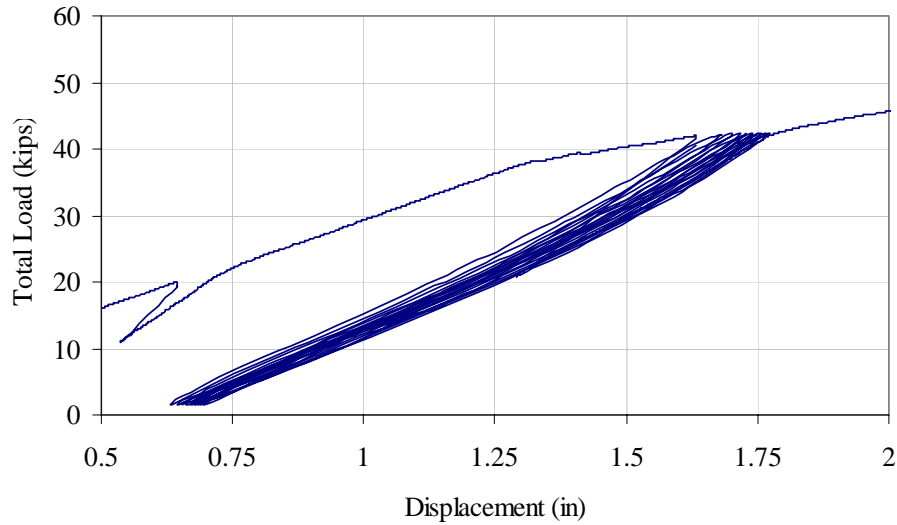
Figure 5.43. Load vs. Displacement plot for inelastic cyclic loading on FRP 3

It can be noted that a decrease in relative displacement is seen by the tenth cycle showing the beam has stabilized and that a permanent set has been added to the beam. The behavior of the strengthened beam was similar to that of other strengthened beams. The ultimate failure mode was also similar and the beam failed when the concrete in the moment span failed in compression. Figure 5.44 shows the concrete compression failure mode for the FRP 3 beam.
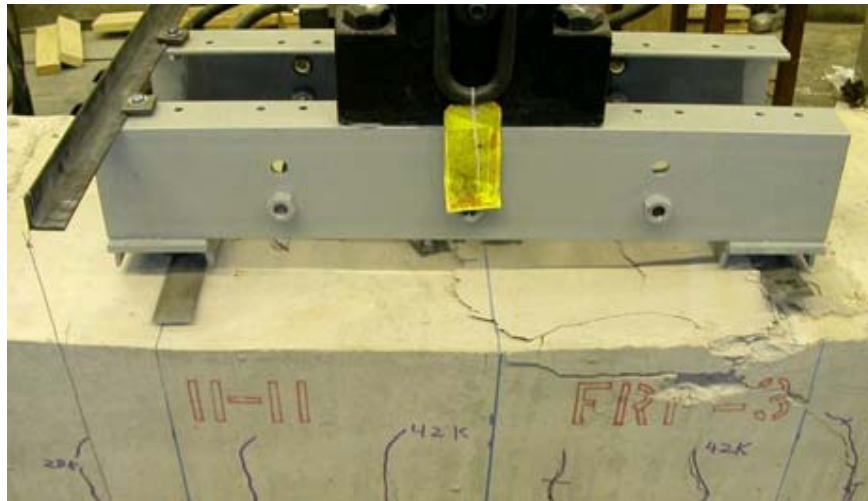
Figure 5.44. Concrete compression failure of FRP 3

An increased stiffness in the elastic and inelastic regions of the loading history was seen for the beam. The load at yield of 38.2 kips was obtained corresponding to a moment of 180 k-ft. The ultimate load of 69.9 kips was obtained corresponding moment of 330 k-ft. The yield strength increase was 25.2 percent while the ultimate strength increase was 58.1 percent. Figure 5.45 shows the comparison between beam FRP 3 and the control beam C-1.
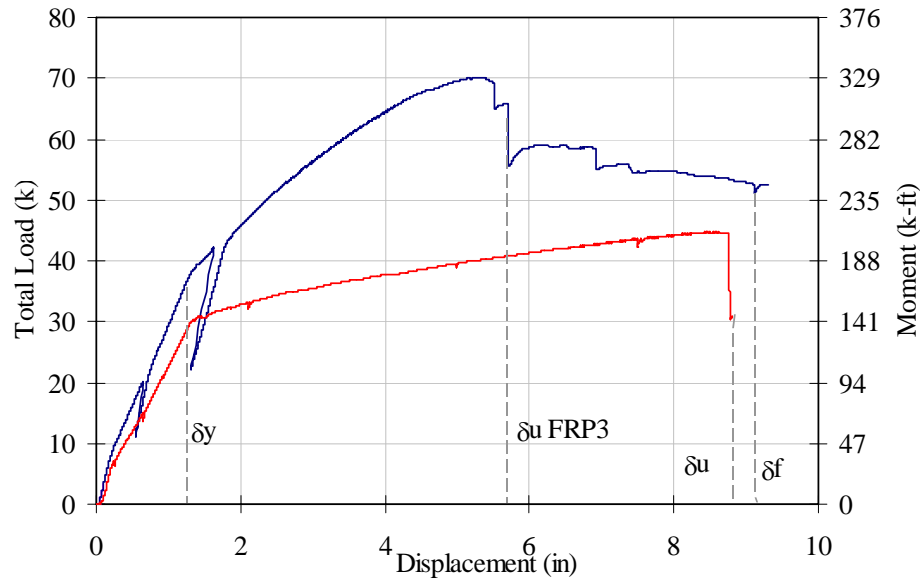
Figure 5.45. Comparison between beam FRP 3 and beam C-1

The ultimate ductility ratio of the strengthened beam was 4.0, however, the final ductility ratio was significantly higher at 7.0. Figure 5.46 and Figure 5.47 show the strain distributions for the beam. The strain versus depth relationship for the beam shows the upward movement of the neutral axis while a negative compression strain at the ends of the beam is seen due to reverse curvature. After concrete compression the beam carried a considerable load. While the strengthened beam continued to hold a substantial amount of load a secondary failure mode was observed.
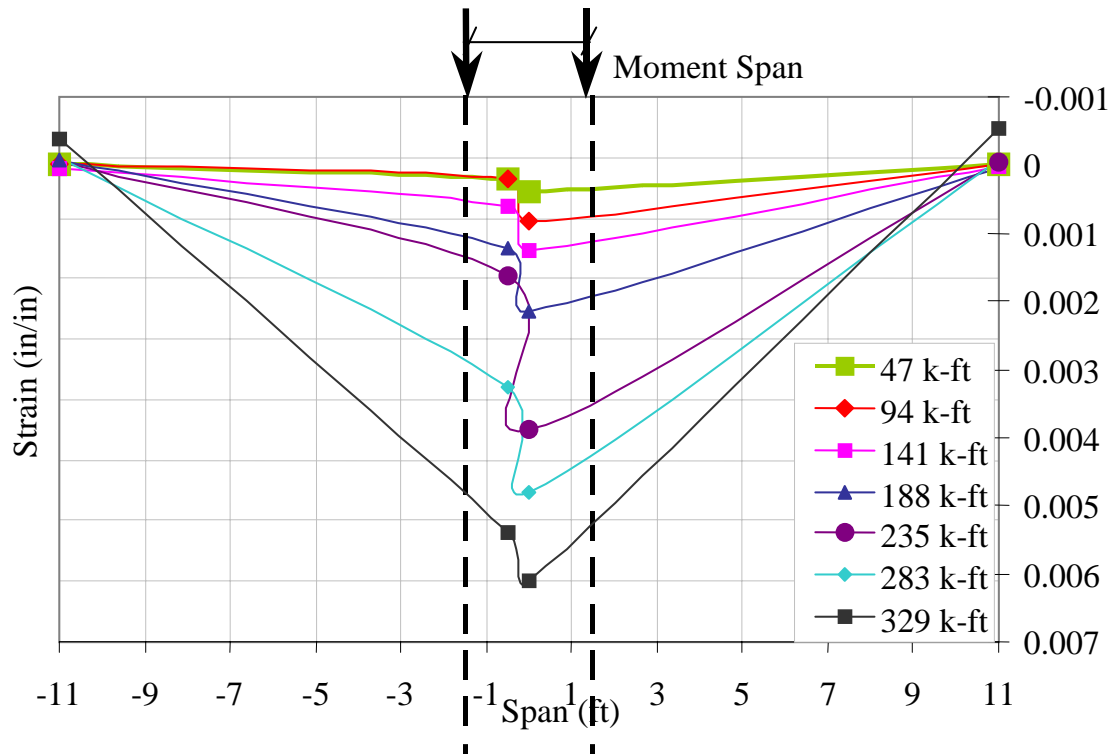
Figure 5.46. Maximum strain distribution for beam FRP 3 along the beam length
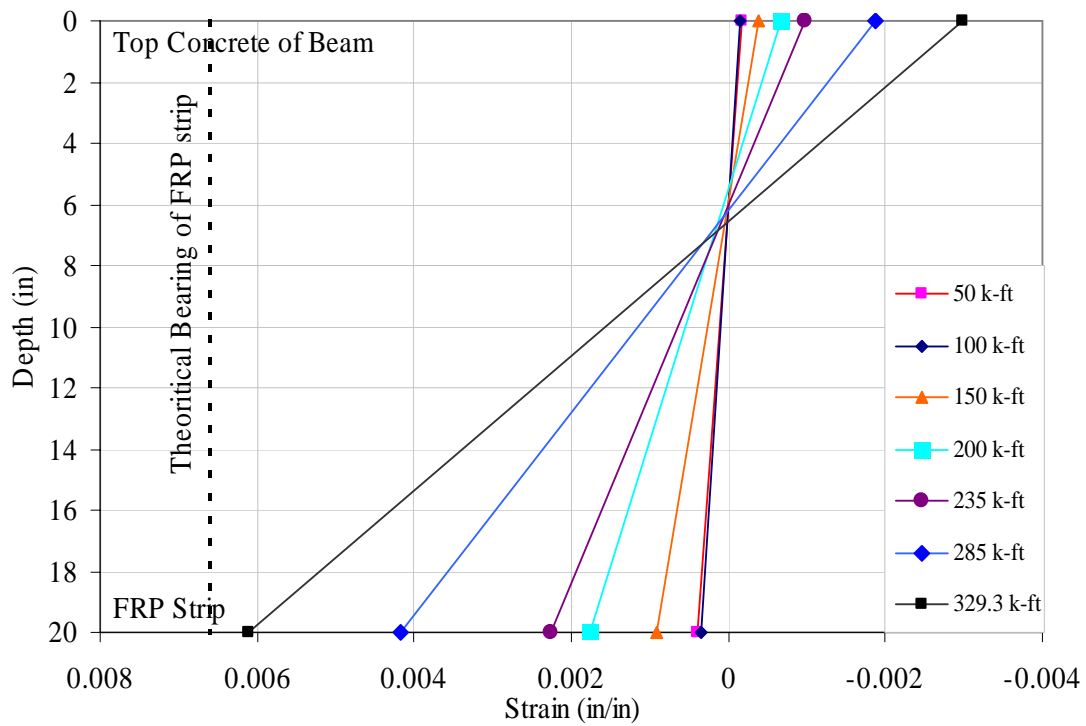
Figure 5.47. Variation of FRP strain through the depth of beam FRP3

92

A cover delamination failure near one of the supports was seen. Figure 5.48 shows the progression of the failure mode.

(a)
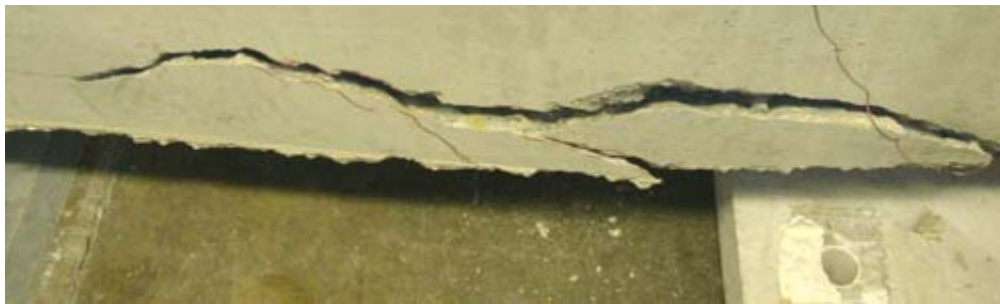
(b)

(c)

Figure 5.48. Cover failure in FRP 3 (a) Crack in the shear span (b) Propagation in concrete cover (c) Cover failure

Following the cover failure the beam finally failed by anchorage pull out. Figure 5.49 shows the pullout failure of the anchors.

Figure 5.49. Final end-anchor pullout failure in beam FRP 3

The failure mode of beam FRP 3 beam was similar to the failure mode seen in FRP 1. However, in FRP 1 the initiator was a flexural-shear crack near the load point. For FRP 3 the failure was initiated by a shear crack in the shear span of the beam. This is a typical failure mode seen in bonded FRP systems and called a concrete "rip-off" failure (FIB, 2001) or an "end peel off" failure (Saadatmanesh and Malek, 1998; Sebastian, 2001). This "rip-off" or "end peel" failure mechanism is activated when the shear stress near the plate end reaches a critical value. The "end peel off" mechanism also explains the eventual anchorage pullout failure. In a recent study conducted on delamination modes of bonded FRP strips, Sebastian (2001) proposes that a reverse bending of the FRP strips is seen in order to develop zero net curvature of the FRP strips at the ends. The reverse bending of the FRP strip causes a high normal stress gradient at the ends of the strip causing the anchors to pull out vertically. Figure 5.50 illustrates the failure mode of end peel off.
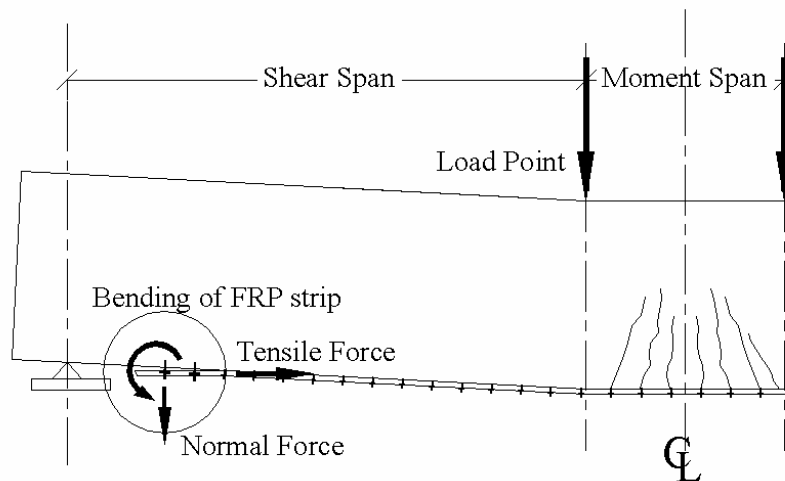
Figure 5.50. Anchorage pullout at the end due to reverse bending of the FRP strip

After the test was completed, the beam was turned over to study the FRP strip. Bearing or slotting of all three FRP strips was observed. Figure 5.51 shows the slotting in one of the FRP strips for FRP 3.

Figure 5.51. Bearing failure mode in FRP strip in beam FRP 3

Discussion on Strain Distribution

As discussed previously, strain gages were attached to the FRP strips in the moment span of the beams and on the compressive face of the concrete beam. Strain gages were also attached to the FRP strips near the supports. Negative strain corresponds to compression and positive strain to tension in the material. The following trends can be seen from the strain distributions:

- Significant strain was measured in the FRP strips confirming the composite behavior of the FRP strip with the reinforced concrete section.

- All strain gauges at the center of the moment span confirmed the crushing of concrete close to a strain of -0.3%.

- Some variability was seen between the strain readings in the moment span. Strains in the concrete and the FRP strips near the load point were higher than the one at the center. This difference may be attributed to local affects in the FRP strip near the locations of the fasteners. The difference however was not significant.

- Some variability was seen in the strain readings in the FRP strips. Higher strains were measured in an FRP strip that failed compared with the strip alongside it. Both average and maximum strains were used in what follows to calculate the stress in the FRP strips.

- The lowest average strain measured in an FRP strip at ultimate failure was 0.55% and the largest average strain in an FRP strip was 0.85%. It can therefore be concluded that all strains in the steel rebar were greater than 0.5% at the ultimate failure.

- The strain distribution through the depth of the section can be used to relate the strain in the concrete to the strain in the FRP strip. The strain history is consistent with the increase in the applied moment. The pre-yield, post-yield and concrete crushing strain measurements clearly show the behavior of the internal forces and the movement of the neutral axis. As the

95

applied moment increased the graphs show an upward movement of the neutral axis. After yielding of the steel reinforcement, the plots show an increase in strain in the FRP strips showing their contribution to the larger internal moment.

- The most important relationship that can be seen in the graphs is the relationship of theoretical strain value at bearing failure of the FRP strip with the strain at ultimate. The theoretical strain corresponding to the bearing of the strip was reached in the FRP strip in beams FRP 1 and FRP 2 at a point in time halfway between the yielding of the steel and the ultimate moment of the beam (Arora, 2003). For the FRP 3 beam, this threshold bearing strain value was not achieved at the ultimate load.

- The strain readings in the FRP strips near their ends were close to zero or negative indicating compression. The largest negative strain seen at the ends of the strips was seen for FRP 3. At ultimate failure the reading was –0.08 % while at the final stage the strain was as high as -0.1 %. The negative strain in the strips is attributed to the reverse bending of the FRP strips and is consistent with anchorage pullout seen in beam FRP 3.

Discussion on Fastener Loads

The strain in the FRP strips at the ultimate load can be used to calculate the force per fastener in the shear span. Table 5.8 shows the average and maximum strains measured in the FRP strips and the calculated fastener loads. The average strain is calculated from the strains measured in each strip.

Table 5.8. Strain and Fastener Force in Laboratory Beams at Ultimate Load						
Beam	FRP Strain		FRP Stress (ksi)		Force per Fastener (lbs)	
	Average	Maximum	Average	Maximum	Average	Maximum
FRP 1	0.0066	0.0075	58.74	66.75	734	834
FRP 2SS	0.0085	0.0100	75.65	89.00	946	1110
FRP 3	0.0055	0.0061	48.95	54.29	612	679
Note: Modulus of strip used = 8,900 ksi, Area of FRP strip = 0.5 in^2 Number of fasteners in the shear span = 35 + 2 end anchor bolts (Each anchor is assumed to carry 2.5 times the fastener load based on the ratio of diameters of the anchor and the fasteners)						

Both the maximum strain and the average strain readings were used to calculate the amount of force at each fastener. The stress in the FRP strip was calculated using the elastic modulus of the FRP strip. The force in the strip was then calculated using the area of the strip and is distributed evenly to the number of fasteners. It is assumed here that all the fasteners experience the same load. The following conclusions can be made:

- The largest force per fastener of 1110 lbs was seen for beam FRP 2SS where the final failure mode was FRP rupture.

- The maximum force per fastener of 1110 lbs is comparable to the 1000 lbs of force per fastener seen in experimental connection tests and recommended for design by Lamanna (2002).

- The lowest 679 lbs force per fastener was seen for beam FRP 3 where three strips were attached. Bearing failure was not reached in the fasteners when beam FRP 3 reached its ultimate load.

- The stainless steel washers appeared to cause premature failure of the strip and did not transfer load to all fasteners in a uniform fashion at the ultimate load.

Analysis of Results

As discussed previously, the results obtained from the experimental beams obtained were used as the control data for the unstrengthened and strengthened capacity of the bridge. The first step needed for this processes was to scale the results of the laboratory tests to a unit width in order to relate the results of the laboratory beams to the required capacity of the bridge. As discussed previously, the beams were representative of an approximately two-unit width section of the bridge. Therefore to obtain data for a unit width section of the bridge, the results were scaled by a factor of 0.6 based on the ratio of the FRP reinforcement per unit width. The scaled capacities of the beams were also compared at a displacement corresponding to L/64, which is significantly higher than typical design limits. This was done to compare the relative improvement in strengthening without the effect of strain hardening in the control beam.

Tables 5.9, 5.10 and 5.11, show the scaled results for the yield, at a L/64 displacement and at the ultimate capacity of the laboratory beams.

Table 5.9. Beam Yield Moments per Unit Width			
Beam	Yield Moment	Yield Moment per Unit Width	Increase
	(k-ft)	(k-ft/ft)	%
C-1	143.6	86.2	-
FRP 1	169.8	101.9	18.2
FRP 2SS	177.0	106.2	23.2
FRP 3	180.0	108.0	25.3
		Average	22.2
		Average for FRP 1 & FRP 2SS	20.7

Table 5.10. Beam Moments @ L/64 Displacement per Unit Width			
Beam	Moment @ L/64	Moment @ L/64 per Unit Width	Increase
	(k-ft)	(k-ft/ft)	%
C-1	177.2	106.3	-
FRP 1	265.1	159.1	49.7
FRP 2 SS	273.9	164.3	54.6
FRP 3	302.7	181.6	70.8
		Average	58.4
		Average for FRP 1 & FRP 2SS	52.2

Table 5.11. Beam Ultimate Moment per Unit Width			
Beam	Ultimate Moment	Ultimate Moment per Unit Width	Increase
	(k-ft)	(k-ft/ft)	%
C-1	208.7	125.2	-
FRP 1	277.2	166.3	32.8
FRP 2 SS	286.9	172.1	37.5
FRP 3	329.9	197.9	58.1
		Average	42.8
		Average for FRP 1 & FRP 2SS	35.2

The results obtained per unit width show an average increase in the capacity of the bridge of more than 50% corresponding to a limit of L/64 and 35% at the ultimate stage. As discussed previously, a 29% increase in the flexural capacity is required to improve the existing Inventory Rating (IR) of the bridge from HS17 to HS25. Figure 5.52 shows graphically the comparison of the scaled experimental results and the nominal capacity requirements for different rating levels.
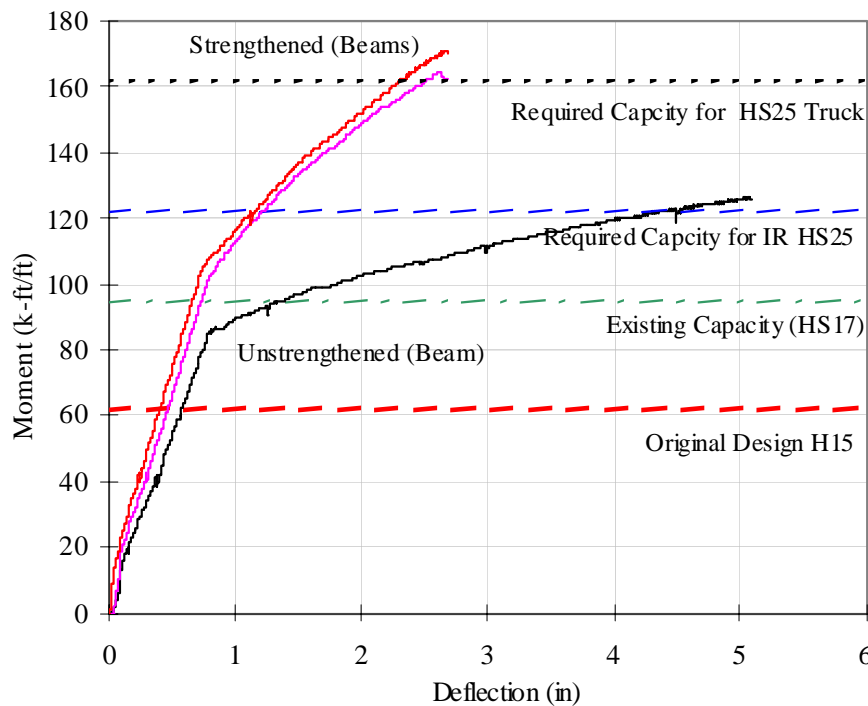
Figure 5.52. Results of laboratory beams compared with different levels of Inventory Ratings

The results obtained from the laboratory beams are compared with predictions made using Strength and Moment-Curvature (M-C) models.   Table 5.12 compares the scaled results of the laboratory beams with the models.

Table 5.12. Comparison of Test Results with Theory					
Beam	Scaled Ultimate Moment per Unit Width	Strength Model	% Diff	M-C Model	% Diff
	(k-ft/ft)	(k-ft/ft)		(k-ft/ft)	
C-1	125.2	94.6	- 24.4	117	-7.0
FRP 1	166.3	154.8*	-7.4	165**	-0.8
FRP 2 SS	172.1		-11.2		-4.3
% difference from experimental =		$\dfrac{\text{calculated} - \text{test}}{\text{test}}$			x 100
* Concrete Compression Failure mode ** FRP rupture Failure mode					

Figure 5.53 shows graphically the comparison of the scaled experimental results and the models used for design.
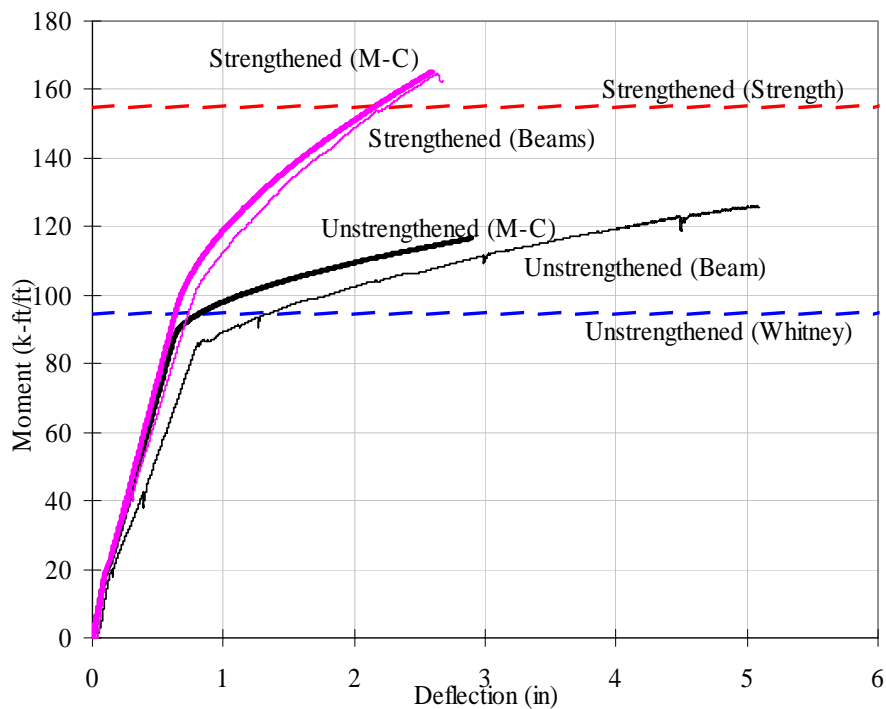
Figure 5.53.   Comparison of predictions from moment-curvature model and strength model with scaled test results (predictions shown in bold and dashed lines)

A -7 % difference is seen between the Moment-Curvature model (Lamanna, 2002) and the test results and a -24% difference is seen between the Strength model and the test results. A negative difference is conservative as both models under predict the capacity of the beams. However, two different failure modes were predicted. As discussed earlier, the M-C model predicted an FRP rupture as the failure mode, while the Strength model predicted a concrete compression failure mode. As observed in the experimental beams a concrete compression failure mode was seen. These shortcomings of the models used for preliminary design and the

predicted failure modes need to be studied in more depth and modifications to the M-C model should be made using this new knowledge gained from the laboratory tests.

General Behavior and Discussion of Strengthened Beams

It can be seen from the laboratory tests that the strengthened beams show increased stiffness both in the elastic and inelastic range, in addition to increased ultimate capacity. The ability of the FRP strip to contribute additional tensile force to the reinforced concrete section is a function of the mechanical behavior of the attached FRP strip. The tensile force in the FRP strip is developed by load transfer through the fasteners located in the shear span (like shear studs in a "composite" beam). Figure 5.54 shows the mechanism for the transfer of the tensile force to the FRP strip.
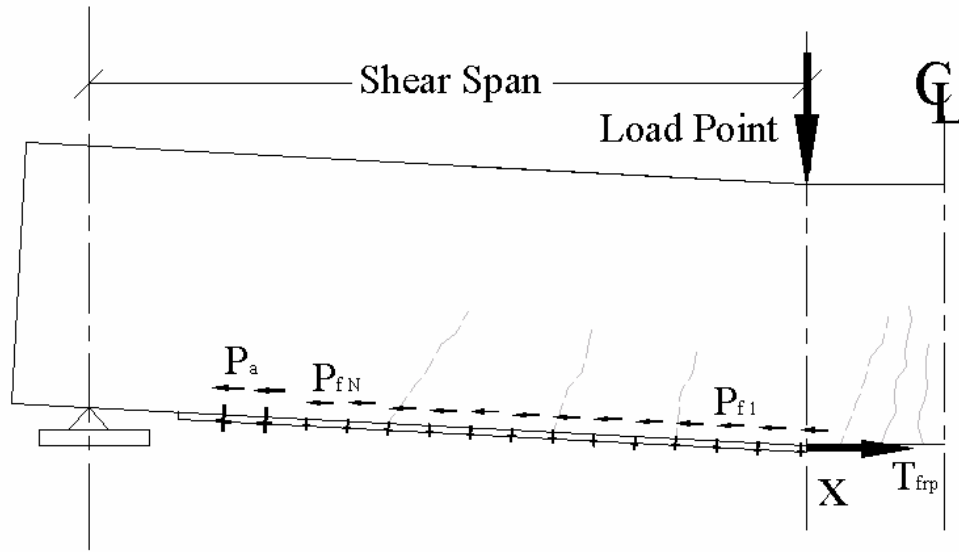
Figure 5.54. Transfer of force to the FRP strip through the individual fasteners and anchor bolts

The tensile force in the FRP strip is developed as force is transferred by the individual powder actuated fasteners ($P_{f1....N}$) and the end anchors ($P_{a\,1..M}$). For force equilibrium in the X-direction,

$$\sum F_x = 0$$

(5.3)

$$T_{frp} = \sum_{1}^{N} P_f + \sum_{1}^{M} P_a$$

where, T_{frp} is the tensile force at section X in the FRP strip, P_f is the force transferred by a powder actuated fastener and P_a is the force transferred by an end anchor.

From the strain readings in the strengthened beams, it is seen that as the applied moment on the beams increased, a bearing failure occurred in the FRP strip sometime after the yielding of the steel reinforcements. The bearing of the FRP strip is initiated at the location of the highest strain, in this case, in the moment span. Once bearing is initiated, the fastener load corresponding to the bearing of the FRP strip is achieved at this location no additional load can be transferred by this fastener (i.e., the load remains constant as progressive bearing failure occurs at the location of the fastener.) Additional load is then transferred to next fastener, which then undergoes a bearing failure and so on until all the fasteners have reached their bearing load. This leads to a pseudo-ductile failure mode in the FRP strip. In order to maintain displacement compatibility larger slotting (progressive bearing failure) must occur at the ends of the FRP strips than in the middle.

For beams FRP 1 and FRP 3, the large amount of slotting seen at the ends is consistent with this behavior. However, for FRP 2SS, no slotting was seen at the ends. This appears to be due to the fact that the embedded stainless steel washers in the FRP strips caused internal failure in the interior of the span. Force re-distribution was not achieved and larger forces were seen at the fasteners since load was not transferred to all the fasteners. The idealized behavior of the MF-FRP strengthened beam may therefore be represented diagrammatically as shown in Figure 5.55.
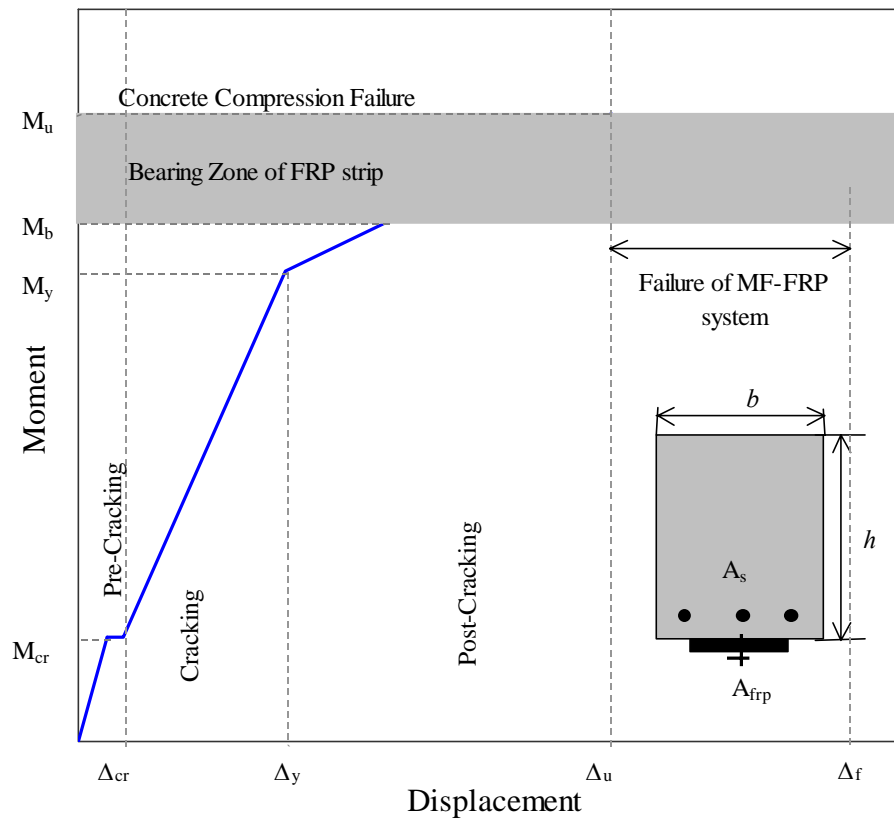
Figure 5.55. Idealized moment versus displacement behavior of MF-FRP strengthened beams

The drop in capacity seen after concrete compression failure is dependent on the amount of confinement offered by the concrete beam. While no further strength gain is achieved after concrete compression, the beam carries a considerable amount of load. The amount of load sustained by the beam and the displacement at which final failure of the beam occurs depends on the detailing of the strengthening system.

In the laboratory beams after compression failure of the concrete occurred, a final failure of the strengthening system was observed. In beam FRP 1 a shear-out failure of the FRP strip at the end was observed. The beam eventually failed by cover delamination, however the bearing failure of the FRP strip at the ends could have sustained loads for a longer period. In beam FRP 2SS the stainless steel washer initiated the final failure mode due to FRP rupture and a smaller period of sustained load carrying capacity was seen for the beam after concrete compression failure. In beam FRP 3, the final failure mode was pullout of the end anchors.

Laboratory Testing Conclusions

The laboratory tests conducted to obtain control data for the unstrengthened and the strengthened capacity of the Edgerton bridge have confirmed the behavior of MF-FRP strengthening system for RC beams. All beams strengthened demonstrated significant strength increases along with a ductile final failure mode. The following conclusions can be drawn from the tests:

- The strengthened beams showed an increase in yield and ultimate moment of up to 25.2 and 58.1 percent respectively. A larger increase of 70.8 percent was seen for the strengthened beams corresponding to a deflection of L/64.

- All the strengthened beams showed an increased stiffness in both the elastic and inelastic ranges and failed ultimately due to concrete compression. A significant improvement in the elastic and inelastic stiffness of the beams was seen.

- A significant amount of ductility was seen for the beams. As expected a decrease in the ductility at the ultimate load of the beam was seen. However, the final ductility ratios demonstrated that the FRP strip did not detach until much later in the loading history.

- All the beams showed a sustained bearing failure of the FRP strip at the final failure of the beams leading to a ductile failure mode of the beams.

- The final failure mode seen after concrete compression is attributed to the failure of the strengthening system and ranged from cover delamination for FRP 1 to FRP rupture for FRP 2SS and anchorage pullout for FRP 3.

- The smaller size X-CR stainless steel fasteners used for FRP 2SS provide similar strength increase as the X-ALH fasteners, however the initial damage caused by the washers appears to have decreased the ductility of the beam as compared to the FRP 1.

- The strains measured in the FRP strips confirmed the composite behavior of the FRP strips and provided useful information on the bearing failure modes observed.

- For FRP 1 and FRP 3 bearing was seen at all fastener locations in the shear span of the beams and the ends of the FRP strips. For FRP 2SS bearing was not seen at all the fastener locations in the shear span only. The stainless steel washers, which inhibited the load transfer to other fasteners, caused a brittle FRP rupture failure mode.

- The larger FRP reinforcement ratio for beam FRP 3 produced a larger increase in strength of the strengthened beams.

- The cyclic loading on beam FRP 3 showed no evidence of causing damage to the strengthening system. Some loss of stiffness was seen due to the cyclic loading in both the elastic and inelastic regimes adding a permanent set in the displacements. However, the displacement difference decreased to a small amount by the tenth cycle showing the beam has stabilized.

- The level of strengthening obtained in beams FRP1 and FRP 2SS of 32% and 37% respectively, met the 29% nominal moment increase requirement for strengthening of the Edgerton Bridge from HS17 to HS25 based on a unit width capacity. This was achieved with a single FRP strip at 12 in. on center and fasteners at 3 inches on-center along the strip length with two end-anchors at each end.

- The level of strengthening obtained in beam FRP 3 of 58% significantly exceeded the 29% nominal moment increase requirement. This was achieved with a FRP strip at 6 in. on-center and fasteners at 3 in. on center along the strip length with two end-anchors at each end.

- The strength predictions obtained using a moment-curvature model and a strength model compared well with the test strengths. The use of the strength model for design calculations is recommended. The load-deflection predictions of the moment-curvature model are reasonably well correlated with the test results. However, the M-C predicts a premature failure due to FRP rupture that was not observed in the testing. Further work is required to refine the moment-curvature model before it can be used in design to predict failure modes and deflections of MF-FRP strengthened beams.

6 Ultimate Load Testing and Performance of Bridge P-53-702

General

As detailed previously, bridge P-53-702 in the City of Edgerton, Wisconsin, was strengthened in August 2002 using the MF-FRP system by attaching fiber-reinforced polymer (FRP) composite strips with powder-actuated fasteners to the underside of the bridge deck. The purpose of the strengthening was two-fold. First, researchers wanted to demonstrate the practicality of the installation method on a real-world structure. Attaching FRP composite strips had proven efficient in terms of manpower and time in the laboratory, but this efficiency needed to be shown in an implementation on an existing structure. Second, three years of studies had proven that the MF-FRP method increased the flexural capacity of laboratory specimens ranging from small-scale model beams to typical full-scale bridge beams (Bank et al, 2002a; 2002b; Borowicz, 2002). The aspects of the implementation have been discussed in Chapter 4. In June 2003, ten months after the installation of the FRP strips on the bridge the MF-FRP strengthened bridge was tested to failure prior to its demolition and eventual replacement. In addition to providing data on the capacity and behavior of the strengthened bridge, the effect of 10 months of environmental exposure on the MF-FRP system was evaluated.

The testing was conducted over a period of five days from June 16th to June 20th, 2003. The testing was a joint project conducted by the University of Wisconsin – Madison and the University of Missouri – Rolla. Assistance was also provided by the United States Military Academy at West Point. The Wisconsin Department of Transportation and the United States Army Corps of Engineers provided funding for the investigation. This chapter outlines the in-place load testing procedures, documents the results of the testing, and draws conclusions as to the effectiveness of the strengthening method.

Objectives

The objectives of the ultimate load testing of Bridge P-53-702 were as follows:

- To conduct load testing to failure of two sections of the strengthened bridge.

- To document failure modes of each test section.

- To gather data on the following: load applied to test sections; deflections of test sections; strain in FRP composite strips; and strain in concrete in compression zone.

- To synthesize the raw data into load versus deflection, moment versus deflection curves, and strain versus deflection plots.

- To determine the flexural capacity of strengthened test sections and compare them to the capacity of an unstrengthened section tested in the laboratory.

- To document any effects on the FRP composite strips or the powder-actuated fasteners due to the environment.

- To determine the in-situ properties of the materials (rebar and concrete) used in Bridge P-53-702.

- To characterize the mechanical properties of FRP strips before and after service.

Test Preparation

General

In order to conduct the testing of the strengthened bridge, two test sections were isolated from the rest of the bridge deck, a field loading system was erected, and a data acquisition system and instrumentation were configured. This was accomplished as follows:

Cutting of Bridge Deck

When constructed in 1930, Bridge P-53-702 had a twenty-inch thick reinforced concrete deck. Over the years, however, this deck thickness was increased to nearly twenty-six inches with the addition of an asphalt overlay. As such, the contractor hired to isolate the two test sections had to use a concrete saw with a fifty-four inch diameter blade. Figure 6.1 shows the contractor making his initial cut (Cut #1) in the bridge deck.

Figure 6.1. Contractor cutting the bridge deck (Cut #1)

Utilizing a rebar locator and construction drawings from the late 1920's, investigators chose the locations of the three longitudinal cuts. The first cut was made six inches west of the

centerline of the bridge and served as the boundary between the two test sections. The second cut was made 43 inches west of the centerline, while the third and final cut was made 33 inches east of the centerline. The result was three cuts running the length of the bridge that separated two test sections. Figures 6.2 and 6.3 show views of the isolated test sections along the top of the bridge deck. Since the FRP composite strips were fastened 12 inches on center, both test sections contained three FRP strips spaced evenly across their respective widths. Figure 6.4 shows the bridge with the test sections marked.
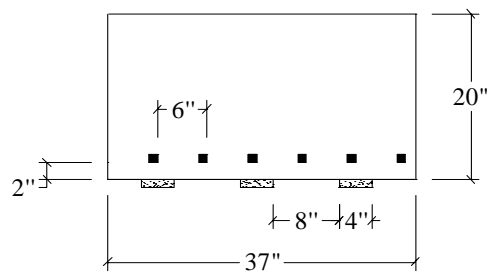
Figure 6.2. Transverse view of west section   Figure 6.3. Transverse view of east section
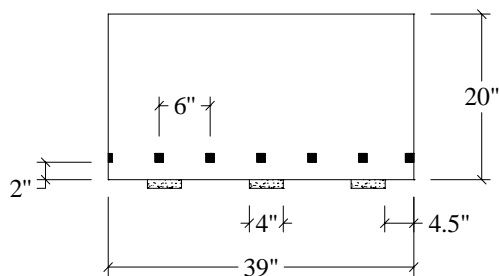
Figure 6.4. Test sections (looking north)

Despite using the largest concrete saw blade available (25-inch cut depth), the contractor was not able to cut through the entire depth of the bridge deck along cuts one and three (See Figure 6.5). In fact, the saw blade never pierced the bottom of the bridge deck along cut one. The blade found its way through the entire depth of deck along cut #3 four feet from the north and south abutments. The result was that the two test sections were not completely separated. Rather, the east and west sections were connected by 1.5 inches of concrete cover along the entire span length at the bottom of the deck. The east section was also partially connected to the adjacent untested portion of the deck by less than one inch of concrete cover.
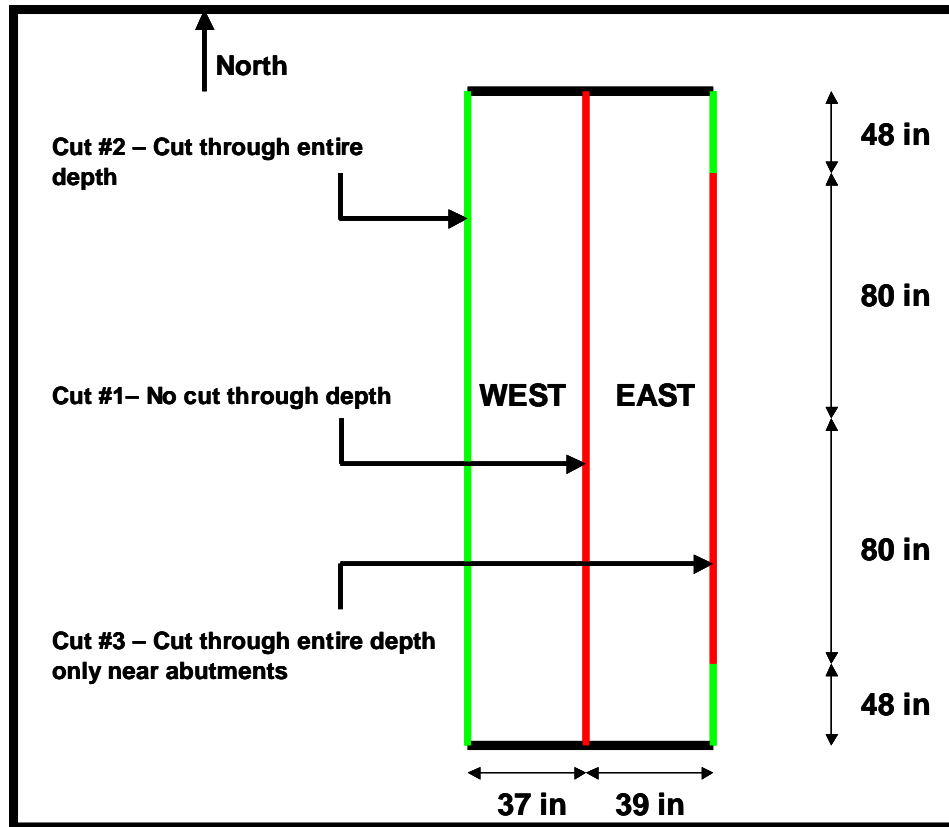
Figure 6.5. Top view of cut penetration

Drilling of Bridge Deck

Four holes were drilled through the full depth of the bridge deck for the installation of the test apparatus. Locations were positioned in accordance with the test assembly schematic and marked with fluorescent orange paint. In turn, the contractor drilled the three-inch diameter holes with a standard concrete coring machine. Figure 6.6 shows the contractor drilling the first hole through the depth of the deck.

Previously, a fifth core had been drilled on an outboard section of the bridge to check the depth of the deck and obtain a suitable concrete core for testing.   However, the concrete crumbled and thus prevented researchers from obtaining a specimen suitable for testing.

Figure 6.6. Contractor drilling through depth of bridge deck

Removal of Asphalt at Center of Test Sections

In order to measure the strain in the concrete at the top of the test sections (compression zone) and observe any compression failures, nearly six inches of asphalt overlay on the bridge deck were removed from the central portion of the test sections (See Figure 6.7) using a 40-pound jackhammer powered by a 250 cfm air compressor. The result was a two-foot long section that spanned both test sections and exposed the original surface of the concrete bridge deck.

Figure 6.7. Removing the asphalt overlay

Installation of Test Apparatus

The test apparatus consisted of the following components:

        a)   Two steel reaction beams
        b)   Two 100 kip hydraulic jacks
        c)   Four DYWIDAG bars with steel plates

These components were arranged in accordance with Figure 6.8 to provide the appropriate test configuration. This configuration placed the test sections in four-point bending with a shear span of 102 inches and a moment span of 52 inches.

First, the four DYWIDAG bars were inserted through the pre-drilled holes in the deck and secured with reaction plates and nuts on both the top and bottom of the deck. Then the 1400 lb north and south reaction beams were lifted on to the DYWIDAG bars with a forklift (See Figure 6.9). When the reaction beams were plumb and level, they were locked into place by tightening down the appropriate nuts. Next, in order to evenly distribute the applied load across the width of the test sections, the area under the jacks was leveled by placing a 36"x12"x1" steel plate on top of a layer of high-strength, quick-setting grout. After the grout cured, the jacks were centered on the steel plates, bringing them into contact with the reaction beams. Finally, members of the Rock County (Wisconsin) Department of Roads and Grounds positioned two dump trucks (loaded to a weight of 55,000 pounds) on alternate ends of the untested sections of the bridge to prevent these sections from lifting off their respective abutments during the testing.
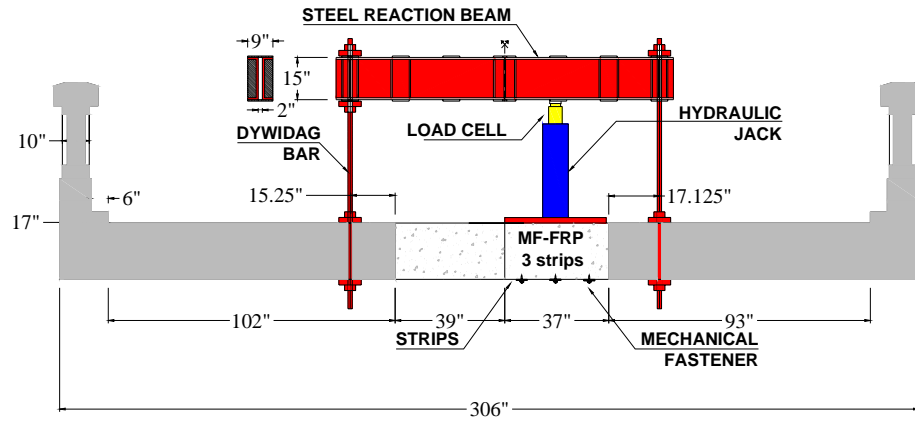
Assembly Details - Test of West Section
(dimensions in inches)
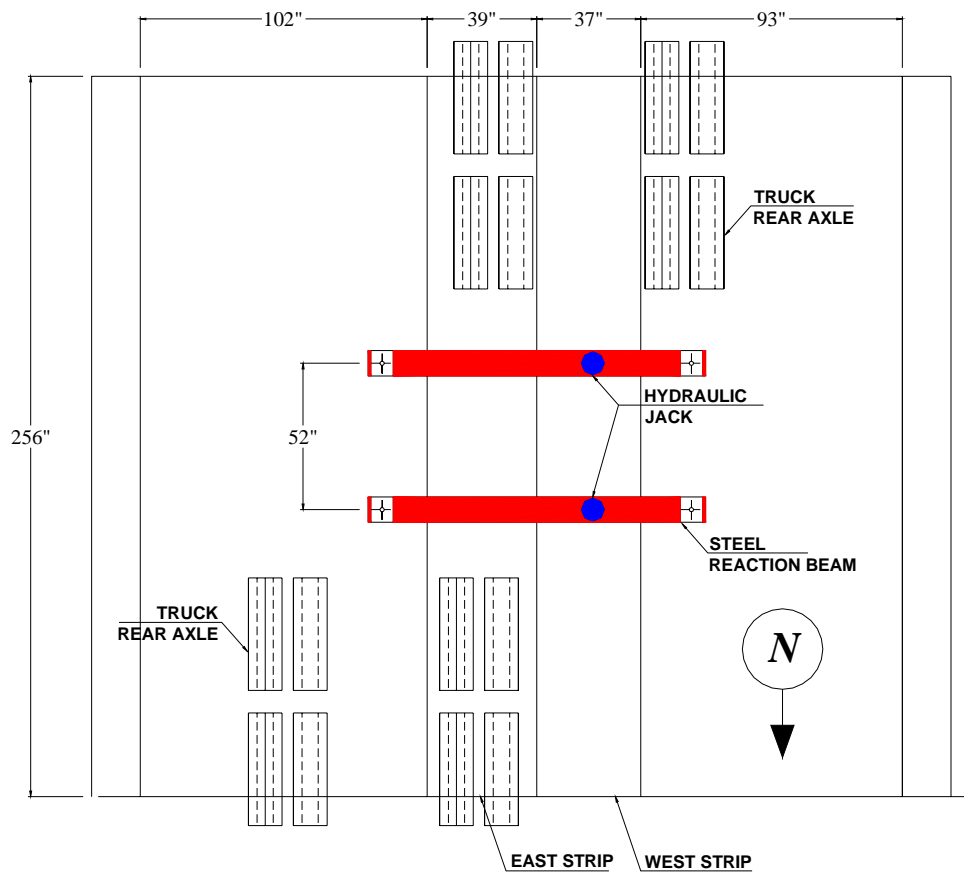
Figure 6.8. Schematic of test assembly

Figure 6.9. Placing the north reaction beam

Installation of Instrumentation

In order to collect sufficient data, nine DC-LVDTs were used to measure displacement and five 120-ohm strain gages were used to obtain the strain in the FRP composite strips fastened to the bottom of the bridge. Figure 6.10 shows the layout of the data collection assets for the west section, while Figure 6.11 shows the arrangement for the east section.

Bottom Sight: Vertical DCVTs (L#)   Ⓝ →

12.5"

● 9   8 ●   7 ● 5 ● 3 ●   2 ●   1 ●

4 ●

6 ●

37"

3 3/4" —48 1/2"— —48.75"— —48 3/4"— —50 5/8"— 3 5/8"

26 1/16"

25 7/8"

Top Sight: Horizontal DCVTs   Ⓝ →

9.5"

18"

9.5"

T-Right

T-Left

37"

3 3/4" —48 1/2"— —48.75"— —48 3/4"— —50 5/8"— 3 5/8"

26 1/16"

25 7/8"

Bottom Sight: Strain Gages and Horizontal DCVTs   Ⓝ →

see detail

18.5"

B-Right

a   b   c   e   d

B-Left

37"

Between the last
bolt and the first
fastener

7 1/8" —45 1/4"— —50 3/4"—

24 1/8"

Detail
Strain Gages

Fasteners in the middle of the strip

2"

1"

1"

e

d

Figure 6.10. West section instrumentation

112

Bottom Sight: Vertical (L#) and Horizontal DCVTs (N) ▶

9 (outside between the 2 loads applied)

17.125"

B-Right

4

39"

B-Left

1 (outside between the 2 loads applied)

15.5"

Top Sight: Vertical (L#) and Horizontal DCVTs (N) ▶

8.96"

B-Right

18"

5

B-Left

39"

9.75"

8● 7● 6● 3● 2●

50 1/4" — 48.75" — 48 3/4" — 54 5/16"

26 1/16"

25 7/8"

Bottom Sight: Strain Gages (N) ▶

see detail

a b c e d

39"

Between the last
bolt and the first
fastener

7" — 47 1/4" — 50 7/16" — 24"

*Detail
Strain Gages*

Fasteners in the middle of the strip

2"

1"

e

1"

d

Figure 6.11. East section instrumentation

113

Test Execution

General

Three major tasks were accomplished during the execution of the load test. First, since both the east and west test sections were still partially attached to adjacent sections, the first load cycle was used to crack the bottom cover that connected the respective sections. Second, a valid load-deflection curve that captured both the yield and ultimate loads of the strengthened test sections needed to be obtained. To that end, the manual application of the load (via hydraulic jacks and hand pump) in discrete cycles was carefully controlled. Finally, once the load had reached a plateau at its ultimate, the point at which the FRP composite strips failed needed to be identified. The intention was to accomplish this by continually applying load until a failure in the strips occurred. Figure 6.12 shows the final preparations prior to testing the west section.

Figure 6.12. Preparing to execute load test on west section

West Section (3 strips)

Since the west section was still connected to the east section at cut #1, the first load cycle was used to crack the 1.5" of concrete cover. This load cycle was started at zero and was taken to a total load of 20 kips (10 kips per jack). The load was then removed and a load sequence (See Figure 6.13) consisting of the following cycles began:

    a)   0 kips to 40 kips total load
    b)   0 kips to 60 kips total load
    c)   0 kips to attempted failure of the west section

Figure 6.13. Testing the west section

East Section (5 strips)

After analyzing the raw data from the test of the west section, it was decided not to test the east section in its initial configuration (see additional discussion in the Test Results section). In an effort to show the strengthening effect of attaching additional FRP strengthening material, two additional four-inch FRP composite strips were attached to the underside of the east section using a single row of ALH fasteners spaced three inches on center (See Figure 6.14). The result was that the East section was strengthened with a total of five FRP composite strips spaced at six inches on center (See Figures 6.15 and 6.16).

Figure 6.14. Pre-drilling the concrete prior to fastening the first additional strip

Strip not well attached due to the spalling
of the concrete during the first test
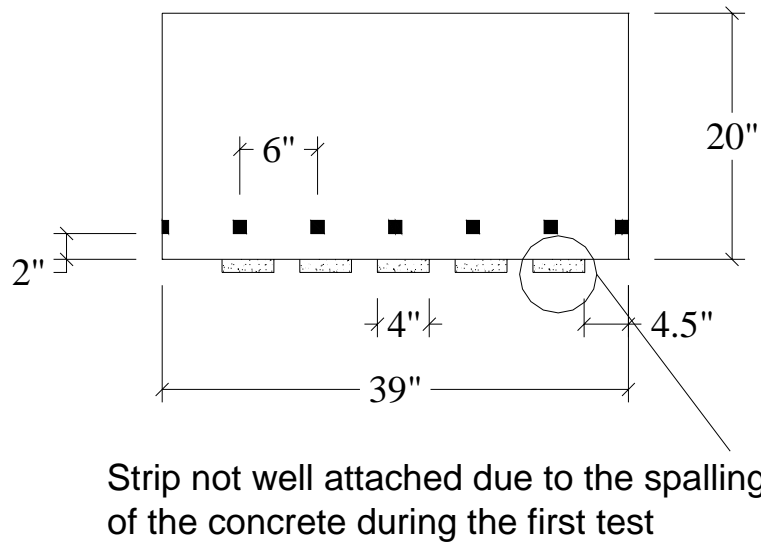
Figure 6.15. Transverse view of east section after addition of two FRP strips
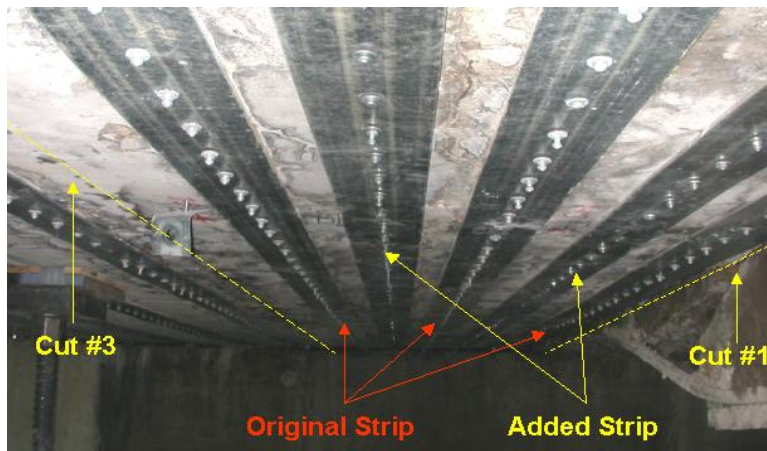
Figure 6.16. View of east section with two additional FRP strips (looking south)

Since the east section was still connected to the untested section of the deck at cut #3, the first load cycle was used to crack the 1.0-inch thick concrete cover along the bottom of the deck. This load cycle was started at zero and was taken to a total load of 20 kips (10 kips per jack). The load was then removed and a load sequence (See Figure 6.17) consisting of the following cycles began:

a)   0 kips to 40 kips total load
b)   0 kips to 60 kips total load
c)   0 kips to 90 kips total load
d)   0 kips to attempted failure of rehabilitated east section

116

Figure 6.17. Testing the east section

Data Collection

At approximately 3.5 inches of midspan deflection during both tests, the final load cycle was stopped and the data collection assets were removed from under the bridge so as not to damage the instruments. The test then continued by imposing a large deflection (approximately eight inches) in an attempt to achieve failure of the FRP composite strengthening system.

Test Results

General

During the testing of each section, load, deflection, and strain data were recorded in accordance with the collection plan outlined. The failure mode of each test section was documented and the condition of the FRP composite strengthening system (including the strips and the fasteners) was noted.

West Section (3 strips)

The west test section failed via concrete crushing in the compression zone. Figure 6.18 shows the crushed concrete along the top of the west section. Despite this failure, load continued to be applied to the structure in an effort to force a failure in the FRP composite strengthening system. This failure came at a midspan deflection of nearly eight inches. Considerable concrete spalling and a large shear crack opened (see Figures 6.19 and 6.20) along the southeastern portion of the west test section causing one of the composite strips to detach. Simply stated, the fasteners no longer had any concrete to "hold on" to in this area.

117

Figure 6.18. Concrete crushing failure along top of west section

Figure 6.19. Shear failure and spalling along southeast portion of west section

Figure 6.20. Flexural cracks at midspan of west section (during test)

Of particular interest during this test was the behavior of the fasteners along the length of the FRP strips. As the west test section continued to deflect, the fasteners did not cause a "slotting" or progressive bearing failure in the FRP composite strip as seen in some laboratory tests. Rather, they remained embedded in the concrete and rotated (head of fastener away from midspan of section) as the deflection increased. Figure 6.21 shows this rotation of the fasteners along the length of the west section.

Figure 6.21. View of rotated fasteners along length of west section

East Section (5 strips)

The east test section failed via concrete crushing in the compression zone (See Figure 6.22). Despite this failure, load continued to be applied to the structure in an effort to force a failure in the FRP composite strengthening system. However, after nearly seven inches of midspan deflection, the FRP composite strengthening system was still in tact (See Figure 6.23). The test was halted at this point for two reasons. First, the east section came in contact with the west section that started to deflect as well. Consequently, safety became a primary concern. Second, the laptop computer used in conjunction with the data acquisition system lost its charge and could not be recharged on site.
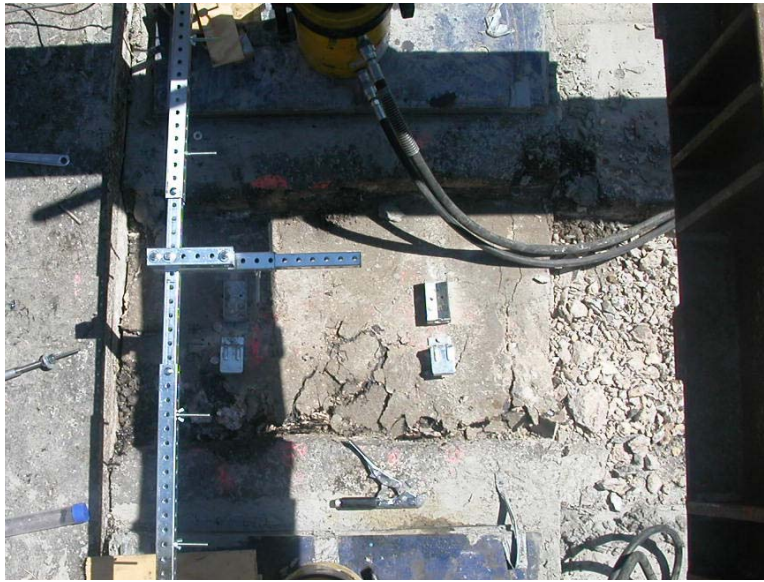
Figure 6.22. Concrete crushing along top of east section

Figure 6.23. View of deflected east section (foreground)

While the FRP strengthening system remained intact, there were signs that the fasteners and composite strips were under considerable strain (See Figure 6.24). First, the fasteners rotated just as they had in the test of the west section. In fact, this rotation caused some of the fasteners to loosen to the point of falling out of the concrete deck. Second, the large force transferred into the composite strips coupled with the great deflection of the section damaged the strip at some fastener locations. It seemed as if that combination of force and deflection was pulling the strip right through some fasteners.
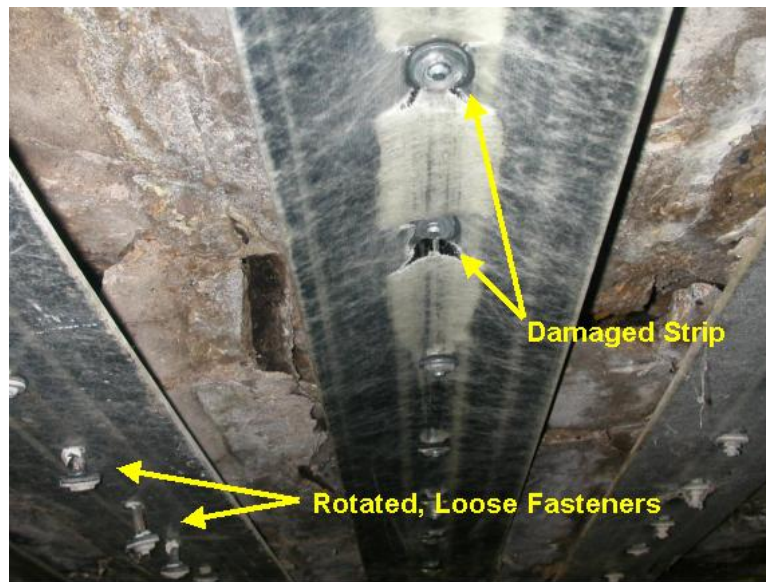
Figure 6.24. View of strips on east section after test completion

Data Analysis

General

Data analysis included the reduction of raw data to a form that would enable evaluation of the performance of the MF-FRP system. Both the amount of strengthening provided and the long-term durability of the system were of interest.   The first step in this process was to determine the material properties of the components of the original bridge and to confirm the mechanical properties of the FRP strips. Next, load vs. deflection and moment capacity vs. deflection graphs were plotted in order to determine the strengthening effect of the system. The strengthening achieved in practice was compared to the original design requirement for the strengthening system discussed in Chapter 4.   Finally, the effect of the environmental exposure on the FRP composite strengthening system was documented.

Verification of Bridge Materials and Original Design

After the testing was completed, the bridge was demolished by a construction contractor. This proved to a valuable opportunity to gather construction materials and verify the layout of

the steel reinforcement in the bridge deck. Plans used to analyze bridge P-53-702 were not specific to its construction since its plans were no longer on file. That is, the plans were of a typical bridge built during that era and left some doubt as to their applicability to bridge P-53-702. Figure 6.25 shows the demolition of the deck. The FRP strips can be seen still partially attached to the test sections.

Figure 6.25. Demolition of the bridge

It was found that the major steel reinforcement was laid out as anticipated. The flexural reinforcement was indeed 1-inch square bars (with deformations) spaced 6 inches on center and covered by 2 inches of concrete along the bottom of the bridge deck. Figure 6.26 shows the spacing of the steel reinforcement in one of the demolished sections of the bridge. Note that contrary to the initial assumptions there were no bars in the compression zone (top of deck). ¼ inch square transverse bars spaced 18 inches on center were used to tie the main bars together. Every fourth main bar was bent at the ¼ point for shear reinforcement. All main bars were hooked on their ends. No reinforcement was found to exist between the abutment and the deck itself. Consequently, the assumption of a simply supported deck (and test sections) was valid.

Figure 6.26. View of flexural steel spaced six inches on center

The strength of the steel reinforcement and the compressive strength of the 73 year-old concrete were also determined. The AASHTO Manual for Condition Evaluation of Bridges (2000) recommends using a tensile strength of 33,000 psi for the steel and compressive strength of 2,500 psi for concrete used in construction during this era for the purposes of load rating calculations. These were used in the design of the strengthening system as described previously. Attempts to extract useable concrete cylinders from the bridge deck were unsuccessful, as the concrete crumbled apart during each trial. Instead, large chunks of concrete were taken to the UW laboratory for testing. Varying lengths of the one-inch square steel bars were also taken for testing.

The concrete was tested using a rebound hammer and was found to have a compressive strength of 2210 psi +\- 553 psi. These results, however, are only a guide in that the effectiveness of the rebound hammer comes into question when it is used on concrete greater than 56 days old and applied to uneven surfaces. Nevertheless, these results imply that using the recommended strength of 2,500 psi is reasonable for analysis.

Two separate lengths of the main steel reinforcement were tested to failure in tension in a universal testing machine. The average yield strength of the steel was 35,000 psi, while the average ultimate strength was 54,000 psi. Figure 6.27 shows the condition of the two test specimens after failure. This confirms the recommendations of the AASHTO manual for the yield strength of the steel reinforcement from this era.
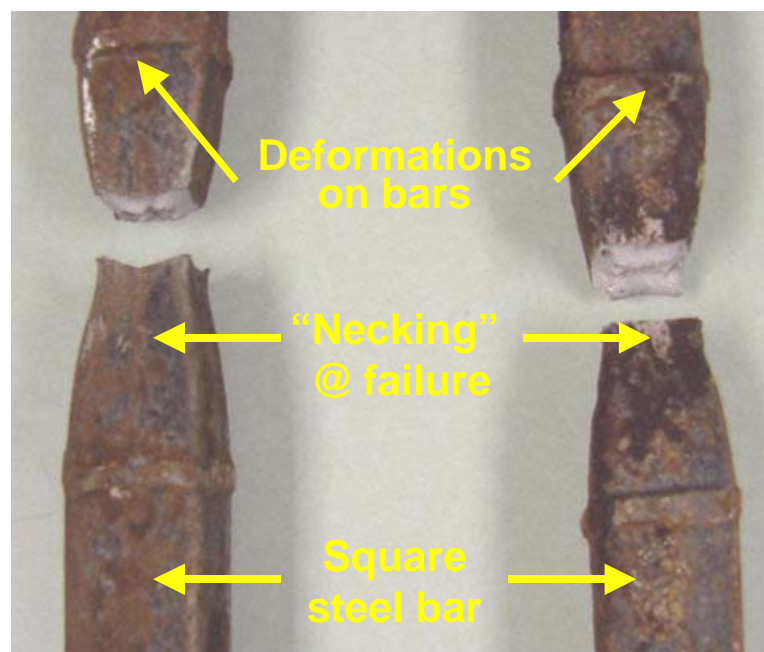

Figure 6.27. Steel samples post-failure

Load and Deformation of the Strengthened Bridge

The total load vs. deflection curve and the bending moment vs. deflection curve were plotted to determine the effectiveness of the MF-FRP composite strengthening system. The total load was taken as the sum of the forces from the two separate actuators, while the midspan deflections was taken from the DC-LVDTs located along the bottom of each section from positions L5 and L4 (see Figures 6.10 and 6.11 for the west and the east sections, respectively.)

The behavior of the strengthened sections was compared to an unstrengthened (control) section. One of the sections was originally intended to be tested as a control section to obtain control data for the bridge, however, this was not done. During the testing it was decided that it would be more beneficial to the research study to attempt to increase the level of strengthening by adding two additional FRP strips to the east section (the second section tested) than to do a control test. The reason for this was that the results obtained from the first (west) section tested were felt to be somewhat inconclusive with regard to the strengthening effect and the attachment of the FRP strips. It was thought that the results might have been affected by the fact that the two sections were still partially connected when the section reached its yield load. In order to obtain control data for the unstrengthened bridge the control beam (C-1) tested in the UW laboratory was used. Test results for the laboratory beam were scaled to account for the larger size of the bridge section and the difference in loading configuration and material properties used in the laboratory. It is important to note that the laboratory beam used steel with a nominal 60 ksi yield strength that may have had more post-yield hardening than the existing ~33 ksi yield steel in the bridge (even though the steel area in the control beam was scaled by the ratio of the yield strengths). Therefore, the post-yield increase in the control beam shown may not truly represent the real bridge, but nevertheless serves as a good indicator of the unstrengthened bridge's behavior. In addition the laboratory control beam had a measured concrete strength of nearly 6000 psi. However, in the parametric studies conducted it was seen that the concrete strength did not significantly influence the load carrying capacity.

While the scaled loads obtained from the laboratory control beam are felt to be representative of the unstrengthened bridge structure, the deflections obtained in the laboratory are not felt to be appropriately scaled to represent the bridge section. It is felt that partial connection between the sections in the small deflection range (< 0.5 in.) probably increased the stiffness of the test sections in the pre-yield regime.

The results of the load-deflection behavior for the strengthened bridge sections are compared to the scaled laboratory control beam in Figure 6.28 and 6.29.
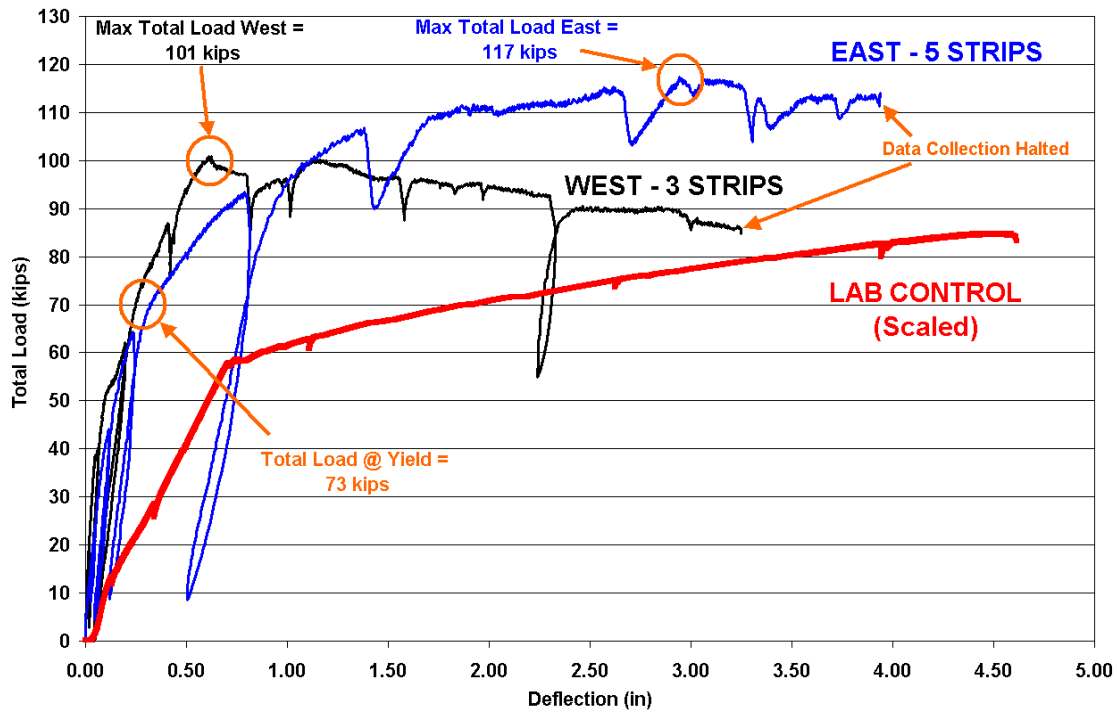
Figure 6.28. Total load vs. midspan deflection results
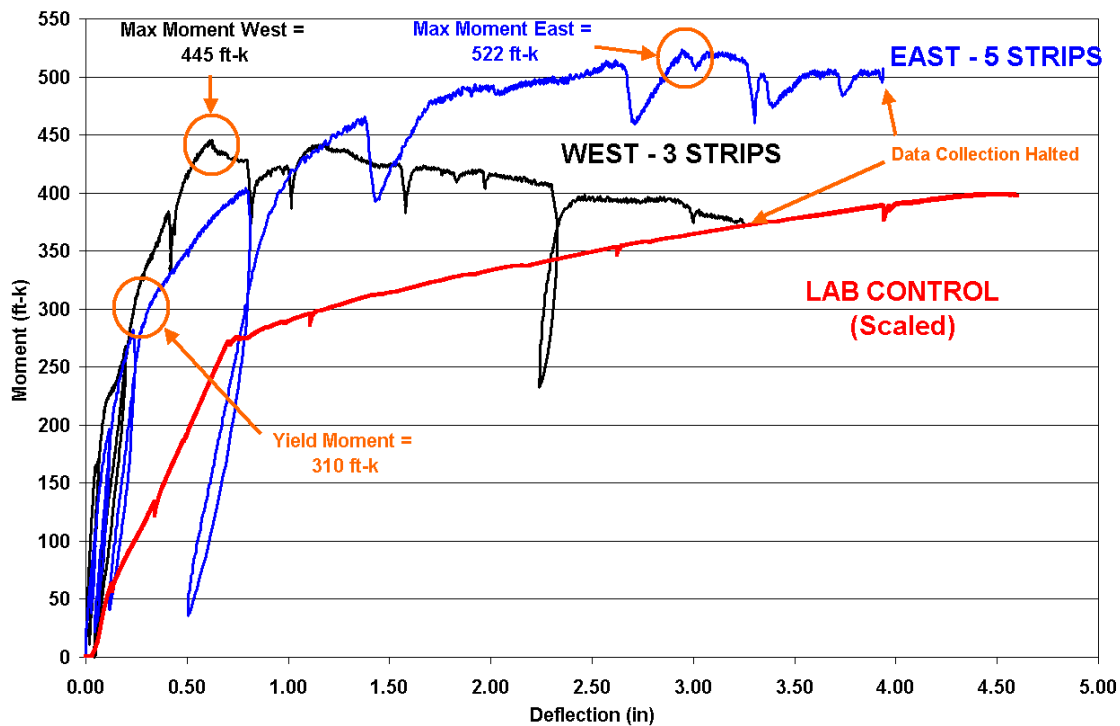
Figure 6.29. Moment vs. midspan deflection results

Figures 6.28 and 6.29 clearly show the strengthening effect of the MF-FRP system. Table 6.1 summarizes the test results for the east and west test sections and compares them to the scaled laboratory control beam. Table 6.2 provides the results per unit width of the bridge for comparison to the design requirements.

Table 6.1. Summary of Ultimate Test Results								
Test Section	# of Strips	Yield Mom.	% Inc	Ult Mom.	% Inc	% inc wrt. own yield	Mom. @ 2"	% Inc
		(ft-k)		(ft-k)			(ft-k)	
Control	None	272	-	399	-	-	333	-
West	3	310	14.0	445	11.5	43.5	417	25.2
East	5	310	14.0	522	30.8	68.4	492	47.7
Note: Failure mode for all sections was concrete compression.								

Table 6.2. Ultimate Test Results per Unit Width					
Test Section	# of Strips	Yield Mom.	% Inc	Ult Mom.	% Inc
		(k-ft/ft		(k-ft/ft)	
Control	None	86.1	-	125.2	-
West	3	95.4	10.8	136.9	9.3
East	5	100.5	16.7	169.2	35.1

The predicted nominal strength per unit width for the existing HS17 rating and the required design nominal strength per unit width to increase the load rating to HS 25 were calculated to be (See Table 4.17), 94.6 k-ft/ft and 122.1 k-ft/ft, respectively. As noted previously a 29% increase in nominal moment capacity was required to increase the load rating.

The compressive strain in the concrete, the tensile strain in the FRP at the midspan and the moment versus curvature for the West section (3 strips) are shown Figures 6.30, 6.31, and 6.32, respectively.
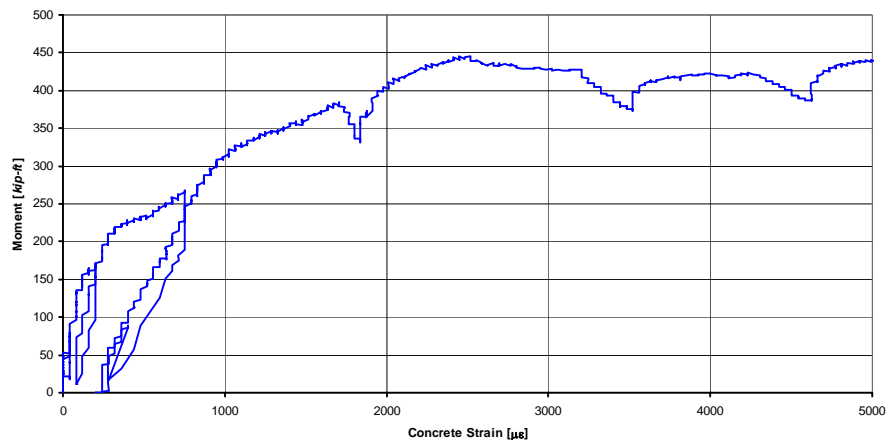
Fig. 6.30. Compressive Strain in Concrete for West section (3 strips)
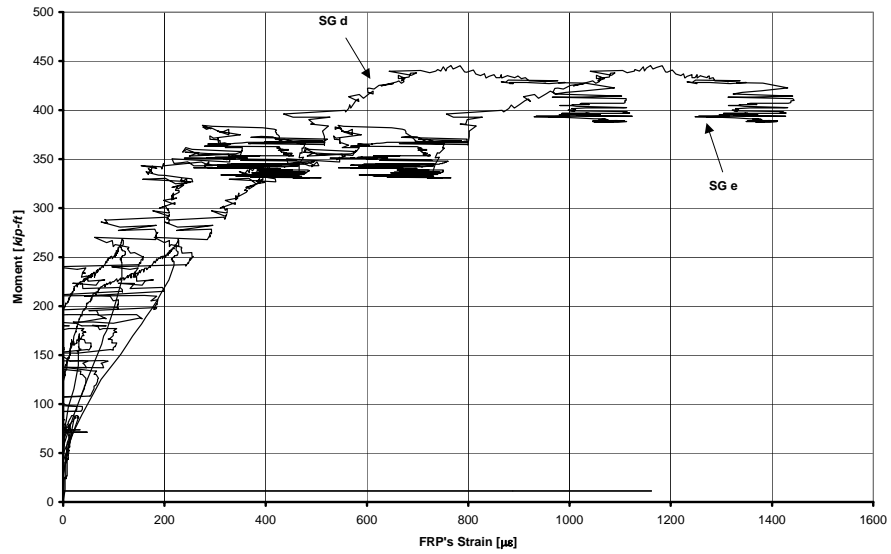
Fig. 6.31. Tensile Strain in FRP strip for West section (3 strips)
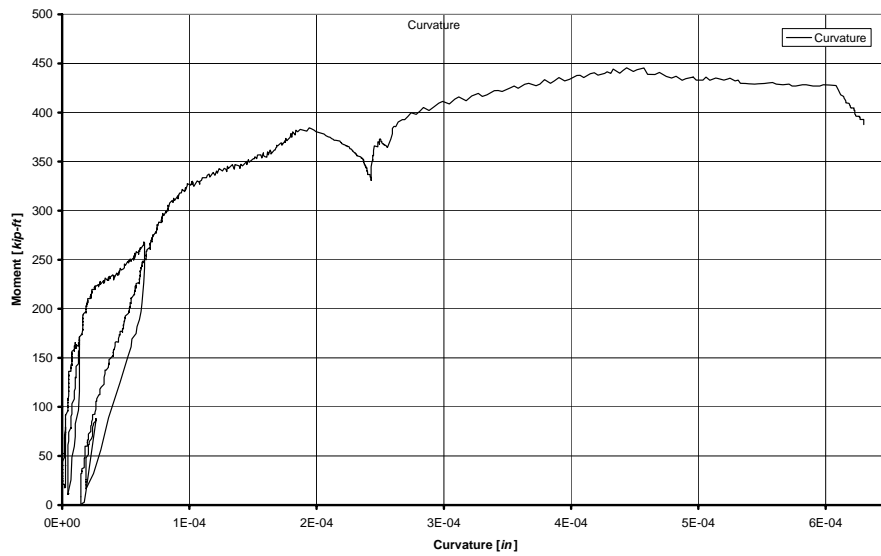
Fig. 6.32. Moment versus Curvature for West section (3 strips)

The compressive strain in the concrete, the tensile strain in the FRP at the midspan and the moment versus curvature for the East section (5 strips) are shown Figures 6.33, 6.34, and 6.35, respectively.

127
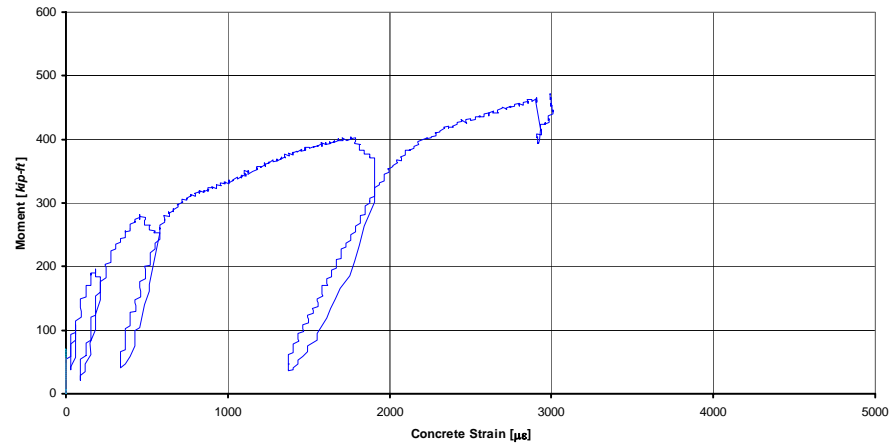
Fig. 6.33. Compressive Concrete strain for East Section (5 strips)
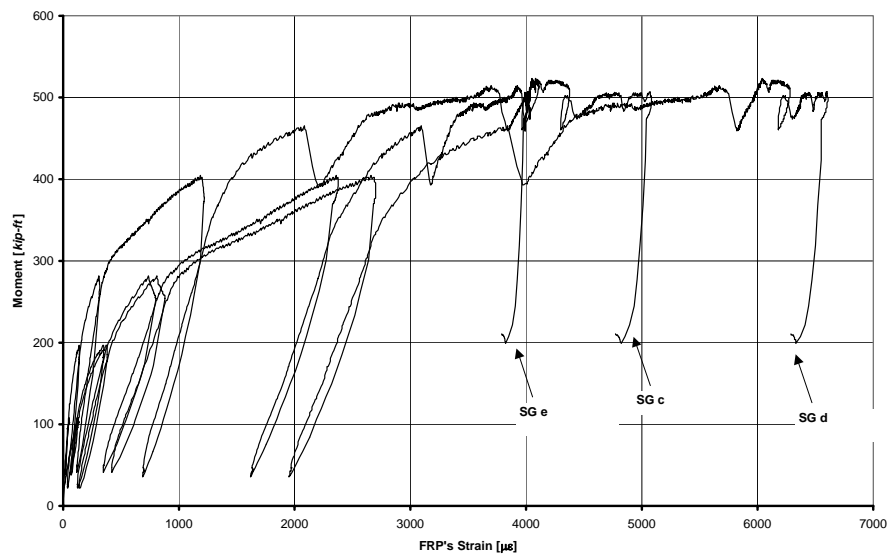
Fig. 6.34. Tensile FRP strain for East Section (5 strips)
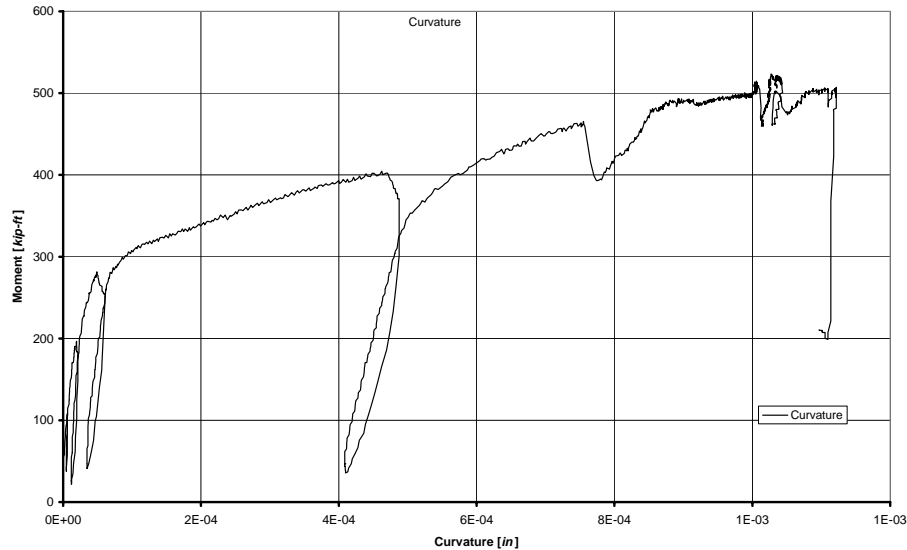
Fig. 6.35. Moment versus Curvature for east section (5 strips)

Discussion of Test Results

The yield moments for the two strengthened sections were similar and approximately 14.0% higher than that of the scaled control beam. Since both test sections yielded at the same load level the results appear to be reasonable. As noted earlier it is not possible to compare the pre-yield stiffness of the two beams. It is difficult to explain why the west section (3 strips) is stiffer than the east section (5 strips) in the post-yielding regime. The effect of loading and unloading close (60 kips) to the yield load may have had some adverse effect on the behavior of the sections near the yield load.

The strengthening on the east section (three strips) appears to have begun to lose its effectiveness soon after the maximum load was achieved. The fastener rotation described earlier may have occurred at this time. In addition, the shear crack in the concrete section itself probably weakened the section at this time. The strengthening system on the west section (5 strips) appears to have remained attached and effective for the full duration of the measured load test. (Recall that the instrumentation was removed at approximately 4 inches of deflection but that the test was continued without recording data.)   Load drops during the loading were due to breaks in the load application (and hence load drop-off due to the loss of hydraulic pressure in the jacks).   This can be confirmed by observing the large hysteresis loop seen at the unloading and reloading cycle at 90 kips.

The ultimate, or maximum, moments carried by the strengthened test sections were considerably higher than the scaled laboratory control beam. These results not only show the increased capacity of the sections due to the MF-FRP composite strengthening system, but also show the benefit of using additional composite strips. With respect to the scaled laboratory control beam, the three strips spaced at 12 inches on center increased the capacity of the west

129

section by 11.5%, while five strips spaced 6 inches on center improved the moment capacity of the east section by 30.8%. Investigation with respect to their own yield moments reveals that the west section and east section improved by 43.5% and 68.4%, respectively. Given that the original bridge may not have had such a pronounced strain-hardening regime as the laboratory control beam, it is possible that the original ultimate strength of the bridge may have been less than the control. If the original section experienced no strain hardening the yield strength of the two test sections can be taken as good indicator of the ultimate capacity of the original bridge. Typical deflection limitations for a structure of this type are L/800 (0.32 inches for Bridge P-53-702). Load carrying capacity was also compared at a deflection of 2 inches of deflection (L/128). At this large deflection, the west section showed a 25.2% greater capacity, while the east section showed a 47.7% greater capacity than the scaled laboratory control. From the results shown in Table 6.2 it can be seen that the required increase in strength was achieved by the east section and probably by the west section however, this depends on the ultimate strength of the existing section which is open to some question.

From the strain and the moment versus curvature data it can be seen that the concrete failed in compression at between –2500 and –3000 microstrain in both the West and the East sections. The strain gages on the FRP strips indicated that in the East section (5 strips) the average tensile strain in the FRP strips was about 6000 microstrain at failure. For the modulus of 9000 ksi this translates to a stress in the FRP strip of 54 ksi. In the West section (3 strips), however, the maximum strain in the FRP strip was only around 1400 microstrain (or a stress of 12.6 ksi). This appears to indicate that in the West strip the load was not fully transferred into the FRP strip as desired.

Environmental Effects on the MF-FRP System

The strengthening system was in place for nearly 10 months and was subjected to the extremes of Wisconsin weather. These extremes included hot, humid summer days with temperatures in excess of 90 degrees and cold winter days with temperatures (including wind-chill) well below zero. Examination of the FRP composite strips and powder-actuated fasteners prior to the ultimate load testing led to the following observations:

- All the strips were attached firmly to the concrete underside and no sign of any damage was seen.

- The underside was in good condition and no additional deterioration was seen as compared to the year before.

- No stalactites were seen on the soffit near or around the FRP strips and the substrate seemed in fair condition. Figure 6.36 shows the overall view of the underside after one winter.

130

Figure 6.36 Overall view of the retrofitted bridge deck after ten months

- In the spring of 2003, the FRP strips were covered with water and some strips were covered with frost. Figure 6.37 shows a high amount of moisture on the FRP strip. However, this did not seem to affect the strips.

- Some corrosion was seen in most of the washers on the X-ALH fasteners and the carbon steel anchors. The southern end of the bridge showed less corrosion as compared with the northern end of the bridge near the abutment. Figure 6.38 shows the corrosion of the ALH fasteners at the southern end of the bridge and Figure 6.39shows the corrosion seen at the northern abutment. The variation in the rate of corrosion was attributed to the larger amount of existing deterioration of the substrate near the North abutment. Figure 6.40 shows the original damaged area near the north abutment.

Figure 6.37. FRP strips covered with moisture (spring, 2003)

Figure 6.38. Small amount of corrosion seen at the southern end

Figure 6.39. Corrosion seen at the northern abutment

Figure 6.40. Original damaged area near the northern abutment

- No corrosion was seen on the stainless steel X-CR fasteners and the anchor bolts. Figure 6.41 shows the unaffected stainless steel fasteners and anchor bolts.

Figure 6.41. Stainless steel fasteners and anchors bolts

- A small amount of corrosion on the ALH fastener shank was observed on fasteners that had achieved improper embedment during the installation of the system. Figure 6.42 shows one of the fasteners exhibiting some corrosion on the fastener shank. The corroded fastener, which was bent originally when the fastener struck hard aggregate, was pulled out to observe the extent of deterioration. Figure 6.43 shows the bent fastener after one winter.

Figure 6.42. Corrosion of ALH fastener shank with incomplete embedment

Figure 6.43. Corrosion on X-ALH fastener seen after ten months

- At the locations of the missing fasteners the FRP strips showed some signs of deterioration. Figure 6.44 shows some deterioration at the location of the missing fastener.

Figure 6.44. Deterioration of FRP strip at location of missing fastener

- The overall condition of the bridge seemed to have been unchanged after one winter. Some additional corrosion of the exposed rebar was seen and it was observed that water had penetrated in between the FRP strips and the concrete deck. This can be seen in Figure 6.45 where the edge of the FRP strips was covered with water.

Figure 6.45. Edge of FRP strips covered with water

The survey of the MF-FRP strengthening system can be described as in "Good" condition as defined by the condition evaluation guidelines by FHWA (2000). The qualitative performance of the FRP strips after one winter was encouraging as no indication of any significant damage to the fastened connection was observed.

Material Properties of FRP Strips

Not only was it important to visually inspect the FRP composite strips, but it was also necessary to determine if ten months of exposure had degraded the properties of the FRP material. As such, both virgin FRP strips and FRP strips recovered from bridge P-53-702 were tested in tension to determine their ultimate strength, open-hole strength and modulus of elasticity.

Tension test conducted on coupons that were 14" long by 1" wide with a gage length of 10" (2" on the ends of the coupons were enclosed by the grips of the test apparatus). Open-hole strength tests had the same dimensions, but a 0.188" hole was drilled in the center of the coupons (7" from either end) prior to the tensile test.   Width and thickness were measured to calculate the average cross-sectional area of each specimen for calculation of the strength and stiffness following ASTM D3039 and ASTM D5766. The strain in each coupon was measured with an extensometer, which was removed at approximately 75% of the ultimate load to prevent damage to the equipment. Figure 6.46 shows the test apparatus, while Figure 6.47 shows typical failed samples.

Figure 6.46. Testing a coupon of recovered material (no hole)

Figure 6.47. Failed coupons of virgin material (left – no hole; right – central hole)

The ultimate load, strain data, and cross-sectional area provided the basis for analysis. The ultimate load divided by the cross-sectional area gave the ultimate strength, while a linear regression of the stress vs. strain curve provided the modulus of elasticity. The results of the two rounds of tensile testing are shown in Table 6.3. Table 6.4 compares the properties of the two materials.

Table 6.3. Average FRP Tensile Test Data

FRP Sample	# of Tests	Ultimate Strength			Modulus of Elasticity		
		Average (ksi)	Std Dev (ksi)	COV (%)	Average (ksi)	Std Dev (ksi)	COV (%)
Virgin D3039	30	121.0	5.4	4.5	8,511	634	7.5
Recovered D3039	5	122.7	6.4	5.2	8,729	667	7.6
Virgin D5766	30	94.4	5.7	6.0	--	--	--
Recovered D5766	5	94.5	2.3	2.4	--	--	--

Table 6.4. Material Property Comparison

FRP Sample	Strength	% Difference from Virgin	Modulus of Elasticity	% Difference from Virgin
	(ksi)		(ksi)	
Virgin D3039	121.0	--	8,511	--
Recovered D3039	122.7	+1.4	8,729	+2.6
Virgin Open Hole	94.3	--	--	--
Recovered Open Hole	94.5	+0.2	--	--

From the above results, it can be seen that the ten months of exposure to the elements had a statistically insignificant impact on the mechanical properties of the FRP composite strips. The ultimate strength, the open-hole strength and modulus of elasticity of the recovered strips remained relatively unchanged with respect to the virgin material. It should be noted, however, that the coupons used for the "recovered" FRP material were cut from the side portions of the strips away from the holes in the strip where some damage may have occurred due to environmental effects or due to the load testing on the bridge. These measured material properties for the FRP strips also compared well with those obtained in testing conducted at UW (Gulbrandsen, 2002) prior to installation of the strips on the bridge. These tests reported an ultimate strength of 122.4 ksi, an open-hole strength of 92.8 ksi and a modulus of 8,893 ksi.

Conclusions of Ultimate Load Testing Study

The ultimate load testing conducted on a flat slab bridge in Edgerton, Wisconsin that had been strengthened previously with the MF-FRP system was the first ever in-situ test of the MF-FRP system. The following conclusions can be drawn for this phase of the study.

- Specially designed FRP composite strips attached with powder-actuated fasteners and expansion anchors were able to increase the ultimate strength of test sections of a 73-year-old concrete bridge.

- The level of strengthening was shown to be a function of the number of strips. A test section with five strips had a higher ultimate load than a section with three strips.

- Both test sections were shown to have improved strength over a scaled laboratory control beam. Both sections also had significant increases in strength after yield of their internal steel.

- The FRP strips remained attached to the underside of the concrete bridge well past the yield point and well into the inelastic large-deformation range. The FRP strips remained attached to the concrete well beyond the compressive strength of the concrete.

- The FRP strips did not appear to be as well attached to the concrete at the locations of the powder-actuated fasteners as had been seen in prior laboratory experiments. Progressive bearing failure, or slotting, of the FRP strips was not seen. Fasteners tended to rotate rather than shear through the strips. This is attributed to the poor properties of the concrete substrate. Nevertheless, load was transferred into the FRP strips.

- Both test section failed due to concrete compression with the strips still firmly attached.

- The FRP composite strip did not appear to have been degraded by 10 months of in-situ environmental exposure.

- The in-situ properties of the steel reinforcing bars and the concrete were measured on samples extracted from the demolished bridge. Properties of the steel and concrete were similar to those recommended by AASHTO and as assumed in the design studies.

- During the design phase of the research it was determined that a 29% increase in the nominal strength of the bridge was required to increase the inventory load rating of the bridge from an HS17 to an HS25. Based on the results of the in-situ ultimate load testing this increase in strength was felt to have certainly occurred in the east section strengthened with five FRP strips and most likely to have occurred in the west section strengthened with three strips.

- The predicted strength of the existing section using AASHTO recommended strengths for steel and concrete in the 1930s and using an effective width corresponding to the inspection inventory load rating show reasonable agreement with the results of the load tests.

7 Conclusions and Recommendations

Conclusions

Based on the results of the research study conducted the following can be concluded:

1. The MF-FRP method can be used to strengthen reinforced concrete sections. The powder-actuated fasteners are seen to offer a rapid and economical method of attaching high strength and high stiffness pre-fabricated FRP material strips to concrete members. The selective use of expansion anchors at the strip ends prevents delamination but does not significantly impact installation time. The strips can be attached using hand-tools and commercially available fasteners.

2. The FRP strips were easily attached to the underside of a deteriorated reinforced concrete flat slab bridge by county maintenance workers. Minimal surface preparation was required prior to the attachment of the FRP strips. Existing cracks, fissures, and surface profile protrusions did not prevent installation of the fasteners.

3. In order to design a strengthening system for a bridge its existing capacity must first be determined from site observations, inspection reports, and theoretical models. The existing capacity of a bridge can be determined using existing AASHTO procedures and existing reinforced concrete models.

4. Conventional reinforced concrete ultimate strength models can be used to predict the capacity of a concrete section strengthened with attached FRP strips in a similar fashion to the method used for epoxy-bonded systems. A moment-curvature model developed at the University of Wisconsin can be used to obtain simulations of the entire load-deformation history of MF-FRP strengthened beams.

5. The cost of labor and materials to strengthen a 23 ft long reinforced concrete flat slab bridge in Edgerton, Wisconsin built in 1930 was $7,995 or $12.72/ft^2. This cost was for an MF-FRP system using 50% stainless steel and 50% galvanized steel fasteners and one FRP strip spaced at 12 inches on center.

6. The MF-FRP strengthening system did not show any significant signs of deterioration after being in-service for 10 months. Stainless steel fasteners were seen to show less corrosion than galvanized steel fasteners but the impact of the corrosion on the strengthening was not possible to quantify. Properties of FRP strips recovered from the field did not show reductions over the virgin material properties.

7. In-situ load testing to failure of the Edgerton Bridge indicated that the MF-FRP strengthening method had increased the load rating of the bridge. The strengthening design was required to increase the moment capacity by 29% and based on experimental test data it appears that this level of strengthening was achieved with one strip spaced at 12 inches on center. A second test section with one strip at 6 inches on center was shown to exceed the 29% design strengthening requirement.

139

8.   MF-FRP strengthened beams representative of the bridge section and tested in the laboratory study showed increases in the yield and ultimate strength of up to 25% and 58% respectively for strips spaced at 6 inches on center. For FRP strips spaced at 12 inches on center yield and ultimate strengthening was 23% and 37%, respectively. This exceeded the 29% strengthening requirement. All beams failed due to concrete compression prior to the FRP strip failing or delaminating.

9.   The FRP strips in beams strengthened in the laboratory with stainless steel fasteners appear to have been damaged due to penetration of the fastener washers into the FRP strips.

10.   MF-FRP strengthened beams loaded cyclically in both the elastic and inelastic ranges did not show any significant decreases in strength or stiffness due to the cyclic loading. Fasteners remained fully embedded and the FRP strips were not damaged.

Recommendations

Based on the conclusions, the following can be recommended:

1.   The MF-FRP method can be used to upgrade the capacity of structurally deficient aging highway bridges. It is recommended for flat slab bridges at this time. The method should be used on a case-by-case basis and must be accompanied by an in-depth engineering analysis and design study (as with any strengthening design). This study must include an evaluation of the existing capacity of the structure intended for strengthening.

2.   The MF-FRP method is especially recommended where the concrete substrate is cracked and deteriorated such that an epoxy-bonded FRP system would not be possible and where short-term strengthening (3-5 years) is desired.

3.   The "optimal" FRP strip used for strengthening with the MF-FRP method has the desired properties for use for strengthening concrete members. The strip has consistent properties and can be easily used in the field. The strip used in this study and produced by Strongwell in Chatfield, MN is recommended for future applications.

4.   It is recommended that DOTs designate an individual in the bridge design section to learn to design strengthening systems for bridges with FRP materials.

5.   Additional research is recommended to determine if the MF-FRP method can be used to strengthen reinforced concrete girder bridges. A follow-up implementation on a girder bridge slated for replacement is recommended in the near future.

6.   Additional research is recommended to determine if the MF-FRP method can be used on prestressed concrete bridge girders. This may be useful for the rapid repair of bridges

that have been damaged due to truck impacts. An initial laboratory study is recommended. This should be followed by a field demonstration.

7.   A study is recommended to determine the relative cost/benefits of strengthening a deficient reinforced concrete bridge with the MF-FRP method to extend the current life instead of replacing the bridge. This is especially important for bridges that are just below a Sufficiency Rating of 50. In this case, the strengthening can be used to improve the Sufficiency Rating to a point where mandatory replacement is not required.

8.   Additional research on the cost/benefits of using more expensive, but more durable, stainless steel fasteners is recommended. The use of a neoprene washer with the stainless steel fasteners is recommended at this time.

9.   In order to educate the bridge design and construction community on the technologies available to strengthen bridges with both conventional and FRP materials, it is further recommended that a workshop and training session be held on this topic for local DOT designers and design consultants. It may be possible to coordinate this activity through the University of Wisconsin Continuing Education Program.

10.   A manual for strengthening bridges with FRP and other materials should be developed for use by DOT engineers. A set of guidelines outlining which types of bridges would be most suited to different types of strengthening methods should be prepared. The guidelines should include a method to make cost comparisons between different alternatives.

References

AASHTO. (1996). <u>Standard Specifications for Highway Bridges, 16th Edition</u>. *American Association of State highway and Transportation Officials,* Washington, DC.

AASHTO. (1998). <u>LRFD Bridge Design Specifications, 2nd Edition</u>. *American Association of State highway and Transportation Officials*, Washington, DC.

AASHTO. (2000). <u>Manual for Condition Evaluation of Bridges, 2nd Edition</u>. *American Association of State Highway and Transportation Officials*, Washington, DC.

ACI Committee 318. (1999). <u>Building Code Requirements for Structural Concrete (318-99) and Commentary (318R-99).</u> *American Concrete Institute*, Farmington Hills, MI.

ACI Committee 440.2R. (2002). <u>Guide for the Design and Construction of Externally Bonded FRP Systems for Strengthening Concrete Structures</u>. *American Concrete Institute*, Farmington Hills, MI.

Alkhrdaji, T., Nanni, A., and Mayo, R., "Upgrading Missouri Transportation Infrastructure: Solid RC Decks Strengthened with FRP Systems<u>," Proceedings of the 79th Annual Transportation Research Board Meeting</u>, Jan 2000, Washington, DC.

Arora, D. (2003). <u>Rapid Strengthening of Reinforced Concrete Bridge with Mechanically Fastened – Fiber Reinforced Polymer Strips</u>. MS Thesis, University of Wisconsin-Madison.

ANSI A 10.3-1995. <u>American National Standard for Construction and Demolition: Powder-Actuated Fastening Systems – Safety Requirements</u>. *American National Standards Institute*, Chicago, IL

ASTM D3039. "Standard Test Method for Tensile Properties of Polymer Matrix Composite Materials," *American Society for Testing and Materials*, West Conshohocken, PA.

ASTM D5766. "Standard Test Method for Open Hole Tensile Strength of Polymer Matrix Composite Laminates," *American Society for Testing and Materials*, West Conshohocken, PA.

ASTM D5961. "Standard Test Method for Bearing Response of Polymer Matrix Composite Laminates," *American Society for Testing and Materials*, West Conshohocken, PA.

Bank, L.C., Lamanna, A.J., Ray, J.C., and Velazquez, G.I. (2002a). <u>Rapid Strengthening of Reinforced Concrete Beams with Mechanically Fastened, Fiber-Reinforced Polymeric Composite Materials</u>. *US Army Corps of Engineers*. Report Number ERDC/GSL TR-02-4. 93 pages.

Bank, L.C., Borowicz, D.T., Arora D., Lamanna, A.J. (2003). Strengthening of Concrete Beams with Fasteners and Composite Material Strips – Scaling and Ancorage Issues. *US Army Corps of Engineers*. Draft Final Report Contact Number DACA42-02-P-0064.

Bank, L.C., Borowicz, D.T., Lamanna, A.J., Ray, J.C., and Velazquez, G.I. (2002b). Rapid Strengthening of Full-Size Reinforced Concrete Beams with Powder-Actuated Fastening Systems and Fiber-Reinforced Polymer (FRP) Composite Materials. *US Army Corps of Engineers*. Report Number ERDC/GSL TR-02-12.

Borowicz, D.T. (2002). Rapid Strengthening of Concrete Beams with Powder Actuated Fasteners and Fiber Reinforced Polymer (FRP) Composite Materials. MS Thesis, University of Wisconsin-Madison.

Chajes, M. J., Mertz, D. R., and Commander, B. (1997). "Experimental Load Rating of a Posted Bridge", *Journal of Bridge Engineering*, Vol. 2, No. 1, pp. 1-10.

FHWA. (2000). Recording and Coding Guide for the Structure Inventory and Appraisal of the Nations Bridges. *Federal Highway Administration*, Report No. FHWA-PD-96-001. Available at http://www.fhwa.dot.gov/bridge/bripub.htm

FHWA. (2001). National Bridge Inventory (NBI), *Federal Highway Administration.* http://www.fhwa.dot.gov/bridge/nbi.htm

FIB (Féderation Internationale du Béton). (2001)."Externally Bonded FRP Reinforcement for RC Structures," *International Federation for Structural Concrete (fib),* Switzerland.

Garden, H. N., and Holloway, L. C. (1998). "An Experimental Study of the Influence of Plate End Anchorage of Carbon Fibre Composite Plates Used to Strengthen Reinforced Concrete Beams," *Composite Structures*, Vol. 42, pp. 175-188.

Gulbrandsen, P.W. (2002). Tensile and Bearing Tests of FRP Composite Strengthening Strips. Hilldale Undergraduate Research Report. University of Wisconsin-Madison.

Hussain, M., Sharif, A., Basunbul, I. A., Baluch, M. H., and Al-Sulaimani, G. J. N. (1995). "Flexural Behavior of Precracked Concrete Beams Strengthened Externally by Steel Plates," *ACI Structures Journal*, Vol. 92, No. 1, pp. 14-22.

Lamanna, A.J. (2002). Flexural strengthening of Reinforced Concrete Beams with Mechanically fastened Fiber-Reinforced Polymer Strips. PhD Thesis, University of Wisconsin – Madison.

Lamanna, A.J., Bank, L.C., and Scott, D.W. (2001a). "Flexural Strengthening of Reinforced Concrete Beams Using Fasteners and Fiber-Reinforced Polymer Strips," *ACI Structural Journal*, Vol. 98, No. 3, pp. 368-376.

Lamanna, A.J., Bank, L.C., and Scott, D.W. (2001b). "Rapid Flexural Strengthening of RC Beams Using Powder Actuated Fasteners and FRP Strips," in Proceedings of the 5th International Symposium of FRP in Reinforced Concrete Structures, (ed. C. Burgoyne), Cambridge, UK, July 16-18, pp. 389-397.

Nanni, A. (1997). "Carbon FRP Strengthening: New Technology Becomes Mainstream," *Concrete International*, Vol. 19, No., 6, pp. 19-23.

Saadatmanesh, H., and Malek, A.M. (1998). "Design Guidelines for Flexural Strengthening of RC Beams with FRP Plates", *Journal of Composites for Construction*, Vol. 2, No. 4, pp. 158-164.

Saraf, K.V. (1998). "Evaluation of Existing RC Slab Bridges," *Journal of Performance of Constructed Facilities*, Vol. 12, No. 1, pp. 20-24.

Sebastian, W.M. (2001). "Significance of Midspan Debonding Failure in FRP-Plated Concrete Beams," *ASCE Journal of Structural Engineering*, Vol. 127, No. 7, pp. 792-798.

Shahrooz, B.M., Miller, R.A., Saraf, V.K., and Godbole, B. (1994). "Behaviour of RC Slab Bridges During and After Repair", *Transportation Research Record 1442*, pp. 128-135.

Sika Corporation, Sika Carbodur Structural Strengthening System – Engineering Guidelines for Design and Application, *Sika Corporation*, 1999.

Spadea, G., Bencardino, F., and Swamy, R.N. (1998). "Structural Behavior of composite RC Beams with Externally Bonded CFRP," *ASCE Journal of Composites for Construction*, Vol. 2, No. 2, pp. 59-68.

Stallings, J.M., Tedesco, J. W., El-Mihilmy, M., and McCauley, M. (2000). "Field Performance of FRP Bridge Repairs," *ASCE Journal of Bridge Engineering*, Vol. 5, No. 2, pp. 107-113.

Teng, J.G., Chen, J.F., Smith, S.T., and Lam, L.,. (2001). FRP-Strengthened RC Structures. *John Wiley & Sons*, NY.

USDC. (1956). Standard Plans for Highway Bridge Superstructures. Bureau of Public Roads, *U.S. Department of Commerce,* Washington, DC.

Velázquez, G.I., Ray, J.C., Borowicz, D.T., Lamanna, A.J., and Arora D., and Bank, L.C. (2002). "Tests of Reinforced Concrete T-Beams Retrofitted with Mechanically Anchored Fiber-Reinforced Polymer (FRP) Plates," 1st International Conference on Bridge Maintenance, Safety and Management, *IABMAS*, Barcelona, SPAIN, July 14-17, CD-ROM.

WBM. (1994). Wisconsin Bridge Manual. *Wisconsin Department of Transportation*, Madison, WI.

WisDOT. (1996). <u>Standard Specifications for Highway and Structure Construction</u>. *Wisconsin Department of Transportation*, Madison, WI.

Bridge Inspection Report and Rating Sheet for P-53-702 provided by WisDOT.

Bridge Inspection Report	Wisconsin Dept. of Transportation
EM30 - 0198 Section 84.17 Wis. Stats.	

Feature On:	LRD STOUGHTON RD	Maintainer: City/Municipal Hwy Agenc	Structure Number: P-53-0702
Feature Under: SAUNDERS CREEK		Sect/Twn/Rng: S04 T04N R12E	
Location: 0.6M N JCT STH 59		County: Rock	Municipality: CITY OF EDGERTON
Inv Rating: HS17	Rdwy Width: 23	Deck Width: 25.9	Existing Posting:	Suff Rating:32.7
Oper Rating: HS29	Total Length: 24	Deck Area: 621	Recom Posting:	Rate Score: 64
Overburden in.: 3 Date: 1/1/1901	Section Loss %:	ADT On: 600 Year: 1980	ADT Under: Year:

Bridge Element / **Quantity in Condition State**

Num	Description	Env	Unit	Tot Qty	1	2	3	4	5	Comments
39	Concrete Slab -	4	(SF)	646	646	0	0	0	0	Deep deter. on deck edges
215	Reinforced Conc	2	(LF)	46	36	10	0	0	0	Cracks and deep spalls both abut. @ corners
322	Bituminous Approach	3	(EA)	2	2	0	0	0	0	
331	Reinforced Conc Bridge	3	(LF)	49	0	49	0	0	0	
359	Soffit of Concrete Deck	4	(EA)	1	0	0	0	1	0	SHOWS HUNDREDS OF STALAGTITES W/
400	Concrete Wingwall	2	(EA)	4	0	4	0	0	0	CRACKS & SPALLS IN ALL WINGWALLS.
405	Drainage	2	(EA)	2	0	2	0	0	0	NEED DOWN SPOUTS.
410	Curb	2	(LF)	49	0	49	0	0	0	spalls entire length

Structure Notes:

CHECK FOR LOAD RATING CAP. POSSIBLY RE-RATED. This bridge should be considered for replacement 2002-2003.

		Old New		Old New		Old New		Old New
NBI RATINGS	Deck	3	Superstructure	3	Substructure	5	Culvert	N

Should structure be re-rated for load carrying capacity? (yes/no) | Y | **Structure Number: P-53-0702**

Other Items	Rating Old	Rating New	Comments
Approach Alignment	8		
Channel Condition	6		
Waterway Adequacy	6		Some silting
Construction Joints	6		
Utilities			

Marking/Signing	Rating Old	Rating New	Comments
Bridge Markers	Y		1 - needs repairs
Narrow Bridge			Need narrow bridge signs
One Lane Bridge			
Vertical Clearance			
Weight Limit Post			

Clearance	Meas. (ft)	Date	New Meas.
Min Vert Clear. Under Cardinal (N or E)		1/1/1901	
Min Vert Clear. Under Non-cardinal		1/1/1901	
Min Vert Clear. Over			
Measured by:		Date:	

EXPANSION JOINTS			
Location	In.	Temp	Type
A.			
B.			
C.			
D.			
E.			
F.			

STRUCTURE TYPE			
Material	Configuration	# Spans	Length
CONCRETE	FLAT SLAB	1	23

Inspection/Maintenance Notes:

This bridge should be rerated for load carryibg capacity.
Recommend - replacement of bridge or other.

Recommendations	Estimated Cost	Year Programmed
BRIDGE REPLACEMENT	56160	1999
Repair bridge marker and install narrow bridge signs	200	

CONSTRUCTION HISTORY			
Year	Work Performed	Year	Work Performed
1930	NEW STRUCTURE		

Routine Inspections		Fracture Critical Inspections		Underwater Inspections						Other Special Inspections	
				Visual/Probing		Diving		Profile/Soundings			
Last Insp	Freq (mo)	Last Insp	Freq (mo)	Last Insp	Freq (mo)	Last Insp	Freq (mo)	Last Insp	Freq (mo)	Last Insp	Freq (mo)
11/15/00	24			11/15/00	12	1/1/01		1/1/01			

Equipment Needs:

Routine	
Fracture Critical	
Underwater	
Other Special	

Inspector:	Date:	Inspection Agency: City/Municipal Hwy Agenc

147

***** SIMPLE SPAN AXLE RATINGS *****

P-702 CTH N ROCK COUNTY
```
22.000   0.205   0.205   0.286   16.000   0.800   10.000
 2.000   2.000   0.0     0.0      0.0     36.000
 0.0     0.0     0.0     0.0     19.500   12.000
 0.0     0.0     0.0     0.0      0.0      0.0
```

SECTION MODULI - REINFORCED CONCRETE SECTION
CONCRETE - 570.2
STEEL   - 30.9

LONGITUDINAL GIRDER RATINGS
ALLOWABLE PERMIT GROSS WEIGHT OF SINGLE AND TANDEM AXLES IN KIPS
MULTIPLE AXLES ARE SPACED AT FOUR FEET.
30 PERCENT IMPACT
1 AXLES = 46.9
2 AXLES = 56.7
3 AXLES = 61.9
4 AXLES = 72.7

ALLOWABLE PERMIT GROSS WEIGHT OF AXLE GROUP COMBINATIONS IN KIPS

TWO SINGLE AXLES
6 FT.SPAC. 61.1 12 FT.SPAC. 85.2 18 FT.SPAC. *****

ONE SINGLE AXLE AND ONE 2-AXLE TANDEM
6 FT.SPAC. 64.2 12 FT.SPAC. 84.8 18 FT.SPAC. *****

ONE SINGLE AXLE AND ONE 3-AXLE TANDEM
6 FT.SPAC. 70.6 12 FT.SPAC. ***** 18 FT.SPAC. *****

TWO 2-AXLE TANDEMS
6 FT.SPAC. 73.0 12 FT.SPAC. ***** 18 FT.SPAC. *****

ONE 2-AXLE TANDEM AND ONE 3-AXLE TANDEM
6 FT.SPAC. 83.7 12 FT.SPAC. ***** 18 FT.SPAC. *****

TWO 3-AXLE TANDEMS
6 FT.SPAC. ***** 12 FT.SPAC. ***** 18 FT.SPAC. *****

H-RATING= 17.5 30 PERCENT IMPACT.
R-RATING= 29.3 30 PERCENT IMPACT.

HS-RATING= 17.6 30 PERCENT IMPACT.   RS-Rating = 29.3 30 Percent Impact (concrete)

P 702

148